EMEP: CCC-Report 1/2016

EMEP Co-operative Programme for Monitoring and Evaluation of the Long-Range Transmission of Air Pollutants in Europe

Air pollution trends in the EMEP region between 1990 and 2012

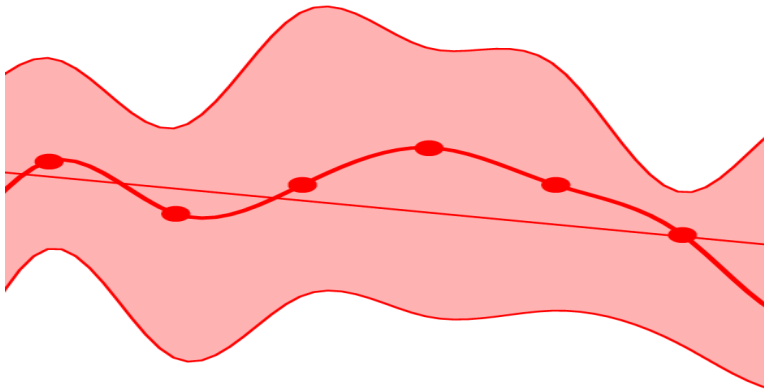

Download report using a barcode skanner:

Joint Report of the EMEP Task Force on Measurements and Modelling (TFMM), Chemical Co-ordinating Centre (CCC), Meteorological Synthesizing Centre-East (MSC-E), Meteorological Synthesizing Centre-West (MSC-W)

NILU : EMEP: CCC-Report 1/2016
REFERENCE : O-7726
DATE : MAY 2016
ISBN : 978-82-425-2833-9 (printed)
ISBN : 978-425-2834-6 (electronic)

EMEP Co-operative Programme for Monitoring and Evaluation of the Long-range Transmission of Air Pollutants in Europe

Air pollution trends in the EMEP region between 1990 and 2012

Authors:
Augustin Colette, Wenche Aas, Lindsay Banin, Christine F. Braban, Martin Ferm, Alberto González Ortiz, Ilia Ilyin, Kathleen Mar, Marco Pandolfi, Jean-Philippe Putaud, Victor Shatalov, Sverre Solberg, Gerald Spindler, Oksana Tarasova, Milan Vana, Mario Adani, Paul Almodovar, Eva Berton, Bertrand Bessagnet, Pernilla Bohlin-Nizzetto, Jana Boruvkova, Knut Breivik, Gino Briganti, Andrea Cappelletti, Kees Cuvelier, Richard Derwent, Massimo D'Isidoro, Hilde Fagerli, Clara Funk, Marta Garcia Vivanco, Richard Haeuber, Christoph Hueglin, Scott Jenkins, Jennifer Kerr, Frank de Leeuw, Jason Lynch, Astrid Manders, Mihaela Mircea, Maria Teresa Pay, Dominique Pritula, Xavier Querol, Valentin Raffort, Ilze Reiss, Yelva Roustan, Stéphane Sauvage, Kimber Scavo, David Simpson, Ron I. Smith, Yuk Sim Tang, Mark Theobald, Kjetil Tørseth, Svetlana Tsyro, Addo van Pul, Sonja Vidic, Markus Wallasch, Peter Wind

Joint Report of :
EMEP Task Force on Measurements and Modelling (TFMM),
Chemical Co-ordinating Centre (CCC),
Meteorological Synthesizing Centre-East (MSC-E),
Meteorological Synthesizing Centre-West (MSC-W)

Norwegian Institute for Air Research
P.O. Box 100, NO-2027 Kjeller, Norway

Contents

Key messages

The present report synthetises the main features of the evolution over the 1990-2012 time period of the concentration and deposition of air pollutants relevant in the context of the Convention on Long-range Transboundary Air Pollution: (i) ozone, (ii) sulfur and nitrogen compounds and particulate matter, (iii) heavy metals and persistent organic pollutants. It is based on observations gathered in State Parties to the Convention within the EMEP monitoring network of regional background stations, as well as relevant modelling initiatives. The main conclusions of this assessment for each type of compounds are as follows.

Ozone:

- Atmospheric measurements show a substantial decrease in the main ozone precursors: ambient NO_2 and NMVOCs (non-methane volatile organic compounds) concentrations in Europe. This decrease is consistent with reported decrease in European emissions of ozone precursors since 1990;
- The magnitude of high ozone episodes has decreased by about 10% between 1990 and 2012, resulting in reductions of 20 to 50% of the number of days exceeding the guidelines of the World Health Organisation or the European long term objective, respectively. It should be noted however that such thresholds are still exceeded at a majority of stations, thereby demonstrating both the efficiency of control measures undertaken over the past 20 years, and the need for further action;
- Annual mean ozone levels measured at EMEP stations were increasing in the 1990s, and show a limited negative trend starting in 2002. This feature is generally attributed to the evolution of the global baseline of tropospheric ozone for which further hemispheric control strategies are needed;
- There was a sharp reduction of the fraction of sites with an upward trend between the 1990s and the 2000s. Over the 2002-2012 time period, none of the considered stations reported significant increase of ozone for any of the metrics (except for the annual mean for which an increase was reported at one site). Most stations reported a downward trend, however, because of the large inter-annual variability of ozone and the relatively short time period, the downward trends are statistically significant at only 30 to 50% of the sites, depending on the metric considered;
- The efficiency of ozone precursor abatement measures is very clear for human and vegetation exposure levels (as measured by SOMO35 and AOT40, respectively) that have experienced a relative decrease of 30 and 37%, respectively, from 2002 to 2012.

Sulfur and nitrogen compounds and particulate matter:

- Observed atmospheric concentrations of gas phase SO_2 decreased by about 92% while particulate sulfate was reduced by 65% and 73% in air and precipitation, respectively, this is in response to sulfur emissions abatement over the 1990-2012 period in the EMEP region;
- Acidifying and eutrophying nitrogen pollutant emissions (NO_x and NH_3) also decreased over the period 1990-2012 but not to the same extent as sulfur emissions, this is also reflected in the reduction of atmospheric concentrations in oxidised nitrogen: 41% for NO_2 and 33% for NO_3^- in precipitation. A

similar overall trend is observed for reduced nitrogen for the 1990-2012 period (29% reduction for NH_4^+ in precipitation) but the decrease appears much slower over the later part of the period, where the trends are not statistically significant at 80% of the sites. The observed trends are broadly consistent with the reported emission reductions in Europe for the same period (49% for NOx and 29% for NH_3).

- Decreases of measured oxidised nitrogen are determined both by emissions and atmospheric chemistry. Particulate matter (PM) composition has shifted from ammonium sulfate to ammonium nitrate so that reductions in emissions are not directly transferred to decreases in concentrations;
- Reduced nitrogen remains a major area for concern as there are either near-zero or increasing trends observed at the majority of available sites over recent years;
- For inorganic aerosols, larger decreasing changes were observed in the 1990-2001 period compared to 2002-2012;
- PM_{10} and $PM_{2.5}$ mass were only measured extensively enough to assess trends after 2001. Over the 2002-2012 period, decreases of 29% and 31% were observed at the sites included in the assessment for PM_{10} and $PM_{2.5}$ respectively;
- Separation of measurements of gas phase and particulate phase atmospheric components for oxidised and reduced nitrogen would allow a clearer understanding of the processes occurring in the atmosphere, which drive trends and environmental impacts.

Heavy Metals and Persistent Organic Pollutants

- Heavy metal deposition decreased significantly, with about 80%, 60% and 35% reductions for lead, cadmium and mercury in EU28 countries based on modelled trends, these numbers being 76%, 49% and 10% in EECCA countries. Most of the reduction occurred in the 1990s;
- Most of the trend is attributed to anthropogenic emission changes within the EMEP region for lead and cadmium. For mercury, the influence of non-EMEP sources is large;
- Where observations are available, the model gives reasonable results. The most important discrepancies are (i) an underestimation of cadmium levels at the beginning of the 1990s, and (ii) an underestimation of the downward trend of mercury concentration in precipitation;
- Amongst the various POPs considered over the 1990-2012 period, the largest modelled reduction is estimated for HCB (90%) and the lowest for B[a]P (30%) for which modelled concentrations revert to an increase over recent years on average in the EMEP region;
- The agreement between model and observation trends is good for POP, except for HCB at sites at the outskirts of the domain that are influenced by non-EMEP sources.

1 Introduction

In the late 1960s, early warnings were issued that air pollution could go beyond the limits of urban areas and industrial facilities, potentially affecting the acidity of precipitations at the scale of the whole European Continent. After a pioneer monitoring network was set up under the auspices of OECD (Organisation for Economic Co-operation and Development) a political consensus emerged for the need to elaborate a specific Convention on Long-range Transboundary Air Pollution (CLRTAP) that was signed in 1979 and entered into force in 1983.

The historical monitoring network was thereafter a full part of the Cooperative Programme for Monitoring and Evaluation of the Long-range Transmission of Air Pollutants in Europe (EMEP, established in 1977), together with numerical modelling and emission reporting capacities. These capacities are supported by five Programme Centres (Centre for Emission Inventories and Projections - CEIP, Chemical Coordinating Centre - CCC, Meteorological Synthesizing Centre-West – MSC-W, Meteorological Synthesizing Centre-East – MCS-E, and Centre for Integrated Assessment Modelling - CIAM). The work of the Centres is evaluated and discussed in Task Forces bringing together EMEP Centre experts and Representatives of the State Parties to the Convention. Such Task Forces are also a forum to further develop working methods and tools. The Task Force on Measurements and Modelling (TFMM) in particular has been set up by the Executive Body in 2000 to perform this role with the Chemical Coordinating Centre, the Meteorological Synthesizing Centre-West, and the Meteorological Synthesizing Centre-East.

One of the first decision of the TFMM at its inaugural meeting was to undertake a review of the status and evolution of air pollution, both modelled and measured, throughout the EMEP region since the onset of the Programme in order to support the EMEP Assessment Report published in 2004 (Lövblad et al., 2004). It is now timely to mobilise the TFMM community to propose an update of this work and assess of the evolution of air pollution in the EMEP region over the 1990-2012 period. The Working Group on Effects of the Convention also published in 2015 a Trend Report, (De Wit et al., 2015), and an Assessment Report of all the activities undertaken under the Convention was published in 2016 (Maas and Grennfelt 2016). **The goal of the present report is to provide the observational and modelling evidences of atmospheric composition and deposition change in response to actions taken by Member countries to control emissions**. **It is also an opportunity to demonstrate the outstanding value of the EMEP monitoring and modelling strategies in supporting to the implementation of environmental policies.**

Consistent with the mandate of the Convention, TFMM focuses its analysis on European regional-scale background ozone as observed at EMEP stations with additional contextual information on ozone trends in the State Parties of the Convention in North America as well as measurements gathered at urban monitoring sites. The trends are considered over the 1990 – 2012 period and the 1990-2001 and 2002-2012 sub-periods.

The monitoring and modelling capacities in support of EMEP have substantially advanced with time as demonstrated in the EMEP Status Reports published

annually[1]. The review of (Tørseth et al., 2012) highlighted the increase of the amount of observational data delivered to the EMEP database[2] thanks to the involvement of State Parties and collaboration with other programmes and initiatives such as the Global Atmosphere Watch (GAW) under the World Meteorological Organisation or the European Research Infrastructure projects, such as the current project on observation of Aerosol, Clouds, and Trace gases Research Infrastructure Network (ACTRIS). This development is illustrated in Figure 1.1 that shows the evolution of contributions received from State Parties.

Numerical dispersion models have also undergone substantial improvements. A recent overview of the EMEP/MSC-W model was presented in (Simpson et al., 2012), and the latest results of the EMEP/MSC-E model were presented in (Shatalov et al., 2014). For the main pollutants covered by EMEP/MSC-W, the collaboration of national experts in modelling mandated by State Parties within the TFMM was implemented through the various phases of the EURODELTA project (Thunis et al., 2008; Bessagnet et al., 2014). This project largely contributed to benchmark the performances of the MSC-W model in terms both comparison with observations and sensitivity to incremental emission changes. EURODELTA is now undertaking a multimodel hindcast experiment which is particularly relevant to support the present work on air quality trends. As far as heavy metals are concerned, collaboration between MSC-E and State Parties was strengthened through various national-scale case studies (for the Netherlands, Croatia, the Czech Republic[3]) initiated by the TFMM.

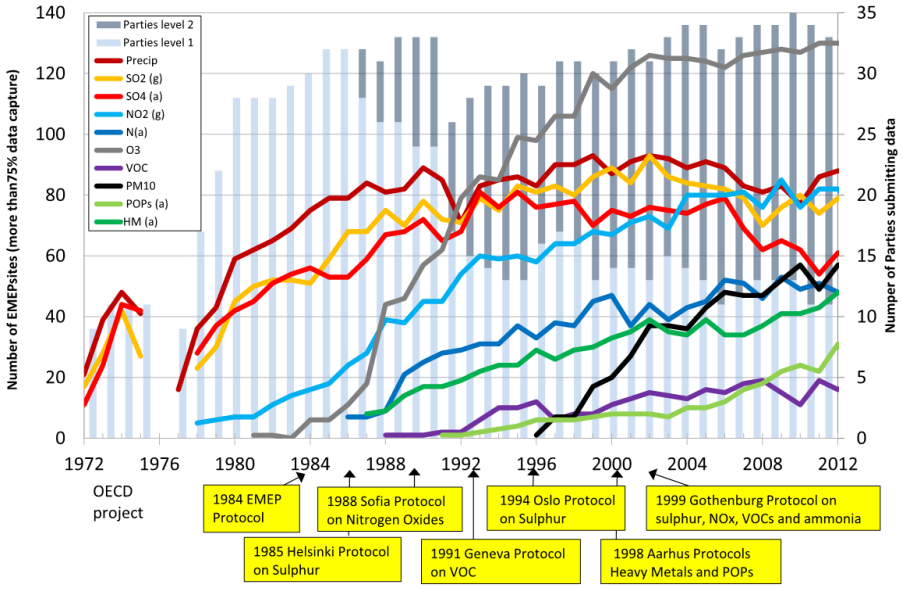

Figure 1.1: *Development of the EMEP monitoring programme. Bars represent the number of parties/countries submitting data according to the level-1 and level-2 monitoring requirements, respectively. Lines indicate the number of sites for which measurements of the various variables have been measured (g) = gaseous, (a) = aerosol, adapted from (Tørseth et al., 2012).*

[1] http://www.emep.int/publ/common_publications.html and http://www.msceast.org/index.php/reports

[2] http://ebas.nilu.no

[3] http://www.msceast.org/documents/CaseStudy_Booklet.pdf

These developments form the basis for the present assessment on air pollution trends in the EMEP region. The methodology to perform trend analyses was discussed at the annual meetings of the TFMM in 2014 (Bologna) and 2015 (Krakow), as well as during a dedicated workshop held in Paris in 2014. State Parties and Centres agreed on the EMEP monitoring stations to be used for such analyses and appropriate statistical methodologies. The quantitative analysis was performed by the Centres and supplemented by specific analyses undertaken by State Parties. The European Environment Agency (EEA) and its European Topic Centre on Air Pollution and Climate Change Mitigation (ETC/ACM) also performed a trend analysis following the agreed methodology for O_3, NO_2 and PM on the whole set of monitoring stations included in the EEA Air Quality e-reporting database[4]. The modelling was performed by the Centres, and supplemented by the input of State Parties (in particular through the EURODELTA exercise).

The present assessment synthesises the results of analyses reported by the group of experts from the TFMM, CCC, MSC-E and MSC-W for ozone trends (Chapter 2), sulfur and nitrogen compounds and particulate matter (Chapter 3), and heavy metals and persistent organic pollutants (Chapter 4). Supplementary material on the methodology for the statistical analysis for the main pollutants and heavy metals and POPs as well as trends in air pollution emission (in collaboration with the Centre for Emission Inventories and Projections - CEIP) are provided in Annex C.

[4] http://www.eea.europa.eu/data-and-maps/data/aqereporting, the former AirBase.

2 Ozone

Main authors: Kathleen Mar, Augustin Colette, Sverre Solberg

Contributors: Mario Adani, Paul Almodovar, Eva Berton, Bertrand Bessagnet, Gino Briganti, Andrea Cappelletti, Kees Cuvelier, Richard Derwent, Massimo D'Isidoro, Hilde Fagerli, Marta Garcia Vivanco, Alberto González Ortiz, Christoph Hueglin, Jennifer Kerr, Frank de Leeuw, Astrid Manders, Mihaela Mircea, Maria Teresa Pay, Jean-Philippe Putaud, Valentin Raffort, Yelva Roustan, Stéphane Sauvage, Kimber Scavo, David Simpson, Oksana Tarasova, Mark Theobald, Kjetil Tørseth, Svetlana Tsyro, Markus Wallasch, Peter Wind.

2.1 Overview of ozone trends

An important challenge when addressing ozone distributions and trends lies in the multiplicity of processes underlying ozone variability. Photochemical ozone production occurs via reactions of nitrogen oxides (NOx) and non-methane volatile organic compounds (NMVOCs) in the presence of sunlight, and is maximized under conditions of high solar radiation and high temperatures (Monks et al., 2015). This leads to ozone diurnal maxima in the afternoon with the highest peaks typically observed in the summer months, when exceedances of regulatory thresholds are most frequent. Once formed, ozone and reservoir species accumulates in the atmosphere, where it can be transported over hemispheric distances, with a typical lifetime of the order of weeks. The concentration of ozone at any particular place and time is the result of complex interactions between precursor emissions of both local and non-local sources by means of chemical transformations, transport and deposition processes.

Systematic ozone monitoring in Europe began in 1957 during the International Geophysical Year, with the longest running time series at Cape Arkona – Zingst on the Baltic Sea coast of Germany. The monitoring network in State Parties to the Convention developed substantially since then so that, since the beginning of the 1990s, an ensemble of high quality records is available for statistical analyses of ozone pollution trends in the EMEP region.

Most EMEP monitoring sites selected for the present analysis are influenced by both hemispheric baseline ozone and by regional air pollution sources, in contrast to remote and free tropospheric observatory sites, which are designed to be free of local and regional influences. The list of stations passing the data completeness filter and thereby included in the present analysis is given in Table A.*1* in Annex A.

An important methodological aspect of any ozone assessments lies in the selection of the metrics (or indicators) because they depict different impacts. Their trends may also show different features. The present assessment focuses on three aspects of ozone evolution: (i) the global baseline, (ii) human and vegetation exposure, (iii) severe photochemical episodes. At rural background sites, baseline ozone trends are well represented by the annual mean, whereas close to emission sources this metric can also be influenced by night-time and wintertime ozone titration. Impacts on health and ecosystems are assessed using the SOMO35 (sum of ozone

daily maxima above 35 ppb) and AOT40 (cumulated hourly ozone above 40 ppb) metrics, respectively. The trends in severe photochemical episodes are assessed by investigating both the number and magnitude of high ozone days. The number of episodes is defined by the number of exceedances of the 50ppb and 60ppb thresholds (WHO and European criteria) for ozone MDA8 (daily maximum of the 8-hour running mean). The magnitude of the episodes is assessed from the fourth highest MDA8 recorded each year, which represents approximately the annual 99th percentile when the data coverage is complete.

The overall evolution of the fourth highest MDA8 and annual mean ozone observed at EMEP monitoring sites is displayed in Figure 2.1 for the 1990-2012 period (see the Methods in Annex A) for details on the station selection criteria). For both metrics we show the median over the whole EMEP network as well as the envelope constituted by the 25th and 75th percentiles. The year to year variability is high for summertime ozone episodes (4th highest MDA8), especially in outstanding years such as 2003 and 2006 (pronounced heat waves). **Since the beginning of the 1990s, a clear downward trend in high ozone episodes was observed when considering the network as a whole. But some further reductions are desirable** given that over recent years, none of the stations in the envelope constituted by the 25th and 75th percentiles reach the WHO ozone air quality guideline of 50 ppb, and only a few reach the European Directive long term objective of 60 ppb. Annual mean ozone was increasing during the first sub-period but decreased slightly in the second sub-period, and appears largely driven by the trend in the hemispheric baseline ozone (see discussion in Section 1.2.2).

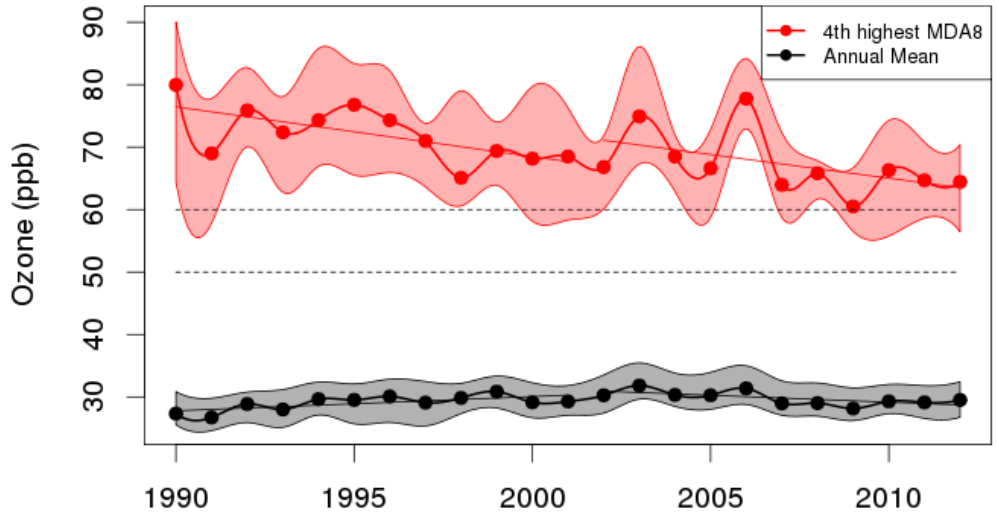

Figure 2.1: *Composite of annual mean ozone (black) and 4th highest MDA8 (red) ozone recorded at 55 EMEP rural monitoring sites between 1990 and 2012. The thick line is the network-wide annual median and lower/higher bounds of the shaded areas are for the 25th and 75th percentiles. Thin straight lines show the linear trend over the 1990-2001 and 2002-2012 periods and dashed lines indicate the WHO air quality guideline (50ppb) and the EU long term objective (60ppb).*

The aggregation of data from many stations into a single median trend for the region masks the variability across the network. To further examine this variability, Figure 2.2 provides the distribution of the percentage of the sites in the EMEP network with statistically significant/insignificant increase/decrease for the first and second sub-periods. Trends are considered statistically significant when

the p-value of their Mann-Kendall statistic is lower than 0.05 (See the Methods section in Annex A). Apart from the metrics presented in Figure 2.1 (annual mean and 4th highest MDA8), some additional commonly-used ozone metrics (see Glossary) are provided in Figure 3: SOMO35 (used to assess health impacts; note however that its significance in terms of human health exposure trends should be considered with care since we focus here on rural sites), AOT40 (vegetation impacts), the number of days where MDA8 is above 50 ppb (WHO guideline) or 60 ppb (corresponding to the 2008/50/EC long-term objective, it is also the target value which means that, at present, the long term objective should not be exceeded more than 25 days per year over three years), and annual MDA8 maximum.

For all ozone metrics, comparing the 1990s and the 2000s demonstrates a sharp reduction in the fraction of sites with an upward trend (Figure 2.2), so that in the 2000s there are virtually no sites where significant increases of any of the ozone metrics are observed (only one site for the annual mean). Consistent with this tendency, a greater percentage of stations within the network showed statistically significant decreases in the 2002-2012 sub-period compared to the 1990-2001 sub-period. However, ozone trends remain statistically insignificant (p-value > 0.05) at the majority of sites (at 75 to 90% for the 1990-2001 period and 52 to 93% of the sites for 2002-2012 period, depending on the metric). This is partly due to the meteorological sensitivity of ozone that makes it variable from year to year, thereby challenging the detection of trends on the basis of 10-year periods. Because there were different trends in the 1990s and in the 2000s, using the whole 23-year period for trend detection only marginally improves the fraction of sites where a statistically significant trend is detected, with 50 to 76% of sites still showing statistically insignificant trends.

There are also important differences amongst the metrics. Annual mean ozone exhibited the largest fraction of positive slopes in the 1990s, and in the 2000s it is the only metric for which statistically significant increases are found (although at just one site). Increases at 35 to 55% of the stations were also found for exposure metrics as well as exceedances of the WHO guideline in the 1990s, whereas a majority of decreases was already found during this earlier decade for highest ozone days (both in magnitude and number of exceedances of the EU long term objective).

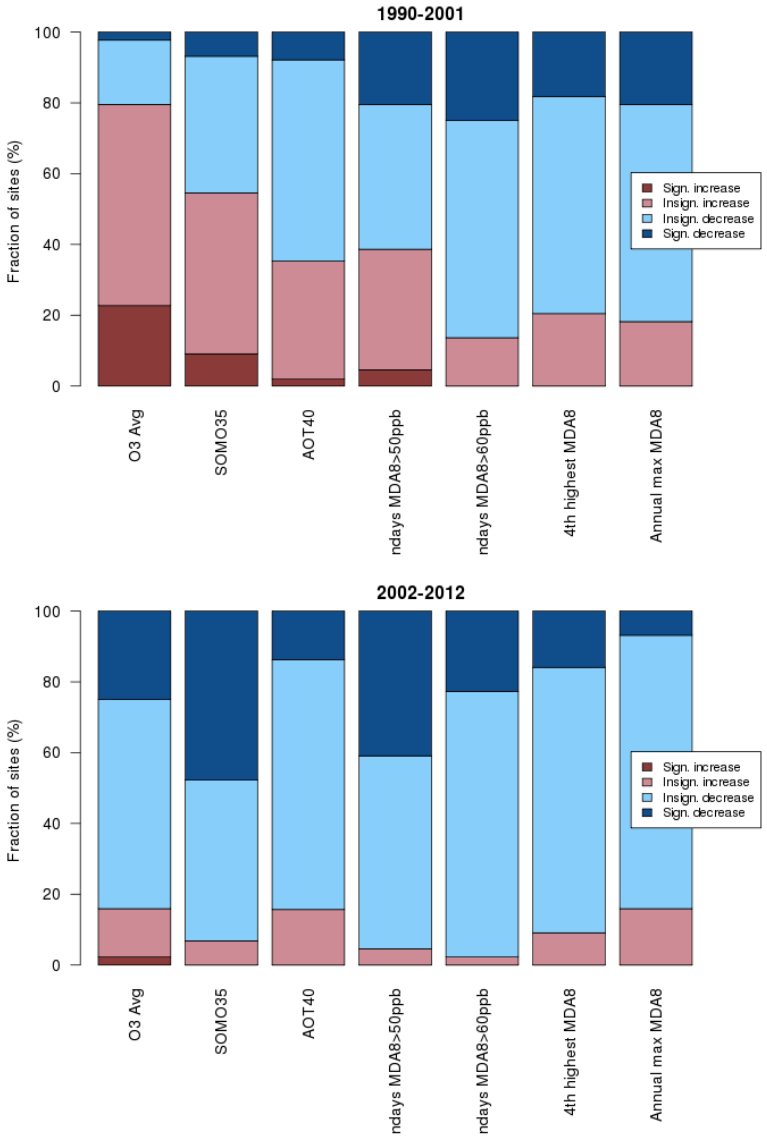

Figure 2.2: *Percentage of EMEP monitoring sites where statistically significant upward trends (dark red), insignificant upward trends (light red), insignificant downward trends (light blue) and significant downward trends (dark blue) were observed in the 1990s (top) and in the 2000s (bottom) for each ozone metric (O3 Avg: ozone annual mean, SOMO35 and AOT40, ndays MDA8>50 and 60ppb: number of days per year where the O_3 MDA8 is above the 50ppb (WHO) or 60ppb (European) threshold, fourth highest MDA8 day and annual maximum of MDA8).*

The network-wide median of the annual relative trend for several metrics is shown in Table 2.1. The relative change (negative for a decrease) over a given period is computed from the Sen-Theil slope (in unit/yr) normalised with the concentration at the beginning of the period (See the Methods section in Annex A). As illustrated in the network-median time series given in Figure 2.1, annual mean ozone was increasing in the 1990s but over the 2002-2012 period, a 7.1% median decrease was observed over the network. **The reduction of summertime ozone episodes (4th highest MDA8) is steady with a relative reduction of 11% and 10% over 1990-2001 and 2002-2012 periods, respectively**. The analysis of regulatory and exposure indicators is complementary to the analysis of 4th highest MDA8. These are based on threshold exceedances and designed to reflect impacts on human health (WHO, European targets and SOMO35) or on vegetation (AOT40). The number of days when the WHO guideline (50 ppb) or European

threshold (60 ppb) are exceeded is closely related to the 4th highest MDA8 metric. Compared to the 2000s, there were many more sites where the number of exceedances of the WHO guideline showed an upward annual trend in the 1990s (Figure 2.2). In the 2000s, a statistically significant downward trend for the number of days where MDA8 was above 50 ppb is seen at less than half of the monitoring sites (Figure 2.2), and the network-wide median slope is not significantly negative (Table 2.1). **The number of exceedances of the EU long term objective decreases steadily, with 41 and 61% median reductions over the 1990s and 2000s respectively**, both being statistically significant over the network. The health impacts metric SOMO35 and the vegetation impacts metric AOT40 show larger decreases than the exceedance metrics over the second sub-period. **From 2002 to 2012, SOMO35 and AOT40 were reduced by 30 and 37%, respectively.** It should be noted that in the 1990s, positive slopes in SOMO35 and AOT40 were reported at a large fraction of sites (Figure 2.2) suggesting that these indicators were at least partly influenced by an unfavourable baseline trend as for annual mean ozone (see discussion in Section 2.2.2).

Table 2.1: *Network-wide median [95% Confidence Interval, CI] of the annual trend and total change (negative for a downward trend) for selected ozone metrics for each considered time periods.*

Ozone Metric	Time period	Median annual trend in, [unit/yr] and 95% CI	Median relative change over the period [%] and 95% CI
Annual mean (ppb)	1990_2001	0.15[0.11,0.25]	5.8[4.6,11]
	2002_2012	-0.21[-0.3,-0.16]	-7.1[-9.5,-4.5]
	1990_2012	0.06[0.009,0.07]	4.1[1.2,5.7]
SOMO35 (ppb.days)	1990_2001	4.9[-16,26]	1.6[-0.41,35]
	2002_2012	-79[-100,-67]	-30[-39,-22]
	1990_2012	-11[-21,-2.4]	-8.3[-14,2.4]
AOT40 (ppb.hours)	1990_2001	-88[-139,12]	-16[-14,23]
	2002_2012	-226[-309,-179]	-37[-40,-14]
	1990_2012	-98[-128,-62]	-31[-47,19]
Ndays MDA8 > 50ppb (days)	1990_2001	-0.41[-0.88,0.15]	-10[-36,83]
	2002_2012	-2.9[-3.3,-2.2]	-47[-84,59]
	1990_2012	-0.41[-0.73,-0.23]	-22[-28,-9.5]
Ndays MDA8 > 60ppb (days)	1990_2001	-0.63[-0.93,-0.42]	-41[-49,-19]
	2002_2012	-0.93[-1.5,-0.82]	-61[-70,-45]
	1990_2012	-0.4[-0.75,-0.37]	-49[-58,-39]
4th highest MDA8 (ppb)	1990_2001	-0.65[-1,-0.5]	-11[-13,-6.7]
	2002_2012	-0.73[-0.92,-0.53]	-10[-13,-7]
	1990_2012	-0.41[-0.62,-0.4]	-12[-17,-11]
Annual max. MDA8 (ppb)	1990_2001	-0.76[-1.3,-0.62]	-11[-14,-7.6]
	2002_2012	-0.65[-0.91,-0.38]	-9[-11,-3.8]
	1990_2012	-0.53[-0.75,-0.49]	-14[-18,-12]

Because of the variety of meteorological conditions, emission sources, and therefore chemical regimes occurring throughout Europe, it is legitimate to inquire whether the trends shown in Table 1 are really representative of the whole European continent. As shown in the Method section in Annex A, the subset of stations available for the first sub-period is significantly smaller than for the second sub-period, and strongly biased to northern and central Europe. To establish the representativeness of the observed trends, Figure 2.3 compares the relative trends observed at EMEP and the EEA's Air Quality e-reporting database (formerly known as AIRBASE) rural background stations for the summertime peaks for the second sub-period only (when both data sets are available). The AIRBASE database includes measurements that are operated by member countries to verify the compliance with the European air quality legislation, although not designed to assess trends of background ozone. They offer an interesting complement to the EMEP network because of their larger coverage (231 stations passing the completeness criteria over the 2002-2012 period instead of 109 for EMEP). The comparison of EMEP and AIRBASE maps of trends shows that there is no outstanding spatial pattern captured by the AIRBASE network that would be missed by the EMEP network. The AIRBASE network-wide median rate of decrease for the 4th highest MDA8 is 12% (fairly close to the 10% reduction for EMEP), and the fraction of sites with significant decreasing trends is also consistent with the EMEP estimate (14% and 15% for the AIRBASE and EMEP networks, respectively). It should be noted, however, that even when only the second period is considered (where there are more measurement records available), neither EMEP nor AIRBASE have good long-term coverage over most of south-eastern Europe but Spain, so that we are not confident that trends are valid for these regions.

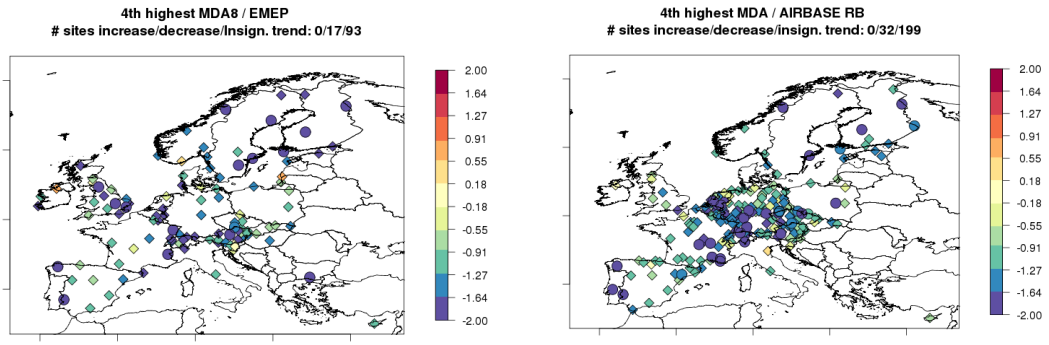

Figure 2.3: *Maps of relative trends over 2002-2012 (%/yr) of the 4th highest MDA8 recorded at EMEP (left) and AIRBASE (right) rural background (RB) sites over the 2002-2012 period. Stations where the trend is significant at the 0.05 level are displayed with a circle, elsewhere a diamond is used.*

Gains are also being made on ambient ozone levels in North America. In Canada annual 4th highest daily maximum 8-hour concentrations decreased by 15% between 1998 and 2012. Between 2003 and 2012, the percentage of Canadians living in communities where ambient concentrations of ground-level ozone exceeded the 2015 Canadian Ambient Air Quality Standard (CAAQS) for ozone[5]

[5] CAAQS for ozone are 63 ppb in 2015 and 62 ppb in 2020. Additional information on the Canadian Ambient Air Quality Standards (CAAQS) can be found at http://www.ec.gc.ca/default.asp?lang=En&n=56D4043B-1&news=A4B2C28A-2DFB-4BF4-8777-ADF29B4360BD

dropped from approximately 50% to 28%. In the United States, national averages of the 4th highest daily maximum 8-hour concentrations declined in the 1980's, levelled off in the 1990's, and showed a notable decline after 2002. From 1990 to 2014 these levels decreased 23%.

2.2 Factors contributing to the ozone trend

Ozone evolution must be put in perspective of the changes in (i) emissions of precursors, (ii) baseline ozone levels (long range transport, including stratosphere-troposphere exchanges), and (iii) photochemical activity in relation to meteorological variability. In this section we discuss the conclusions that can be drawn about the importance of these factors, to the extent possible on the basis of an analysis of surface observations.

2.2.1 Ozone precursors

This section presents to what extent measurements of atmospheric concentrations of ozone precursors (NO_2 and NMVOCs) can be used to confirm the magnitude of the change reported in emission inventories as detailed in Annex C.

2.2.1.1 Concentrations of nitrogen oxides (NO_x)

The network-wide median of annual mean NO_2 measured at EMEP and AIRBASE sites across Europe (separated by station type) is displayed in Figure 2.4. NO_2 is shown here as a proxy for NO_x ($NOx=NO+NO_2$), for which a limit value has been established under Air Quality Directive 2008/50/EC (EC, 2008). Furthermore, NO_2 is measured at a greater number of European stations than total NO_x. Note that there are about half as many EMEP stations passing the completion criteria for NO_2 as for O_3. *Figure 2.4* shows that on average, important decreases in NO_2 concentrations were observed over Europe since the beginning of the 1990s. **Over the full 23-year period between 1990 and 2012, the average relative NO_2 reduction based on the Sen-Theil slope is very consistent at EMEP (39%) and AIRBASE rural background (41%) sites**. The relative reduction is 39% at urban sites, which is slightly smaller than the 51% decline in reported NO_x emissions over EU between 1990 and 2012.

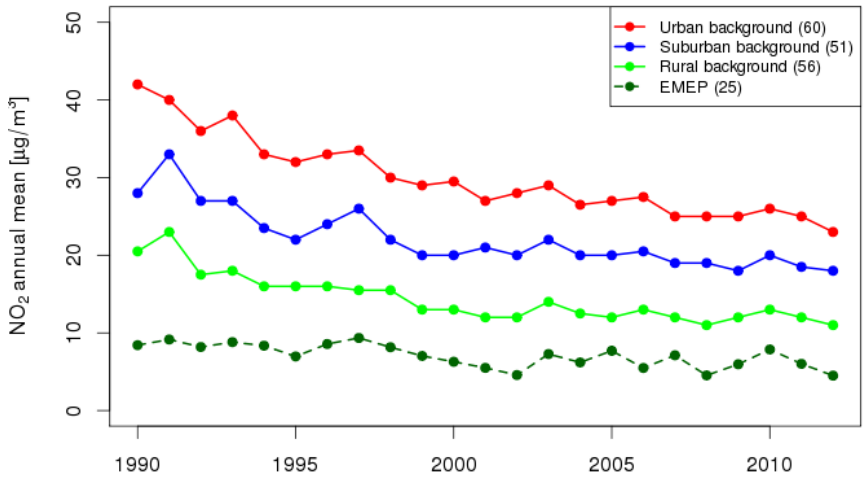

Figure 2.4: *Median NO_2 time series (µg/m^3) at EMEP and AIRBASE stations (for urban, suburban and rural background sites) passing the completeness criteria. For each type of site, the number of stations in the composite is given in the legend. Adapted from (Colette et al., 2015).*

Figure 2.5 shows trends in anthropogenic NMHC (non-methane hydrocarbons), a major group of NMVOC species, at 12 EMEP sites in north-central Europe (in the UK, France, Germany, and Switzerland). An overview of NMVOC monitoring within the EMEP programme is provided in (Tørseth et al., 2012), and the selection of stations and treatment of NMHC data in this study is described in Chapter A.1.3. Although time series are too short or too interrupted to detect trends at many sites, the general picture is that the ambient concentrations of NMHCs have decreased since the mid 1990s, qualitatively consistent with the reported decrease in emissions. With the stringent data capture criteria used in this report, quantitative trends could only be computed at two stations. To increase the representativeness of the trend estimate, we computed the trends for a composite data set of all stations composed of the network median of annual mean values. Over the 2002-2012 period, a decrease of 40% is found, which is in line with the 31% relative reduction of reported NMVOC emissions for the 2002-2012 period.

In general, the summed NMHCs presented in *Figure 2.5* have a relatively short atmospheric lifetime (about a few days in summer), which means that observed concentrations should reflect regional pollution sources: the influence of hemispheric baseline NMHCs should be minimal. This is in contrast to ozone, which, due to its longer atmospheric lifetime, is expected to be influenced by hemispheric baseline ozone at all EMEP sites, see discussion in Section 2.2.2.

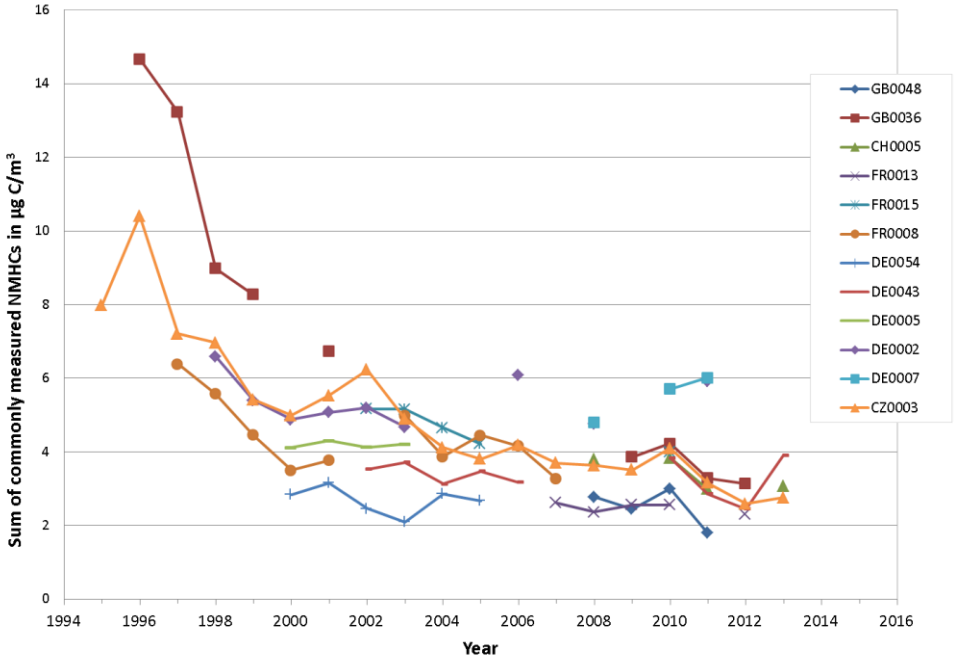

Figure 2.5: *Sum of commonly-measured NMHCs at selected EMEP stations in µgC/m^3, shown as annual averages over time periods with available data. NMHCs included in the total are acetylene (ethyne), benzene, i-butane, n-butane, ethylene, hexane, i-pentane, n-pentane, propene, and toluene. For more information about the selection of NMHC data, see Section A.1.3.*

Trends in ambient NMVOC concentrations have also been addressed in several peer-reviewed publications. (Derwent et al., 2014) presented a detailed analysis of NMVOC trends at a large number of kerbside and urban monitoring stations in the U.K. (in addition to the two rural sites included in *Figure 2.5*), where they find large declines of NMVOCs. At urban sites, trends in NMVOC concentrations should be more easily detectable than at rural sites because of the proximity to emission sources and the relatively short atmospheric lifetime of most NMVOCs. However, it should be noted that analysis of trends at urban stations requires local knowledge of emissions sources in order to avoid misinterpreting a situation where an emission source has simply been moved from one place to another (e.g., due to a change in traffic patterns) as a decreasing trend.

There are some exceptions to the pattern of observed declines of NMVOC concentrations, in particular for ethane and propane, which are not included in *Figure 2.5*. (Derwent et al., 2014) present evidence for some increases in propane and ethane concentrations at U.K. sites. (Tørseth et al., 2012) also report increasing trends in ethane and propane at two German sites (DE0002 and DE0008) and (Sauvage et al., 2009) report an increasing trend for ethane at the French rural site Donon (FR0008). Although the precise reason for this behaviour is unclear, it should be noted that ethane has a longer atmospheric lifetime than other NMHCs, which may require further mitigation actions at the hemispheric scale.

The Pallas-Sodankylä station in Northern Finland is another case in which robust declines of NMVOC were not found. Over the 1994-2013 period, (Hellén et al., 2015) report that acetylene (which is one of the NMVOCs that is the most closely connected to vehicle emissions) is the only NMVOC with a statistically

significant decreasing trend, although they did find small, statistically insignificant negative slopes for most alkanes and benzene. They conclude that the lack of trends at Pallas-Sodankylä is likely related to a significant influence from non-European emission sources.

In addition to anthropogenic NMVOCs, the contribution of biogenic VOC (BVOC) to summertime ozone production is extremely important. BVOC emissions are controlled by land use, temperature and solar radiation. As BVOCs play a role as ozone precursor, the effect of reductions in anthropogenic NMVOCs on ozone production can be dampened at times and locations where BVOC emissions are high, namely in the summer and in highly vegetated regions (Peñuelas and Staudt, 2010).

Despite the relative scarcity of long-term observations of NMVOC concentrations, the available evidence points to a significant decrease in NMVOC concentrations in the EMEP region (40% over the 2002-2012 period). It is very likely that a major driver of the observed decreases was the European vehicle emission standards, which led to significant NMVOC emission reductions, but other factors related to gas extraction, refineries and handling could have contributed to increase some specific NMVOCs such as ethane and propane.

2.2.2 Baseline ozone

In addition to the influence of local emissions and chemistry, European ozone concentrations are also impacted by hemispheric-scale baseline ozone, where "baseline" ozone refers to concentrations in air masses that are not influenced by recently-emitted local anthropogenic emissions (Dentener, F. et al., 2010). For diagnosis of trends in baseline ozone, we rely on a handful of remote European measurement sites where long-term observations are available (Cooper et al., 2014) (Figure 2.6), and contribute to both EMEP and GAW observation networks. These observations show a trend of increasing baseline ozone since the start of the records (in the 1950s and 1980s) until at least the mid-1990s. This is qualitatively consistent with upward ozone trends seen at other remote sites in the Northern Hemisphere (in North America, Japan and the Pacific) and with global increases in emissions of ozone precursors NO_x and VOC until around 2000.

Trends in hemispheric baseline ozone are influenced by several factors, including variability in transport of stratospheric ozone to the troposphere, natural variability in biogenic emissions, and anthropogenic emissions of ozone precursors. When interpreting trends in baseline ozone, it should also be kept in mind that emissions of ozone precursors have an influence on ozone concentrations far from the source regions – for instance North American emissions of NO_x and VOC have an influence on European ozone concentrations (Dentener, F. et al., 2010). But the hemispheric baseline ozone is also influenced by precursor emissions from Europe so that Europe contributes to its own baseline ozone levels.

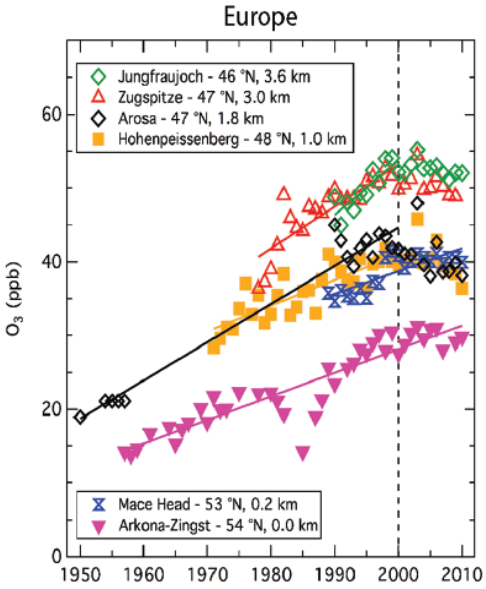

***Figure 2.6**: Surface ozone time series at six rural remote sites in Europe. Trend lines are fit through the yearly average ozone values using the linear least-square regression method through the full time series at each location, except for Jungfraujoch, Zugspitze, Arosa, and Hohenpeissenberg where the linear trends end in 2000. This figure is modified from the original that appeared in IPCC (2013) and taken from (Cooper et al., 2014) .*

Another important ozone precursor at the hemispheric scale is methane, which is long-lived and therefore distributed more uniformly that ozone across the globe. Global anthropogenic CH_4 emissions, which have generally increased since 1950, were stable in the 1990s, but increased again in the 2000s, with current growth mainly taking place outside of Europe (Dentener, F. et al., 2010). Although global CH_4 concentrations are complicated by strong inter-annual variability of natural sources and sinks, they show an underlying long-term trend consistent with the trend in anthropogenic emissions. Even if it is clear that the trend in hemispheric background ozone is not fully explained by trends in global CH_4, modelling studies suggest that CH_4 will have a large influence on hemispheric ozone concentrations under future prospective scenarios.

2.2.3 Peak ozone concentrations

European-wide emissions of ozone precursors NO_x and VOCs have substantially decreased since 1990, and this led to a decrease in ambient levels of NO_2 and VOC over the same time period (*Figure 2.4* and *Figure 2.5*). Since peak ozone concentrations mainly result from local, "fresh" photochemistry, we are confident that the decrease in peak ozone and related metrics (e.g. SOMO35 and number of days above thresholds) at the most polluted European sites is due to the decrease in European precursor emissions.

Looking further into the trends in peak ozone (represented by the 4th highest MDA8), Figure 2.7 shows the scatter plot between the rates of change over the 1990-2012 period vs. the magnitude of ozone peaks at the beginning of the period (estimated with a linear fit of the time series to minimize the impact of interannual variability, see the Method section in Annex A). **The largest negative trends were observed at the stations with the highest levels of peak ozone in the**

beginning of the period. Those sites are typically located in the areas with high photochemical ozone production, where the impacts of precursor emission reductions are seen the most clearly. Sites where peak ozone levels were more moderate in the 1990s tend to show smaller, insignificant trends.

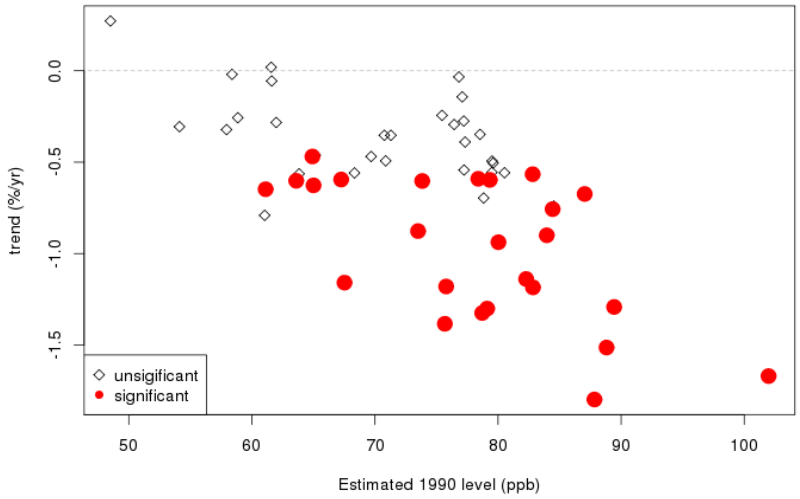

Figure 2.7: *Scatterplot of annual relative trend (%/year) in 4th highest MDA8 for the 1990-2012 time period, versus the values (in ppb) at the beginning of the time period for each EMEP station meeting the data capture criteria. Sites where the trend is statistically significant are plotted in red.*

2.2.4 Seasonal cycles

Further insight into the phenomenology of European surface ozone can be provided by the evolution of the seasonal variability observed at EMEP sites. In Figure 2.8, we display the average monthly cycles in 5-year increments (3-year increment for 2010-2012) in order to dampen the effect of interannual variability. Monthly averages are given along with the monthly maxima in order to differentiate the evolution of baseline and peak values. Two features illustrated by these plots are especially pertinent. First, **summertime ozone peaks have decreased substantially for the months of May to August. This decrease is largest in July and August leading to the shift of the seasonal maximum of daily maxima toward the earlier month of the year**. Secondly, an increase in winter- and springtime mean ozone occurred, which is generally attributed to changes in baseline ozone (both intercontinental transport and stratosphere-troposphere exchange) and also local effects such as the longer lifetime of ozone because of reduced availability of NO (reduced titration).

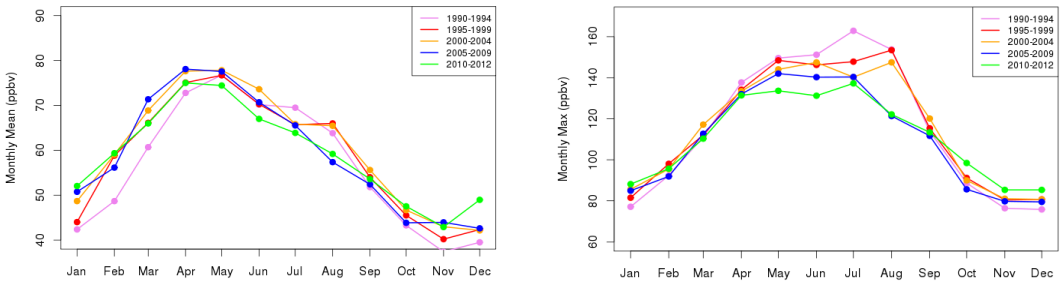

Figure 2.8: *Monthly ozone cycles at EMEP sites with valid data over 1990-2012 for the monthly means (left) and monthly daily maxima (right) by groups of 5 years since 1990 (except for 2010-2012 where the average is over 3 years).*

2.3 Modelled ozone trends

Diagnosing and understanding trends in ozone is complex due to its non-linear dependence on emissions, its regional nature, and its large interannual variability. Analysis of EMEP (and AIRBASE) long-term measurements shows that levels of European regional-scale ozone have been decreasing since at least the early 2000s. Between 2002 and 2012, observations demonstrate that the health exposure metric SOMO35 has decreased by about 30%, and the vegetation exposure metric AOT40 has decreased by 37%. Beyond baseline changes, part of these decreases is related to the substantial reduction in European emissions of ozone precursors NO_x and VOCs since the 1990s. European emission regulations entered into force in the 1990s, and strong decreases in NOx and VOCs emissions and concentrations have been observed since then.

Quantitative attribution of the respective role of baseline and local emission changes can be performed by means of modelling experiments such as illustrated in *Figure 2.9* that presents the EURODELTA 6-model ensemble mean for annual SOMO35. The chemical transport models involved in the ensemble are EMEP-MSCW, Chimere, CMAQ, Lotos-Euros, MINNI, and WRF-Chem (See the Methods details in Section A.4). The model runs were performed using 1990 and 2010 emissions, but the same 2010 meteorology was used to eliminate the effect of meteorological conditions. The relative change in SOMO35 attributed to the 1990 vs. 2010 changes in precursors' emission is of the order of 30%, which would explain most of the observed trend over the period (Section 2.1). However, further analysis is required to validate the model results against observations and also quantify the role of meteorological and emission variability as well as boundary conditions.

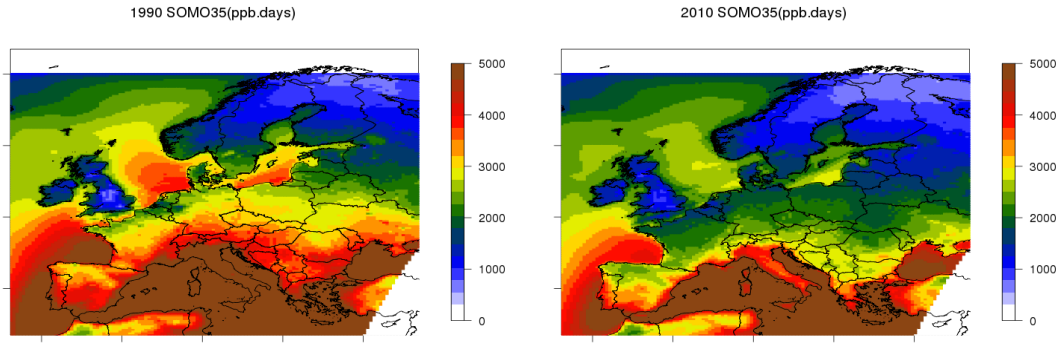

Figure 2.9: *Modelled SOMO35 (ppb day) in the EURODELTA 6-model ensemble using 1990 (left) or 2010 (right) emissions and 2010 meteorological year and boundary conditions.*

3 Sulfur and nitrogen compounds and Particulate Matter

Main authors: Christine F. Braban, Wenche Aas, Augustin Colette, Lindsay Banin, Martin Ferm, Alberto González Ortiz, Marco Pandolfi, Jean-Philippe Putaud, Gerald Spindler

Contributors: Mario Adani, Paul Almodovar, Eva Berton, Bertrand Bessagnet, Gino Briganti, Andrea Cappelletti, Kees Cuvelier, Massimo D'Isidoro, Hilde Fagerli, Clara Funk, Marta Garcia Vivanco, Richard Haeuber, Christoph Hueglin, Scott Jenkins, Jennifer Kerr, Jason Lynch, Astrid Manders, Kathleen Mar, Mihaela Mircea, Maria Teresa Pay, Dominique Pritula, Xavier Querol, Valentin Raffort, Ilze Reiss, Yelva Roustan, Kimber Scavo, Mark Theobald, Svetlana Tsyro, Ron I. Smith, Yuk Sim Tang, Addo van Pul, Sonja Vidic, Peter Wind.

3.1 Overview of sulfur and nitrogen compounds and particulate matter trends

This chapter is organized by key inorganic compounds affecting ecosystems through acidification and eutrophication, as well as health. The past trends of the oxidized forms of sulfur and nitrogen (SO_x and NO_x) are reviewed, as well as the reduced forms of nitrogen (NH_x). For a recent review of the main science and policy issues regarding nitrogen cycle, refer to (Fowler et al., 2015). Furthermore, we also consider the trends in measured total $PM_{2.5}$ (finer than 2.5µm) and PM_{10} (finer than 10µm), the pollutants detrimental to human health, to which inorganic aerosol particulate matter (hereafter PM) fraction contributes with a substantial part.

In common to other sections of this report, the methodology used for the statistical analysis is presented in Annex A. A common dataset was selected by the Chemical Co-ordinating Centre of EMEP (follow-up of earlier analysis published in (Tørseth et al., 2012)), and supplemented by additional analyses provided by State Parties, the European Environment Agency through its European Topic Centre on Air Pollution and Climate Change Mitigation, as well as modelling results of the EURODELTA ensemble of regional chemistry-transport models.

Sulfur and nitrogen compounds in the gas, particulate and precipitations phases, as well as the total particulate matter mass concentration, have overall declined over the EMEP region during the 1990-2012 period, with most of the improvement being achieved in the 1990s. The trends for each of the pollutant categories are summarised in *Figure 3.1*.

The decrease of the deposition of sulfur and nitrogen compounds has led to a significant decrease of acidification (De Wit et al., 2015). **For oxidised sulfur compounds significant negative trends were observed at more than 70% of the sites in the 1990s, and the decline was continuing at more than 50% of the sites over the 2002-2012 period**. For oxidised nitrogen species, the negative trend is slightly lower, but still significant in the 1990s at the majority of sites for atmospheric concentrations (both gaseous and particulate species). However, for oxidised nitrogen in precipitation, the negative trend was only significant at 30 to 35 % of the sites.

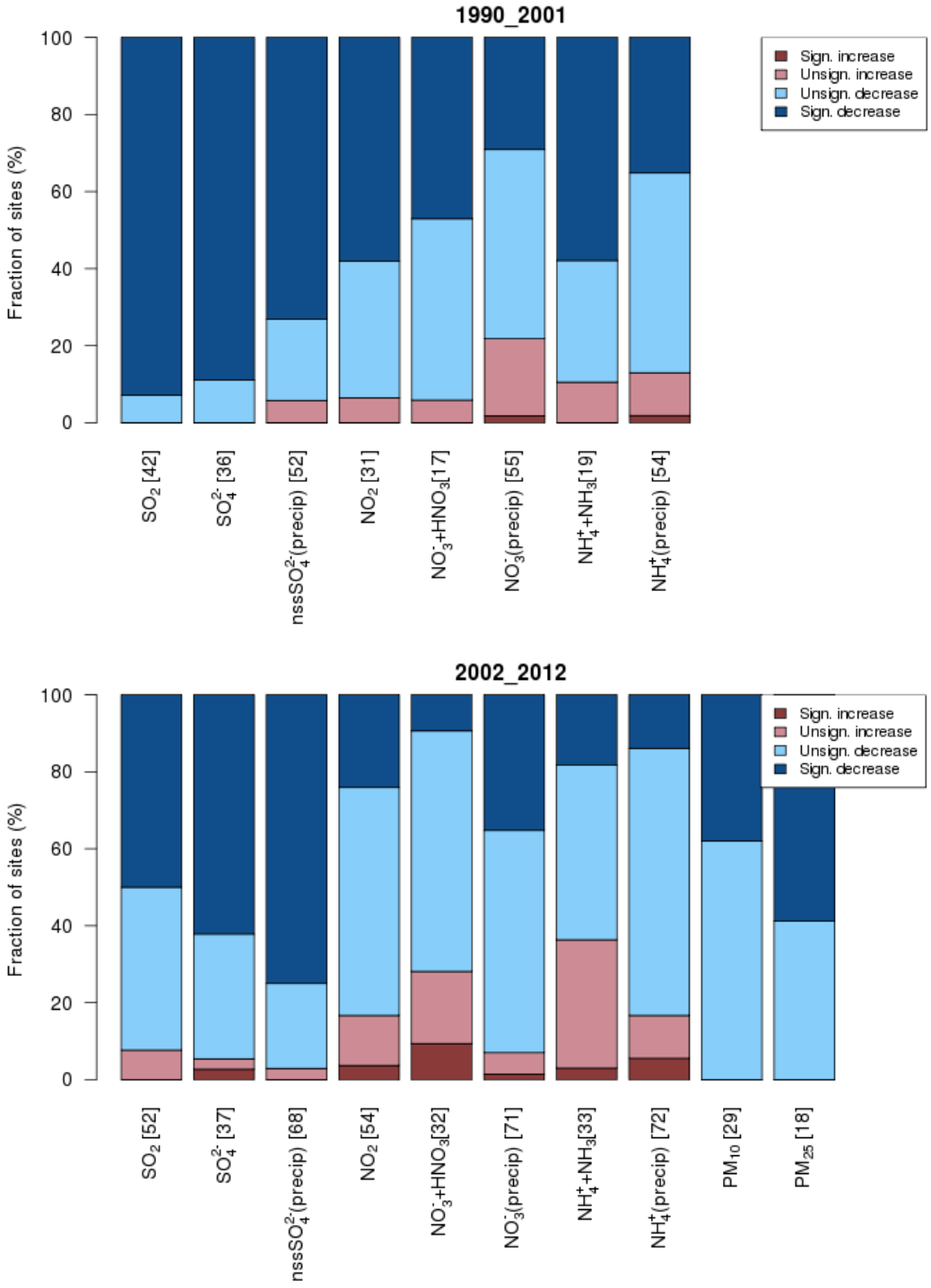

Figure 3.1: *Percentage of EMEP monitoring sites where significant positive trends (dark red), insignificant positive trends (light red), insignificant negative trends (light blue) and significant negative trends (dark blue) were observed in the 1990s (top) and in the 2000s (bottom) for various eutrophying and acidifying compounds: gaseous sulfur dioxide (SO_2), particulate sulfate (SO_4^{2-}), sulfate in precipitations ($nssSO_4^{2-}$ (precip), i.e. sea-salt corrected), gaseous nitrogen dioxide (NO_2), particulate nitrate and gaseous nitric acid ($NO_3^-+HNO_3$), nitrate in precipitations (NO_3^- (precip)), gaseous ammonia and particulate ammonium ($NH_4^+ + NH_3$), and ammonium in precipitation (NH_4^+ (precip)). The same diagnostics are also given for PM_{10} and $PM_{2.5}$ mass over the 2002-2012 time period. The number of sites for each compound is given in brackets.*

For reduced nitrogen in air, there were significant negative trend between 1990 and 2001 at the majority of sites though in the latter period such significant downward trends are only found at 20% of the sites. Similarly, the reduced nitrogen load in precipitation is decreasing at a lower pace in the 2000s compared to the 1990s. The magnitude of exceedances of critical load of nitrogen continues to be high and occurring over a wide European area making the slow rate of the reduction of emissions (and therefore of depositions) of nitrogen compounds of great concern (De Wit et al., 2015). Note that the representativeness of the conclusions is hampered by the limited spatial coverage of the available dataset. Measurement protocols allowing to separate out the gas phase and particulate phase oxidised and reduced nitrogen would be beneficial to document this feature.

The trend in particulate matter mass (both PM_{10} and $PM_{2.5}$) can only be assessed over the 2002-2012 time period, when the network became sufficiently dense. **Overall negative trends are found; they are significant at 40% and 60% of the sites for PM_{10} and $PM_{2.5}$, respectively**.

3.2 Oxidized Sulfur

SO_2 emission reductions started in the 1980s-1990s, therefore changes in concentrations will have occurred earlier than the 1990 start of this assessment. However, concentrations have continued to decrease over the 1990-2012 monitoring period. The timing of concentrations decreases varies between countries according to national implementation of emission reduction strategies, but on average over the EMEP network (Figure 3.2), the decrease was larger in the early 1990s and levelled off since then. The quantitative trend assessment is based on Sen-Theil slopes, using an estimate for the beginning of the period to derive a relative change, and their significance is assessed with a Mann-Kendall test and a p-value of 0.05 (see the details in the Methods Section in Annex A). All 31 sites passing completion criteria for the 1990-2012 time period show a significantly negative trend in SO_2 air concentrations at an median rate (over the network) of -0.066 µgS m^{-3} yr^{-1} (confidence interval for 95% of the sites of [-0.13, -0.055] µgS m^{-3} yr^{-1}), that is a **median change for SO_2 of -92% ([-97,-86]) since 1990** (Table 3.1). However, when the data are considered for the two time periods 1990-2001 and 2002-2012, the annual slopes are -0.13 and -0.027 µg S m^{-3} yr^{-1} respectively, reflecting an 80% decrease in the first followed by a much slower 48% decrease in the second period. This exponential shape of the decrease has been pointed out previously in both national and international assessments (Fowler et al., 2005;Fowler et al., 2007).

As it is shown in *Figure 3.2*, **the relative change of particulate sulfate (SO_4^{2-}) air concentration and sulfate in precipitation is important, yet smaller than that of its main precursor gas SO_2 (-65% and -73%, respectively vs. -92% for SO_2 in 2012 compared to 1990).** While the consistency is acceptable over the 2002-2012 period (relative change of -39%, -48% and -48% for particulate sulfate, sulfate in precipitation and SO_2), it is over the 1990-2001 time period that the evolution differs substantially: -52%, -49%, and -80% respectively. This

feature has been analysed by means of numerical modelling (Banzhaf et al., 2015). This study shows that the reduced acidity of clouds initiated by SO_2 emission reduction favours sulfate formation, and therefore acts as a positive feedback to further enhance this SO_2 sink. This mechanism contributes to the non-linear evolution of SO_2 concentration, and to the incremental efficiency of particulate sulfate formation resulting from a given change in SO_2 emissions.

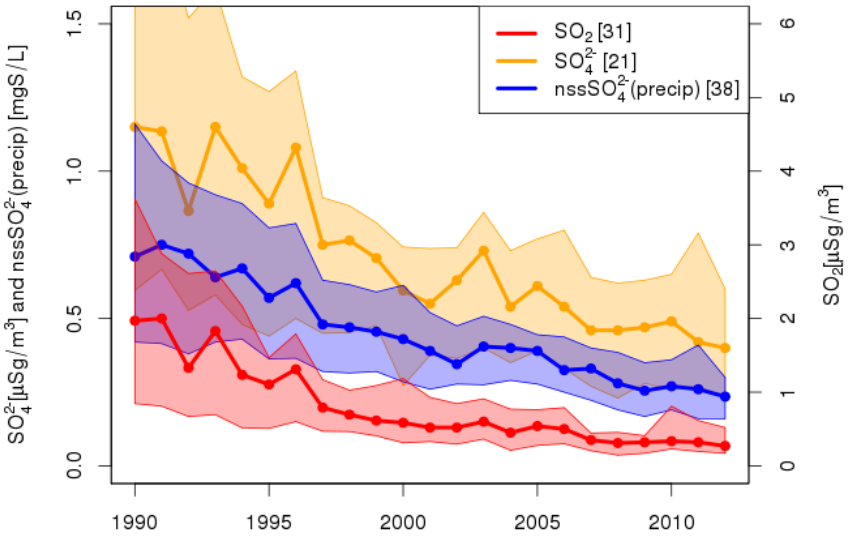

***Figure 3.2**: Median time series across the EMEP network and 25th and 75th quantiles over 1990-2012 for annual mean concentrations of gaseous sulfur dioxide (SO_2), particulate sulfate (SO_4^{2-}), and sulfate concentration in precipitation excluding sea-salt ($nssSO_4^{2-}$(precip)). The number of stations contributing to the median differ but, over time, a consistent set passing completion criteria is used for each compound.*

***Table 3.1:** Trend statistics for oxidized sulfur monitored in the EMEP network: gaseous sulfur dioxide (SO_2), particulate sulfate (SO_4^{2-}), and sulfate concentration in precipitation excluding sea-salt (nss SO_4^{2-}). For three periods (1990-2001, 2002-2012, and 1990-2012), the following is shown: the number of stations, the median and 95% confidence interval over the network for the annual trend (in µgS m^{-3} yr^{-1} for air concentration and mgS L^{-1} yr^{-1} for precipitation chemistry) and the relative change over the relevant time period (in %).*

Compound	Time period	Number of stations	Median annual trend in, [unit/yr] and 95% CI	Median relative change over the period [%] and 95% CI
SO_2	1990_2001	42	-0.13[-0.27,-0.12]	-80[-82,-72]
	2002_2012	52	-0.027[-0.054,-0.028]	-48[-53,-38]
	1990_2012	31	-0.066[-0.13,-0.055]	-92[-97,-86]
SO_4^{2-}	1990_2001	36	-0.050[-0.072,-0.044]	-52[-56,-46]
	2002_2012	37	-0.024[-0.035,-0.019]	-39[-42,-27]
	1990_2012	21	-0.029[-0.043,-0.023]	-65[-69,-56]
$nssSO_4^{2-}$	1990_2001	52	-0.029[-0.044,-0.027]	-49[-50,-37]
	2002_2012	68	-0.019[-0.035,-0.015]	-48[-49,-39]
	1990_2012	38	-0.026[-0.029,-0.019]	-73[-73,-65]

The maps provided in Figure 3.3 show that the spatial variability of the changes in oxidized sulfur compounds over the 1990-2012 time period is not very large, except for slightly larger decreases over central Europe compared to Nordic countries.

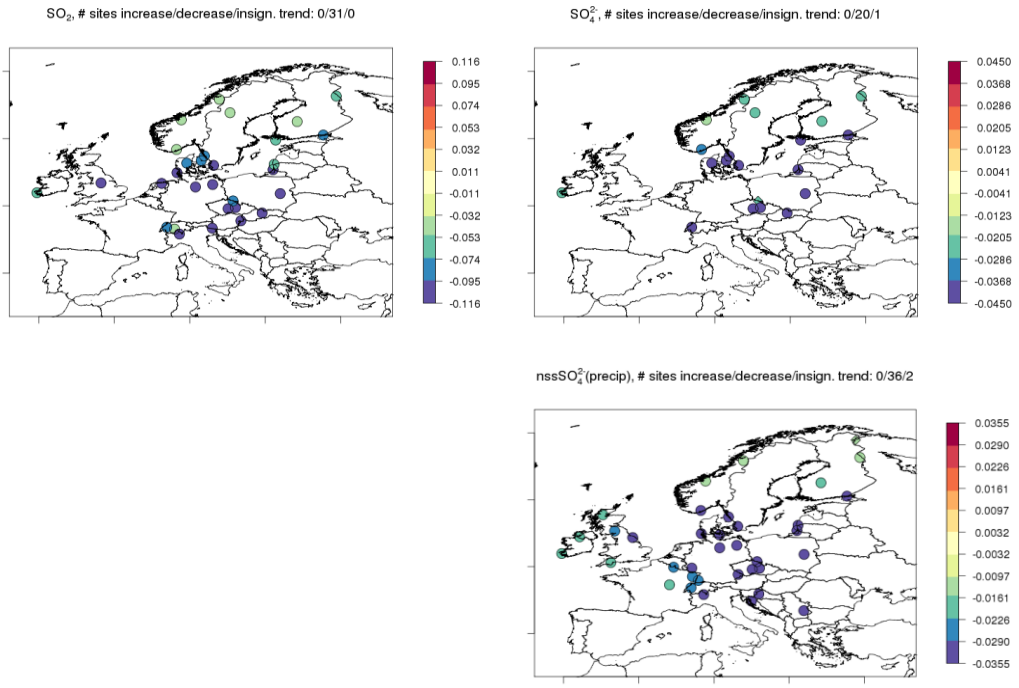

Figure 3.3: *Maps of annual trends at EMEP sites over the 1990-2012 time period for gaseous sulfur dioxide (top left), particulate sulfate (top right) (in µgS m^{-3} yr^{-1}) and sea-salt corrected sulfate concentration in precipitation (in mgS L^{-1} yr^{-1}) (bottom right). Stations where the trend is significant at the 0.05 level are displayed with a circle, elsewhere a diamond is used.*

3.3 Oxidized Nitrogen

The measurements of NO_2 show that for the period 1990-2001 the fraction of sites where significant negative trends were observed was high (58%) but it slowed down and between 2002 and 2012 only 24% of the sites had a significant negative trend. A comparison of NO_2 and NO trends was not attempted here, but it should be noted that in countries where the contribution to NOx emissions due to diesel motorisation increased, the downward NO_2 trend is less evident at traffic sites compared to EMEP sites (Querol et al., 2014). Over the first part of the period (1990s), the median change in NO_2 concentration reached -28% (95% confidence interval: [-34,-19]) while the change in the 2000s was limited to -17% ([-20,18]) still the average evolution over the full 1990-2012 is substantial with -41% ([-47,-16]).

Due to the impossibility in separating gas and particle phase for the inorganic nitrogen compounds using the EMEP recommended filter pack method, the sum of gas phase nitric acid (HNO_3) and particulate nitrate (NO_3^-(p)) has been assessed for trends. Some sites report the individual compound, as also recommended in the EMEP programme, but very few for the whole period. Larger changes in the 1990s (24% median reduction) are found than in the 2000s (7.1% median reduction), to the extent that **significantly negative trends for nitric acid and**

particulate nitrate are only found at 9% of the sites over the 2002-2012 period compared to 47% for the 1990-2001 period. Part of this difference can be directly related to the larger changes observed for NO_2 in the 1990s. But the reduction of sulfur emissions also contributed to decrease particulate ammonium sulfate concentrations, leaving more ammonia available to form the semi-volatile particulate ammonium nitrate, which would contribute to slowing down the negative trends in particulate nitrate observed here.

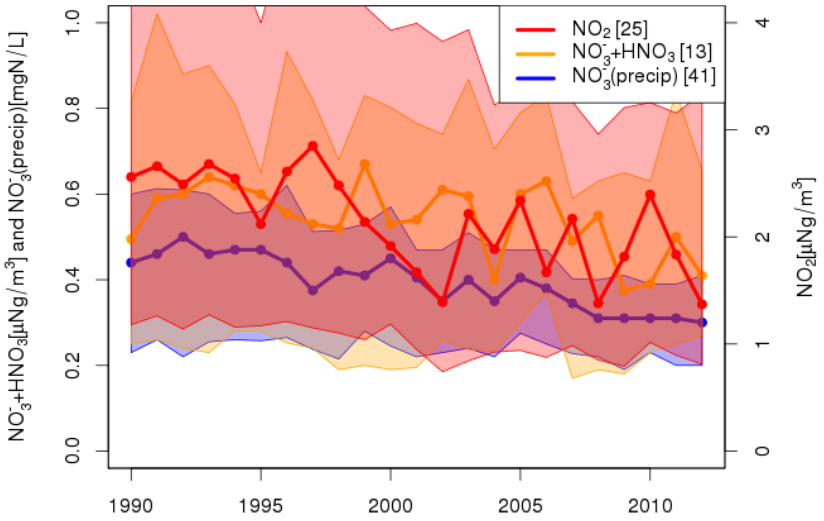

Figure 3.4: *Median time series across the EMEP network and 25th and 75th quantiles over 1990-2012 for annual mean concentrations of gaseous nitrogen dioxide (NO_2), particulate nitrate cumulated with gaseous nitric acid ($NO_3^-+HNO_3$), and nitrate concentration in precipitation (NO_3^- (precip)). The number of stations contributing to the median differs but, over time, a consistent set passing completion criteria is used for each compound.*

Table 3.2: *Trend statistics for oxidized nitrogen monitored in the EMEP network: gaseous nitrogen dioxide (NO_2), particulate nitrate cumulated with gaseous nitric acid ($NO_3^-+HNO_3$), and nitrate concentration in precipitation (NO_3^-precip). For three time periods (1990-2001, 2002-2012, and 1990-2012), the following is shown: the number of stations, the median and 95% confidence interval over the network for the annual trend (in µgN m^{-3} yr^{-1} for air concentration and mgN L^{-1} yr^{-1} for precipitation chemistry) and the relative change over the relevant time period (in %).*

Compound	Time period	Number of stations	Median annual trend in, [unit/yr] and 95% CI	Median relative change over the period [%] and 95% CI
NO_2	1990_2001	31	-0.048[-0.11,-0.043]	-28[-34,-19]
	2002_2012	54	-0.029[-0.051,-0.012]	-17[-20,18]
	1990_2012	25	-0.041[-0.077,-0.031]	-41[-47,-16]
$NO_3^-+HNO_3$	1990_2001	17	-0.0071[-0.024,-0.0053]	-24[-39,-9.8]
	2002_2012	32	-0.0028[-0.0071,0.0042]	-7.1[-12,18]
	1990_2012	13	-0.0044[-0.012,-0.0027]	-22[-34,-4.2]
NO_3^-(precip)	1990_2001	55	-0.0050[-0.0096,-0.0025]	-19[-19,-2.6]
	2002_2012	71	-0.0083[-0.011,-0.0058]	-23[-26,-14]
	1990_2012	41	-0.0075[-0.0083,-0.0053]	-33[-35,-24]

The spatial variability of oxidised nitrogen changes is not very important (*Figure 3.5*), with slightly larger trends for NO_2 over Western Europe, while the nitrate load in precipitation decreased substantially more over Central Europe. For all compounds, it is over the Nordic countries that the trend is less pronounced.

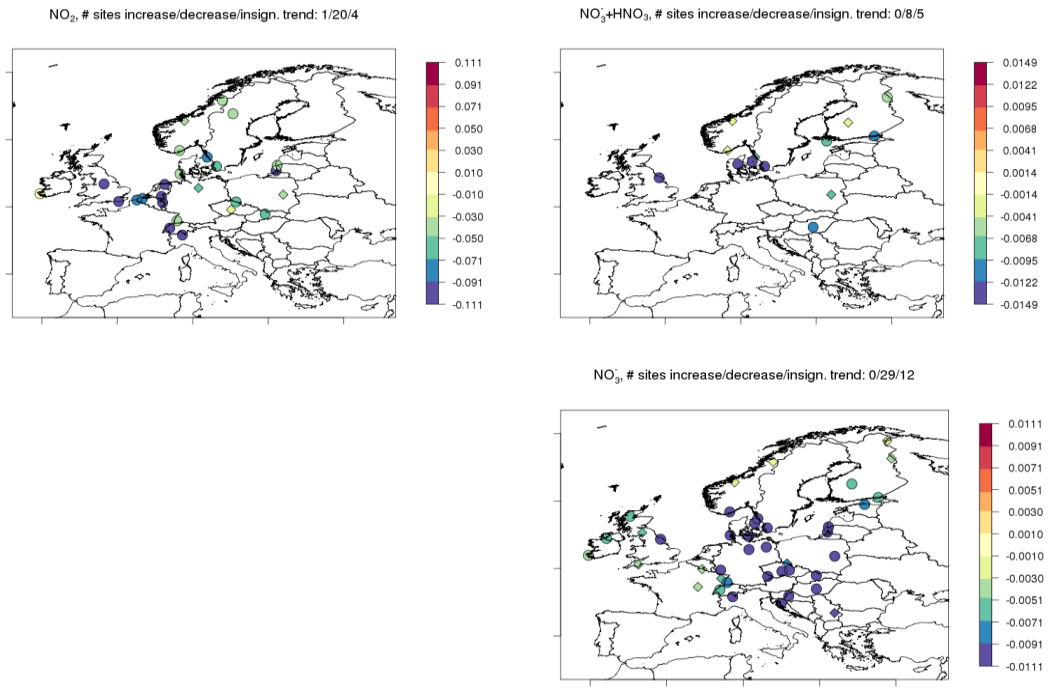

Figure 3.5: *Maps of annual trends at EMEP sites over the 1990-2012 time period for gaseous nitrogen dioxide (top left), particulate nitrate cumulated with gaseous nitric acid (top right) (in µgN m^{-3} yr^{-1}) and nitrate concentration in precipitation (in mgN L^{-1} yr^{-1}) (bottom right). Stations where the trend is significant at the 0.05 level are displayed with a circle, elsewhere a diamond is used.*

3.4 Reduced Nitrogen

As with oxidized N, the reduced N atmospheric components (ammonia gas: NH_3, and particulate phase: NH_4^+) are summed together for the EMEP reporting. The average trend is shown in *Figure 3.6* and is not decreasing as much as the sulfur and oxidized nitrogen compounds. **The change of reduced nitrogen in the air relative to the beginning of the time period reaches -40 % ([-47,-19]) in the 1990s**, with the majority of sites exhibiting a significantly negative trend. In contrast, **such decreases are much more limited in the 2000s**, the median of trends across the EMEP network is close to zero, and increases are found at several sites as shown by the positive upper bound of the confidence interval.

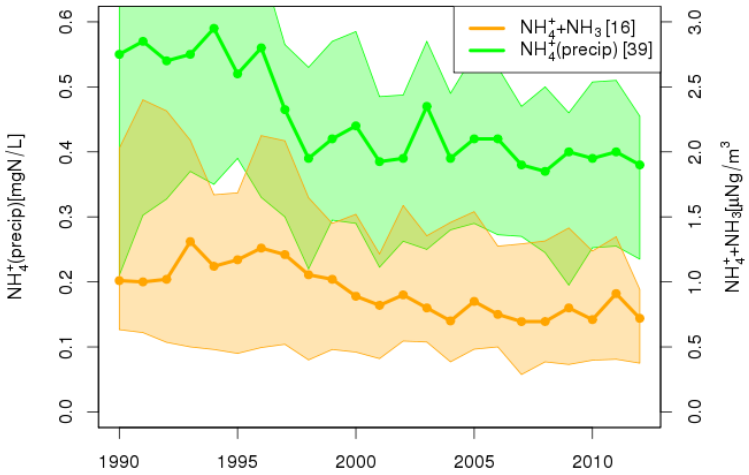

Figure 3.6: *Median time series across the EMEP network and 25th and 75th quantiles over 1990-2012 for annual mean concentrations of particulate ammonium cumulated with gaseous ammonia ($NH_3+NH_4^+$), and ammonium concentration in precipitation (NH_4^+(precip)). The number of stations contributing to the median differs but, over time, a consistent set passing completion criteria is used for each compound.*

Reduced nitrogen concentrations in precipitation follow a similar trend, with a relative change of - 30% ([-34,-11]) and -16% ([-17,16]) over the 1990-2001 and 2002-2012 period, respectively.

Table 3.3: *Trend statistics for reduced nitrogen monitored in the EMEP network: particulate ammonium cumulated with gaseous ammonia ($NH_3+NH_4^+$), and ammonium concentration in precipitation (NH_4^+(precip)). For three time periods (1990-2001, 2002-2012, and 1990-2012), the following is shown: the number of stations, the median and 95% confidence interval over the network for the annual trend (in µgN/m3/yr for air concentration and mgN/L/yr for precipitation chemistry) and the relative change over the relevant time period (in %).*

Compound	Time period	Number of stations	Median annual trend in, [unit/yr] and 95% CI	Median relative change over the period [%] and 95% CI
$NH_3+NH_4^+$	1990_2001	19	-0.029[-0.11,-0.03]	-40[-47,-19]
	2002_2012	33	-0.010[-0.026,0.014]	-14[-15,23]
	1990_2012	16	-0.024[-0.054,-0.014]	-50[-59,-14]
NH_4^+(precip)	1990_2001	54	-0.012[-0.024,-0.011]	-30[-34,-11]
	2002_2012	72	-0.0066[-0.0086,-0.0026]	-16[-17,16]
	1990_2012	39	-0.0069[-0.012,-0.0055]	-29[-36,-15]

The annual trend for the whole period (1990-2012) at each EMEP station are displayed on the maps of *Figure 3.7*. They show that the largest downward trends of reduced nitrogen were observed over Central Europe, with slower evolution over the United Kingdom and Nordic countries.

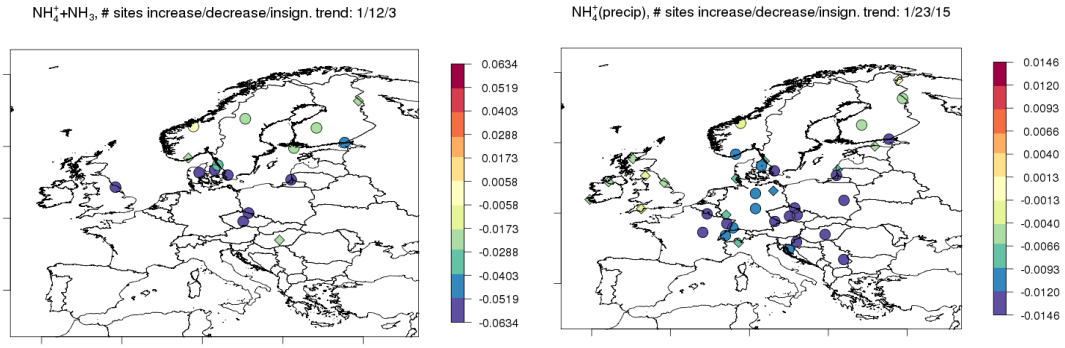

Figure 3.7: *Maps of annual trends at EMEP sites over the 1990-2012 time period for particulate ammonium cumulated with gaseous ammonia (left), and ammonium concentration in precipitation (in mgN L^{-1} yr^{-1}) (right). Stations where the trend is significant at the 0.05 level are displayed with a circle, elsewhere a diamond is used.*

The dominant source of NH_3 emissions is agriculture, and it should be noted that unlike NOx and SO_x emissions, only a small decrease in NH_3 emissions was recorded in Europe after the beginning of the 1990s, with only few countries decreasing their emissions significantly in the past decade (see the emission trend analysis in Annex C. As noted above, the decrease of sulfur emissions has caused the PM composition to shift from stable ammonium sulfate towards the semi-volatile ammonium nitrate. Thus, as SO_2 emissions decrease the correspondingly lower levels of SO_4^{2-} (oxidised from SO_2) do not balance NH_4^+, shifting the chemical equilibrium to favouring formation of NH_4NO_3 (Martin, 2000), leading to change longer atmospheric lifetime of gas phase NH_3. Finally, potentially warmer conditions favouring volatilisation of ammonium nitrate also lead to increased residence time of NH_3 and HNO_3. It is noted however that the inter-annual variability of meteorology, land use and emissions, and the relatively short measurement time series, do not facilitate simple causal connections to be made.

The currently used EMEP recommended measurement method (filter pack measurements) does not allow the separation of NH_3 and NH_4^+. From these considerations, any negative trends in particulate NH_4^+ are likely to be masked by the changes in NH_3 concentrations. However, the separate NH_3 and NH_4^+ are measured for some sites and reported allowing some comments to be made. Two examples are provided in *Figure 3.8*: (i) at the Swedish sites of Rörvik/Råö where the filter pack measurement indicate insignificant trends of NH_3 concurrent with decreases of NH_4^+ comparable to those of SO_4^{2-} for the whole period, and (ii) at sites over the UK with no trend in NH_3 concentrations in the average of 75 sites, and decreases of NH_4^+ in $PM_{2.5}$ over the period 1999-2012.

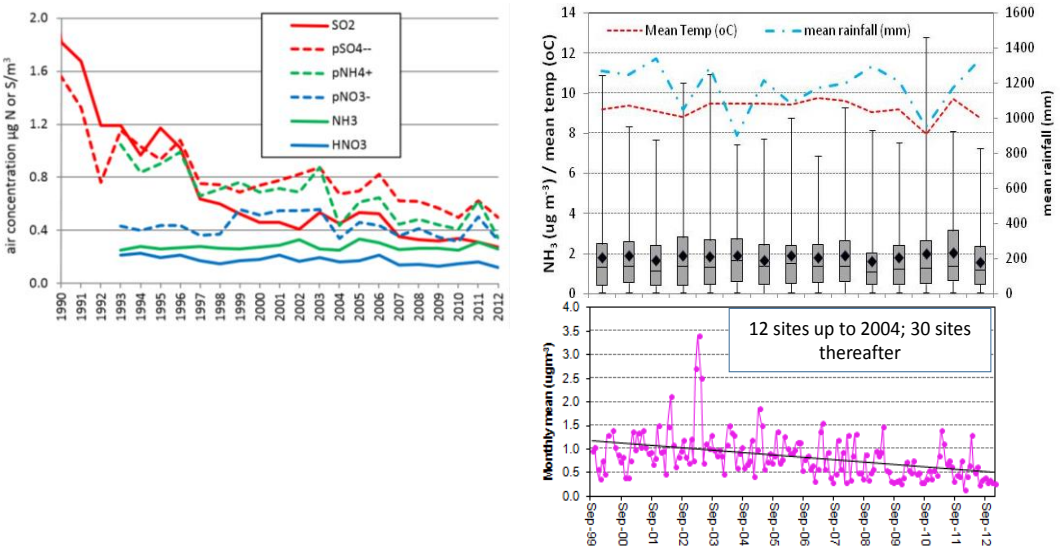

Figure 3.8: *Left: Variation of HNO_3, SO_2, NH_3 and particulate nitrate, sulfate and ammonium at closely located Swedish sites Rörvik (up to 2001)/Råö (2001-present); Right: UK National Ammonia Monitoring Network[6] (NAMN) annual mean NH_3 for 75 sites (1998-2012; sites with short data runs excluded) and meteorological data; Lower panel: UK NAMN NH_4^+ monthly mean in $PM_{2.5}$ (2000-2014).*

3.5 Wet deposition trends in North America

Figure 3.9 shows the United States–Canada spatial patterns of observed wet sulfate (sea salt–corrected) deposition for 1990, 2000 and 2012. Deposition contours are not shown in western and northern Canada, because Canadian experts judged that the locations of the contour lines were unacceptably uncertain due to the paucity of measurement sites in all of the western provinces and northern territories. To compensate for the lack of contours, wet deposition values in western Canada are shown as coloured circles at the locations of the federal/ provincial/ territorial measurement sites.

Wet sulfate deposition is consistently highest in eastern North America around the lower Great Lakes, with a gradient following a southwest to northeast axis running from the confluence of the Mississippi and Ohio rivers through the lower Great Lakes. The patterns for 1990, 2000 and 2012 illustrate that wet sulfate deposition in both the eastern United States and eastern Canada have decreased in response to decreasing SO_2 emissions. The wet sulfate deposition reductions are considered to be directly related to decreases in SO_2 emissions in both the United States and Canada.

The patterns of wet nitrate deposition show a similar southwest-to-northeast axis, but the area of highest nitrate deposition is slightly north of the region with the highest sulfate deposition. Major reductions in wet nitrate deposition occurred in the period between 2000 and 2012, when large NO_x emission reductions occurred in the United States and, to a lesser degree, Canada.

[6] http://uk-air.defra.gov.uk/networks/network-info?view=nh3

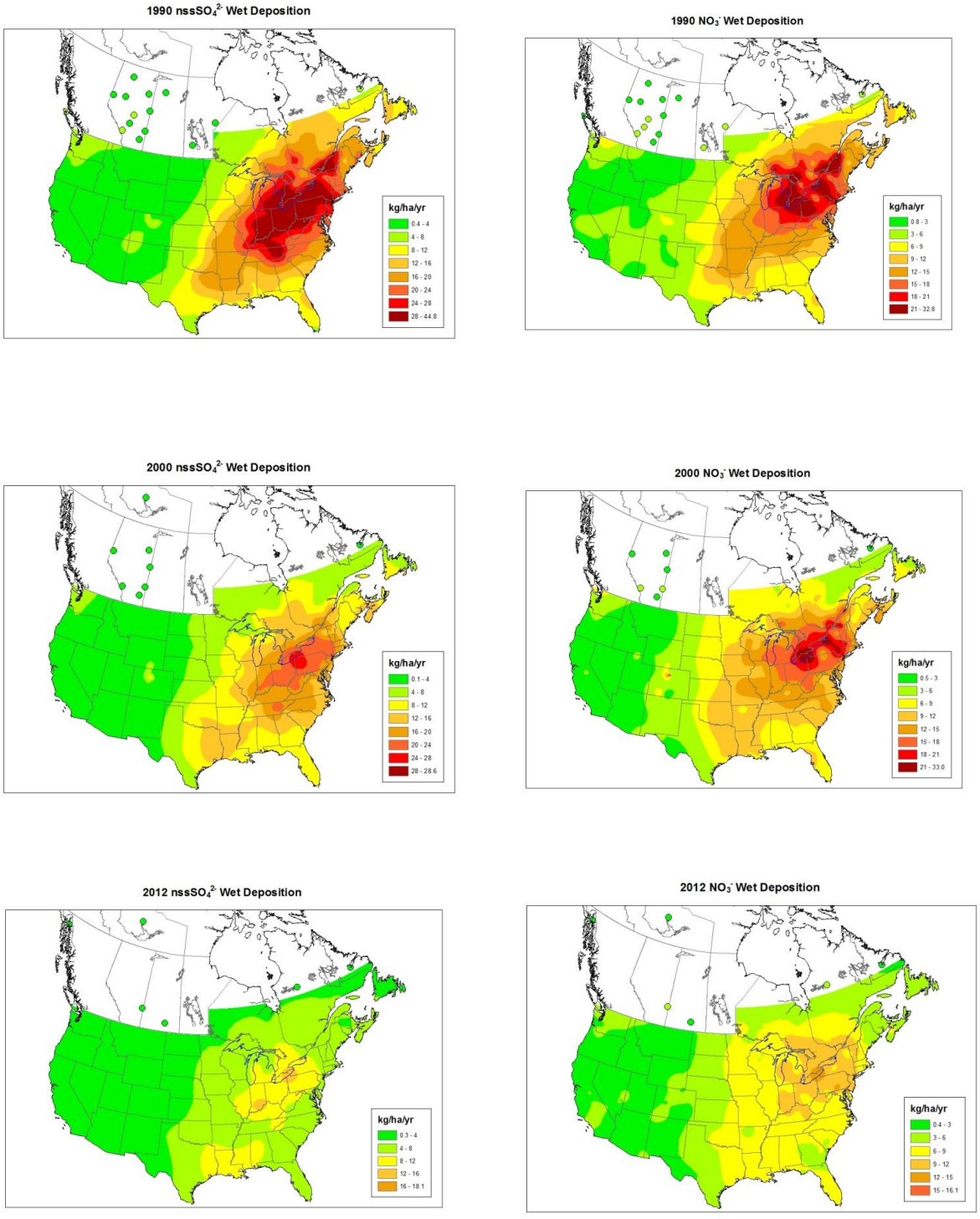

Figure 3.9: *1990-2012 Annual wet sulphate and wet nitrate deposition in North America (Source: National Atmospheric Chemistry Database (NAtChem) Database (www.ec.gc.ca/natchem) and National Atmospheric Deposition Program (nadp.isws.illinois.edu), 2016)*

3.6 Particulate matter

3.6.1 PM_{10} and $PM_{2.5}$ mass

Measurements from 29 and 18 sites were used for PM_{10} and $PM_{2.5}$ respectively for the assessment. In both cases, only data for the 2002-2012 time period could be used because of the low coverage before then. **Significant negative trends were found at 38% and 55% of the sites, with a relative change over the decade of -29% ([-29,-19]) and - 31% ([-35,-25]) for PM_{10} and $PM_{2.5}$, respectively**.

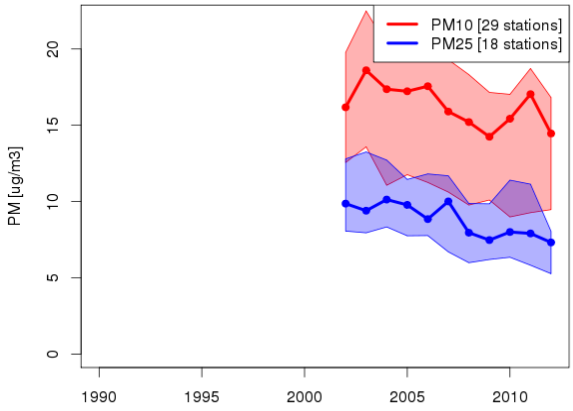

Figure 3.10: *Median time series across the EMEP network and 25th and 75th quantiles over 2002-2012 for annual mean concentrations of PM_{10} and $PM_{2.5}$. The number of stations contributing to the median differs but, over time, a consistent set passing completion criteria is used for each compound.*

Table 3.4: *Trend statistics for particulate matter mass (PM_{10} and $PM_{2.5}$). For the time period 2002-2012 the following is shown: the number of stations, the median and 95% confidence interval over the network for the annual trend (in µg/m³/yr) and the relative change over the relevant time period (in %).*

Compound	Time period	Number of stations	Median annual trend in, [unit/yr] and 95% CI	Median relative change over the period [%] and 95% CI
PM_{10}	2002-2012	29	-0.35[-0.54,-0.32]	-29[-29,-19]
$PM_{2.5}$	2002-2012	18	-0.29[-0.5,-0.23]	-31[-35,-25]

As far as PM_{10} is concerned, the analysis at EMEP sites can be supplemented by the denser European Air Quality data base (AIRBASE), collected and maintained by EEA. This database also covers urban areas and, apart from background stations, it also consists of sites close to traffic and industrial sources. The distribution of annual mean trends by location and site typology is given in Figure 3.11. It shows that larger downward trends were observed close to the sources (traffic and industrial sites) compared with urban, suburban and rural background sites.

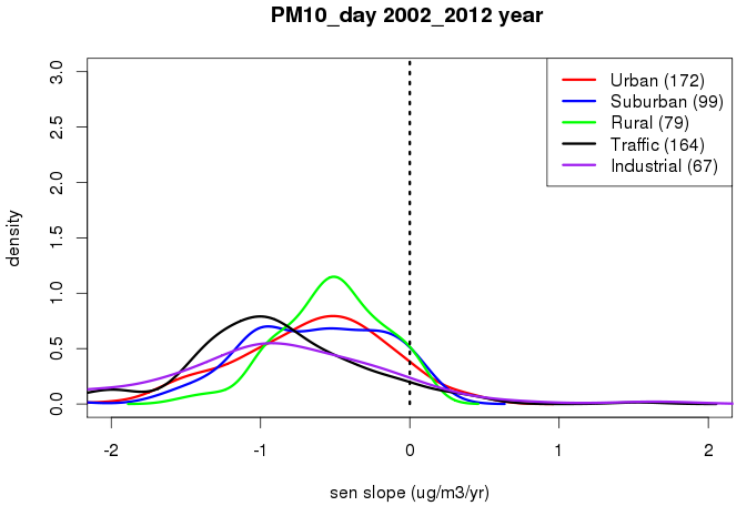

Figure 3.11: *Probability density function of PM_{10} trends (µg $m^{-3}yr^{-1}$) for the 2002-2012 period by location and site typology. The number in brackets shows the number of sites in the distribution, (Colette et al., 2015).*

By season, the decrease is larger in summer for all background stations (urban, suburban and rural) compared with winter (see *Figure 3.12*, upper panel as an example of rural background). This feature could be induced by (i) changes in meteorological conditions by season or (ii) different trends for the various sources contributing to the PM mix (for instance: a compensation of the decrease in fossil fuel combustion related emissions by an increase of biomass use for residential heating in the recent past). This second argument is supported by the fact that such differences in the trend statistics are even found at traffic sites (also partly influenced by residential emissions) but not at industrial sites (see *Figure 3.12*, lower panel).

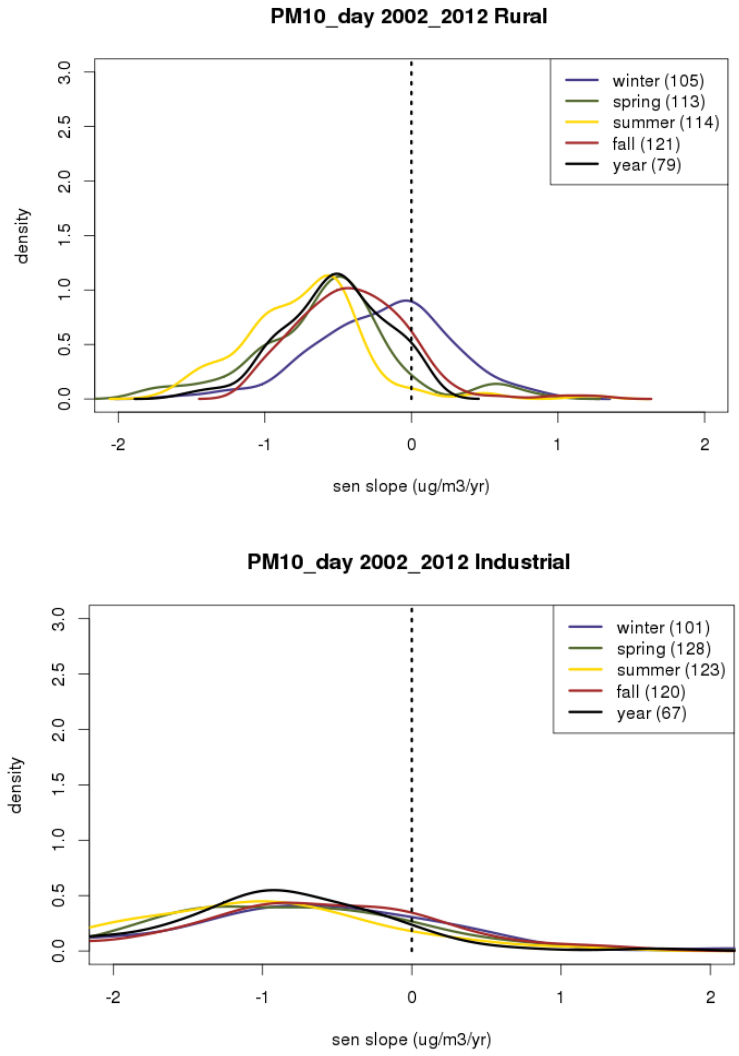

Figure 3.12: *Distribution of PM_{10} trends over the 2002-2012 period for the four seasons and the annual trends in rural background stations (upper panel) and industrial sites (lower panel). The number in brackets shows the number of sites in the distributions.*

The particulate matter trends over the European part of the EMEP region can be put in perspective with the $PM_{2.5}$ trends over North American. In the United States and Canada, ambient concentrations of $PM_{2.5}$ have diminished significantly. More specifically, between 2000 and 2012 the national U.S. average annual and 24-hour concentrations of $PM_{2.5}$ decreased by 33% and 37%, respectively. In Canada, the national averages of the annual and the 24-hour concentrations of $PM_{2.5}$ decreased by 4% and 6.5%, respectively over this same period. However, between 2003 and 2012, the percentage of Canadians living in communities where ambient concentrations of $PM_{2.5}$ exceeded the 2015 Canadian Ambient Air Quality Standards (CAAQS[7]) for $PM_{2.5}$ dropped from approximately 40% to 11%. In 2012, ambient concentrations reported at most monitoring sites in the United

[7] The Canadian Ambient Air Quality Standards (CAAQS) for $PM_{2.5}$ include annual levels of 10 µg/m3 in 2015 and 8.8 µg/m3 in 2020; and 24-hour levels of 28 µg/m3 in 2015 and 27 µg/m3 in 2020. Additional information on the CAAQS can be found at http://www.ec.gc.ca/default.asp?lang=En&n=56D4043B-1&news=A4B2C28A-2DFB-4BF4-8777-ADF29B4360BD

States along the Canadian border met the U.S. annual and 24-hour National Ambient Air Quality Standards for $PM_{2.5}$ set in 2012[8]. In Canada, data from the filter-based monitoring network indicate that average annual concentrations (2008–2010) met the 2015 CAAQS.

3.6.2 Particulate matter composition

Analysis of trends in PM composition can allow further understanding of the main driving factors and contributing sources. Whereas such analysis could be performed at more individual EMEP sites, only two case studies are presented here for illustration purposes.

The first case study has been performed for Melpitz, Germany, where compositional analysis provides further useful information as to what is driving the total PM trends (*Figure 3.13*). The measurements in Melpitz are representative for a large area that is typical for East and North-East Germany where the influence of week-day activities (traffic, production, agriculture) can be felt. PM_{10} mass concentration decreased in 1993-1999 for all seasons (with a higher relative decrease in winter) and remained approximately constant for the last 15 years, at about 22 µg m^{-3} (± 13%). Particulate sulfate concentration also decreased noticeably until the end of century, but much more moderately afterwards. Particulate nitrate remained more constant.

The origin of air masses can be tracked using 96-hour back trajectories and clustered by season (Spindler et al., 2012;Spindler et al., 2013). The highest elemental carbon (EC) concentrations were found for winter-easterly air masses. The trends for the mean concentrations of total carbon (TC) in PM_{10}, sum of elemental and organic carbon (EC+OC), in summers (May-October) and winters (November-April) differs for air-mass inflows from the West or the East. The mean concentration shows a negative trend for the three cases “Summer East”, “Winter West”, “Summer West” and remains more constant for the air mass inflow “Winter East”. This is attributed to the long-range transport of emissions from combustion processes, especially individual coal fired ovens.

[8] The health-based U.S. National Ambient Air Quality Standards (NAAQS) for $PM_{2.5}$ are an annual standard with a level of 12 µg/m3 and a 24-hour with a level of 35 µg/m3. Additional information on these standards can be found at https://www3.epa.gov/ttn/naaqs/standards/pm/s_pm_history.html.

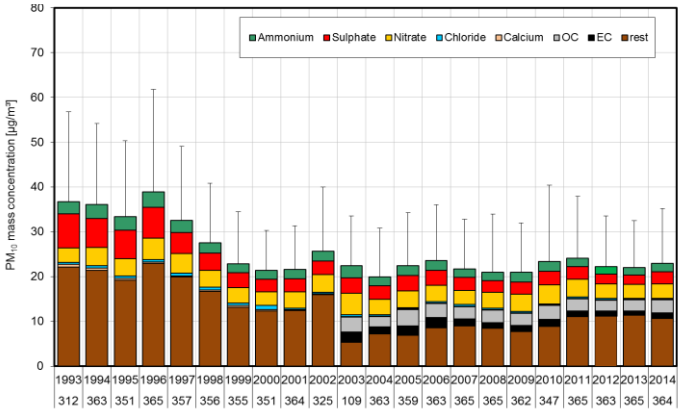

Figure 3.13: *Yearly means of particulate composition at Melpitz, Germany, within the years also the numbers of days for the yearly mean are given in the abscissa*

The second case study regards Montseny, Spain, located approximately 35km away from the Barcelona Metropolitan Area and representative of the typical regional background conditions in the Western Mediterranean Basin. To explore the effectiveness of the emission abatement strategies, the trend analysis of source contributions to ambient PM concentrations can be a useful tool. Source contributions are often obtained from receptor models such as the Positive Matrix Factorization (PMF; e.g. (Paatero and Tapper, 1994)) if chemically speciated particulate data are available. The Montseny station have provided such chemically speciated data for $PM_{2.5}$ since 2002.

Following the procedure described by (Querol et al., 2009), up to 60 different chemical species were determined from 24h quartz fiber filter analysis at this station. The annual data coverage from filters was around 30%. PMF analysis assigned 8 sources contributing to the $PM_{2.5}$ mass at regional background level in the Western Mediterranean Basin during 2002 – 2012. Secondary aerosol sources such as ammonium sulfate ($(NH_4)_2SO_4$) and ammonium nitrate (NH_4NO_3) contributed on average 3.7 µg/m^3 (30%) and 1.2 µg/m^3 (10%), respectively, for the whole study period. Particulate organic matter source peaked in summer indicating mainly a biogenic origin but also including other secondary organics and contributed to 2.9 µg/m^3 (23%) of total $PM_{2.5}$. Smaller components at this station include: primary emissions from heavy oil combustion sources (traced mainly by V, Ni and SO_4^{2-}), which contributed 1.5 µg/m^3 (12%) from industries and shipping; industrial source (traced mainly by Pb, Cd, As, and Cr), which contributed 0.8 µg/m^3 (7%); aged marine source (traced by Na and Cl mainly but also enriched in nitrates) contributing 0.3 µg/m^3 (2 %), mineral source (traced by typical crustal elements such as Al, Ca, Ti, Rb, Sr of both natural and anthropogenic origin (i.e. cement and concrete production)) contributing 1.0 µg/m^3 (8%), and other combustion-related PM (traced by EC and K mainly) including road traffic and biomass burning and contributing 0.9 µg/m^3 (7%).
The evolution of $PM_{2.5}$ composition and sources at Montseny is diagnosed using the exponential decay model used in Chapter 4 and described in the Methods section of Annex B to compute the total reduction (TR; %) and average reduction per year (%) during the period 2002-2012 shown in Figure 3.14. The largest

statistically significant decline (68%) over the period is found for the industrial source that explained around 70%, 60% and 50% of the measured concentrations of Pb, Cd and As, respectively (which showed TR of about 65%, 75% and 60%, respectively, significant at the 0.05, 0.01 and 0.001 confidence level). NH_4NO_3 and $(NH_4)_2SO_4$ sources also exhibit statistically significant sharp declines. The $(NH_4)_2SO_4$ source explained around 65% of the measured concentrations of SO_4^{2-}, which showed a TR of 45% significant at the 0.05 confidence level. The $(NH_4)_2SO_4$ source contribution showed TR and average reduction per year of 51% and 7%, respectively. The NH_4NO_3 source explained around 90% of the measured concentrations of NO_3^- which showed TR of 50% significant at 0.05 confidence level. NH_4NO_3 source contribution showed TR and average reduction per year of 53% and 7%, respectively. The combustion source was only ranking fourth in the total magnitude of decline (not statistically significant) over the 2002-2012 period. The decreasing trends (not statistically significant) of fine mineral and organics source contributions were likely driven by the anthropogenic contributions to these sources. The reduction in the aged marine source was not statistically significant and likely due to the enrichment in nitrates.

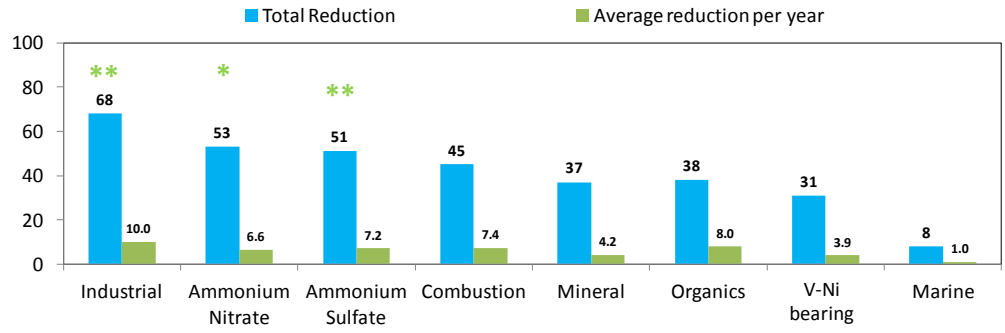

Figure 3.14: *Total reduction and average reduction per year (in %) of PM mass from the 8 sources, detected from PMF analysis, explaining the gravimetric PM2.5 mass measured in the period 2002 – 2012 at Montseny station (Spain). Green symbols highlight the statistically significance of the trends following the Mann-Kendall test: *** (p-value < 0.001), ** (p-value < 0.01), * (p-value < 0.05). No star means no statistically significant trend at p<0.05 confidence level over the considered period.*

3.7 Modelled particulate matter trends

The observed trends in sulfur and nitrogen compounds can be compared with the modelled change between 1990 and 2010. *Figure 3.15* presents the results of the EURODELTA ensemble of six regional chemistry-transport models (EMEP-MSCW, Chimere, CMAQ, Lotos-Euros, MINNI, and WRF-Chem) using respectively 1990 and 2010 emissions, but the same meteorological year and boundary conditions (2010), see details in Annex A.

The modelled change of about 60% in particulate sulfate is well in line with the observed average reduction of 65%. For particulate nitrate, the modelled change is more variable in space but in the range of 20 to 30% reduction, which is again consistent with the observed 20% reduction. Increases appear clearly over ship tracks and oil rigs, where large SO_x emission abatement occurred, favouring the formation of ammonium nitrate instead of ammonium sulfate. Note that although

shipping has become cleaner due to SO_x emission abatement, the total shipping activity has increased resulting in more NO_x emissions, which could also play a role in the increased nitrate formation. The modelled change in ammonium lies within 40 to 50%, which is close to the observed 38% reduction.

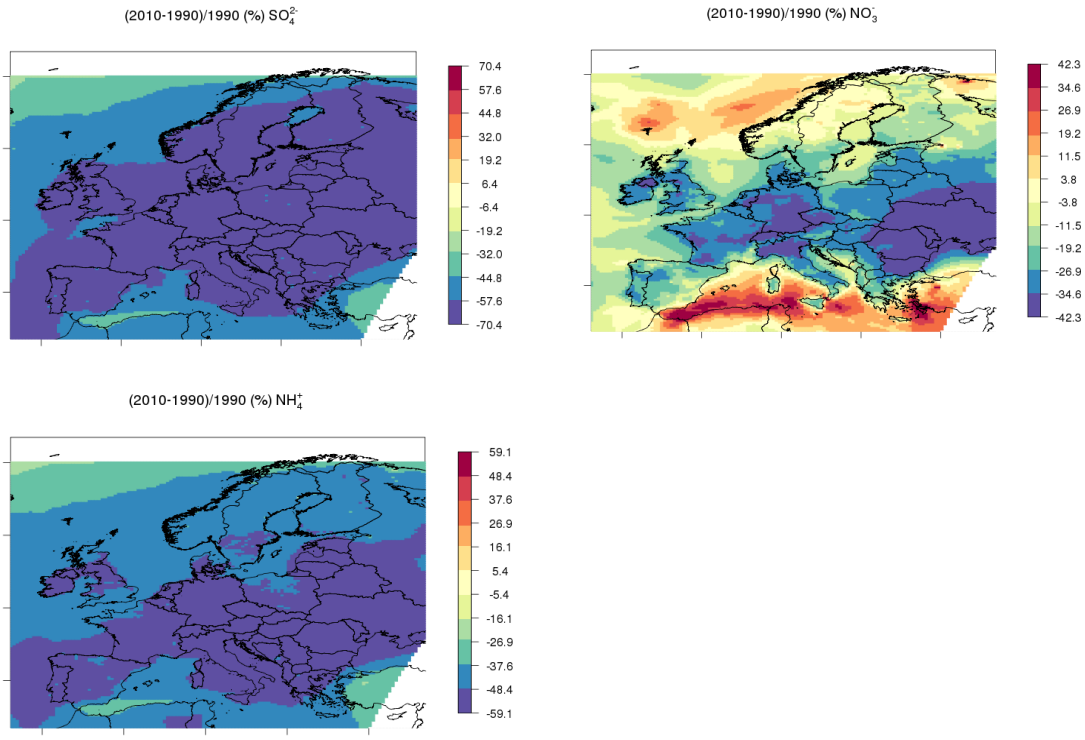

Figure 3.15: *Modelled relative change between 1990 and 2010 (%) obtained with the EURODELTA 6-model ensemble for sulfate (top left), nitrate (top right), and ammonium (bottom left).*

Figure 3.16 shows the results from EURODELTA model ensemble for the total PM mass, i.e. the mean concentrations in 1990 and 2010 and the changes between 1990 and 2010 and between 2000 and 2010. Only the changes in the latter period can be compared with observed trends reported in Section 3.6.1.

The model ensemble estimates a maximum reduction of 20%, which is slightly lower than the observed 29% reduction but still in the right order of magnitude. Over the 1990-2010 the model change is about 40%, which cannot be directly validated with observations.

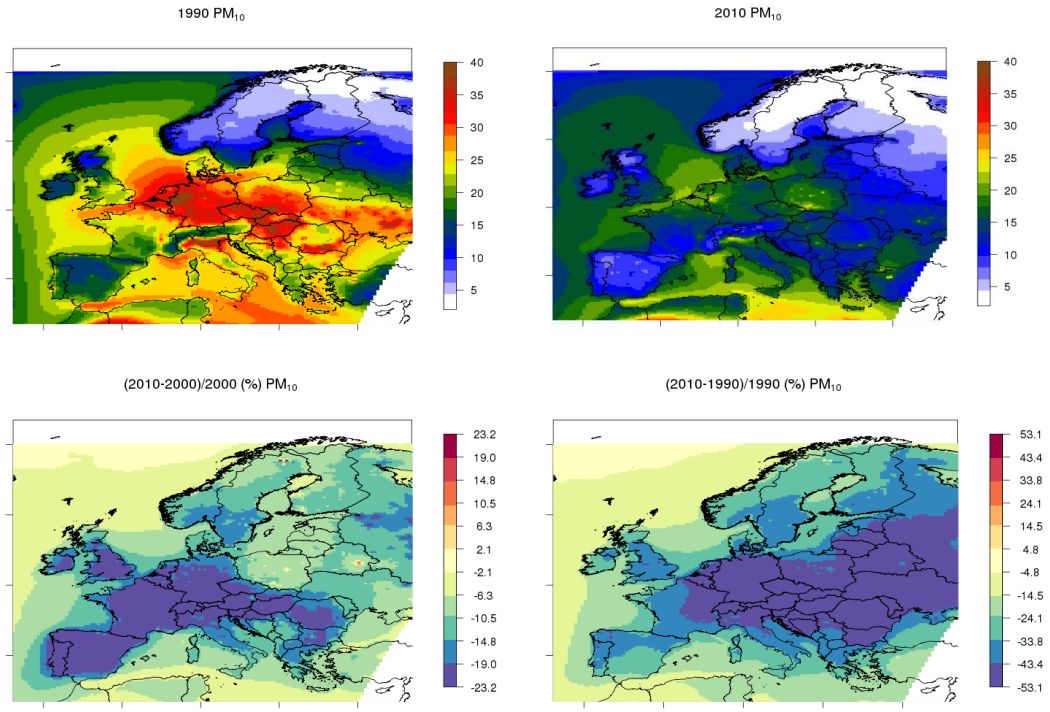

Figure 3.16: *Modelled PM_{10} ($\mu g/m^3$) from the EURODELTA 6-model ensemble using 1990 (top left) or 2010 (top right) emissions and relative change (%) between 2000 and 2010 (bottom left) and 1990 and 2010 (bottom right).*

4 Heavy Metals and Persistent Organic Pollutants

Main Authors: Milan Vana, Ilia Ilyin, Victor Shatalov

Contributors: Wenche Aas, Pernilla Bohlin-Nizzetto, Knut Breivik, Jana Boruvkova

The analysis of long-term trends of heavy metals (HMs) and persistent organic pollutants (POPs) concentrations of the EMEP region has been performed for the period from 1990 (reference year) to 2012 on the basis of the methodology elaborated by MSC-E (see details on Methods in Annex B). This method is based on fitting exponential decays, and therefore the trend is expressed in terms of reduction rates that are, by convention, positive for a downward trend and negative for an upward trend. The following species were included in the analysis: lead (Pb), cadmium (Cd), mercury (Hg), benzo(a)pyrene (B[a]P) (as an indicator species of PAHs), PCDD/Fs (total toxicity), PCB-153 (as an indicator congener of PCBs), and HCB.

Measurements of POPs and HMs were included in the EMEP monitoring programme in 1999 but earlier data are available for some compounds and some sites in the EMEP database (http://ebas.nilu.no). Detailed information about the sites, measurement methods and results for 2013 can be found in the EMEP/CCC's annual data report on heavy metals and POPs (Aas and Bohlin-Nizzetto, 2015). The EMEP monitoring programme for HMs and POPs aims for comparable and consistent monitoring data and recommended methods are described in the EMEP manual for sampling and analysis. It should however be noticed that comparing data across sites and compounds is a complicating factor when interpreting especially POP measurements, due to differences in sampling and analytical methodologies that might affect the comparability (Schlabach et al., 2011;Melymuk et al., 2014).

The analyses of long-term trends of POPs and HMs are performed using modelling results (Travnikov and Ilyin, 2005) and measurement data from the EMEP monitoring network. Due to the deficiency of monitoring data for sufficiently long-term periods as well as a limited spatial coverage of the POPs and HMs sites in Europe, the trend evaluation is based mainly on model calculations complemented by joint analysis of measurement data and calculation results at locations of monitoring sites.

4.1 Heavy Metals

4.1.1 HM deposition trends based on modelling results

Trends of HM levels were analysed for the EMEP region and particular countries. The analysis of HM levels in the EMEP region and in particular countries is focused on modelled total deposition, as this parameter is used for the evaluation of negative effects (e.g., exceedances of critical loads) of heavy metals on the biota and human health (De Wit et al., 2015).

The average annual time series and trends of total deposition over the EMEP region are given in *Figure 4.1*. Rates of deposition reduction of lead and mercury

were higher in the beginning and lower in the end of the two-decade period, but the reduction rate for mercury is smaller than that for lead. The rate of cadmium annual decline remained constant.

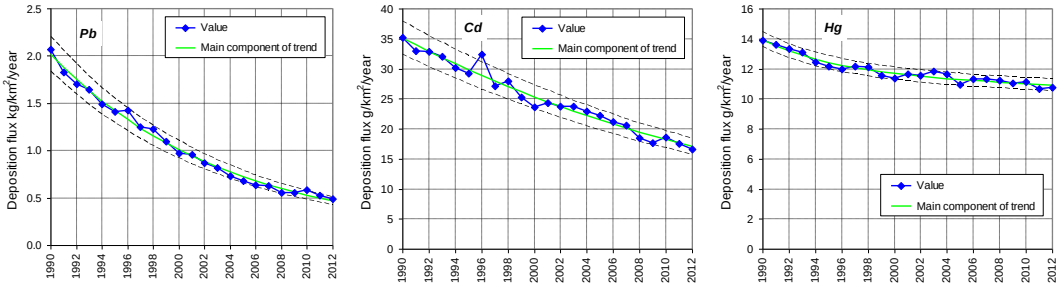

Figure 4.1: *Long-term changes of modelled total deposition flux and of the main component of its trend for lead (a), cadmium (b) and mercury (c). Dashed lines indicate 95% confidence interval.*

Table 4.1 summarizes the main quantitative characteristics of these long-term trends in the EMEP region for the full considered period (1990-2012) and for two sub-periods: 1990-2001 and 2002-2012. Lead was characterized by the highest, and mercury by the lowest magnitude of total reduction and average rate of reduction during all three periods. Deposition trends of all three metals were characterized by a seasonality of around 30-40%. Since emission data did not include information on seasonal variations of heavy metal releases to the atmosphere, the estimated seasonality is fully attributed to the effect of meteorological variability.

Table 4.1: *Main characteristics of the modelled long-term deposition trends and range of annual reduction rates within the period (in brackets) of lead, cadmium and mercury, 1990-2012*

Parameter	Pb	Cd	Hg
Total reduction (full period), %	78	53	23
Total reduction (1990-2001), %	56	32	19
Total reduction (2002-2012), %	50	30	5
Average reduction (full period), % per year	6.4 (5.9 – 6.8)	3.2 (3.2 – 3.2)	1.2 (0.4 – 3.5)
Average reduction (1990-2001), % per year	6.7 (6.5 – 6.8)	3.2 (3.2 – 3.2)	1.8 (0.8 – 3.5)
Average reduction (2002-2012), % per year	6.2 (5.9 – 6.5)	3.2 (3.2 – 3.2)	0.5 (0.4 – 0.7)
Seasonal variations, %	34	36	42

For analysis of long-term pollution changes in the EMEP countries over the whole period (1990-2012) two groups of countries were singled out: EU28 and EECCA. **The highest total reduction of modelled metal deposition was noted for EU28 countries. On average, this decrease occurred to be more than 80% for lead, 60% for cadmium and 35% for mercury** (*Figure 4.2*). **In the EECCA countries the decline of heavy metal pollution levels is smaller: total reduction for 1990-2012 amounted to 76% (lead), 49% (cadmium) and 19% (mercury).** Both within EECCA and EU28 groups the variability of total reduction among countries is large. In some countries the total reduction of cadmium and mercury is even negative, which means that pollution levels tend to increase in long-term perspective. These countries are Armenia and Azerbaijan (Cd, Hg) and Georgia (Hg).

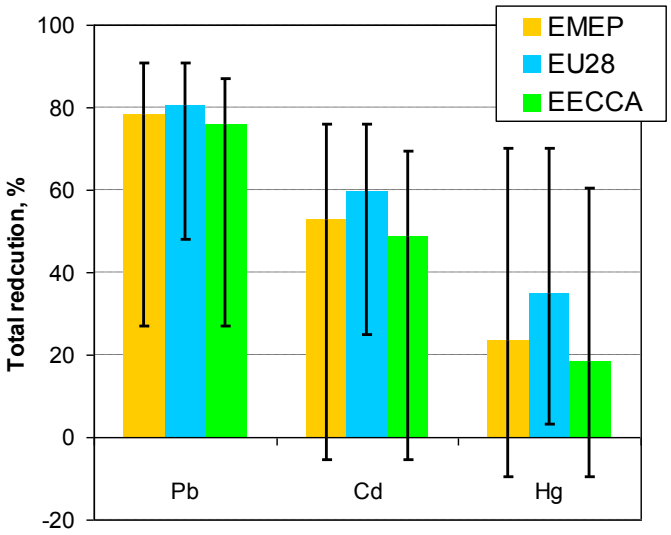

Figure 4.2: *Total reduction of modelled lead, cadmium and mercury deposition in the EMEP region as a whole, in EU28 and in EECCA countries. Whiskers indicate range of the reductions among the countries. Negative values stand for an increase.*

In addition, it is important to note that the rate of pollution reduction differs in time. In the beginning of the period (1990-2001) the reduction rate is the highest, while at the end (2002-2012) the rate is the lowest, and, in some countries, even negative. These countries are Cyprus, Armenia, Azerbaijan (Cd, Hg), Georgia, Italy and Finland (Hg) where there is a concern, if the current trend is maintained, that HM pollution levels may increase in the future.

Another important parameter describing long-term evolution of pollution levels is seasonality. In particular countries seasonality ranged from 8% to 95% for the considered metals (*Figure 4.3*). On average it amounted to 30-40%. Seasonality for mercury was somewhat lower than that for lead and cadmium, mostly due to long (about a year) atmospheric life time of mercury.

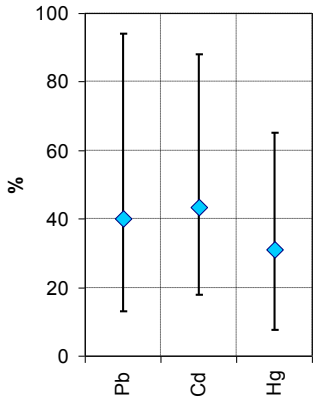

Figure 4.3: *Modelled seasonality of lead, cadmium and mercury deposition averaged among the EMEP countries. Whiskers indicate seasonality range between particular countries.*

4.1.2 Factors contributing to the heavy metals trends

Long-term trends of pollution levels depend on a number of factors including changes of anthropogenic and secondary emission data, long-term climatic trends, changes of land-use, etc. According to the modelling results, the main factors affecting the changes in the EMEP region from 1990 to 2012 seem to be anthropogenic and secondary emissions. Besides, changes of pollution levels within each country were also caused by an evolution in the respective contribution of national and foreign sources.

The reduction of anthropogenic emission of lead and cadmium for the period 1990- 2012 resulted in a decline of calculated deposition from anthropogenic sources of up to 90% and 64%, respectively (*Figure 4.4*). However, the total deposition reduction to the EMEP region was smaller (*Figure 4.1* and *Table 4.1*). The reason for this was a significant contribution of secondary sources to pollution levels in the EMEP region, whose reduction was smaller: around 50% for lead and cadmium.

The situation for mercury differed from that for lead and cadmium. The relatively low (23%) reduction of mercury deposition in the EMEP region was caused by two factors. The first factor is intercontinental transport: contribution of non-EMEP sources (both anthropogenic and secondary) ranged from about 65% to about 80% over the considered period (*Figure 4.4*). However, in absolute terms their contribution remained almost the same for the whole period, because global emissions of mercury had not changed much. The second factor is speciation of mercury emissions. A major part of the mercury was emitted as long-living elemental form (around 70% for anthropogenic sources and 100% for secondary sources), most of which was transported outside the EMEP region.

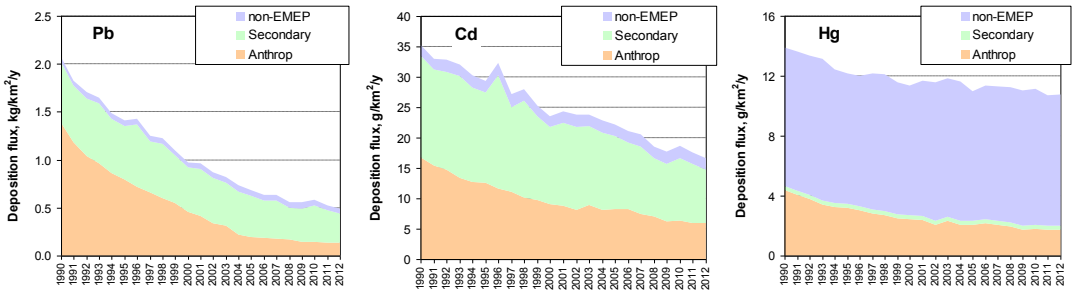

Figure 4.4: *Modelled deposition fluxes of lead (a), cadmium (b) and mercury (c) caused by anthropogenic and secondary sources within EMEP region and by non-EMEP sources*

4.1.3 Comparison of modelled and observed HM levels

Model results on long-term time series of heavy metal pollution levels were available for each grid cell of the EMEP domain. For those grid cells where monitoring stations were located, an analysis of trends could be done jointly on the basis of both modelled and measured values (*Figure 4.5*, *Figure 4.6*, *Figure 4.7*). There were 19 EMEP stations measuring lead and cadmium and 8 stations measuring mercury with long time series. The selected stations were located mostly in the central and the northern parts of Europe. Trends in the other parts of the EMEP region were characterized entirely by the modelling. As seen from *Figure 4.5*, *Figure 4.6* and *Figure 4.7* according to the model the highest mean reduction rate of heavy metal pollution levels took place in the central and

western parts of Europe, whereas in its eastern part and in the Central Asia the rate of reduction is smaller. Nevertheless, marked reduction rate is also noted in some countries in the eastern part of Europe, e.g., in Belarus, Latvia, Lithuania, Estonia (air concentrations of Pb) or in Ukraine (concentrations and wet deposition of Pb, Cd and Hg). Some increase of Hg wet deposition was noted for the north of Scandinavia (which is confirmed by available long-term measurements) and for the Mediterranean region.

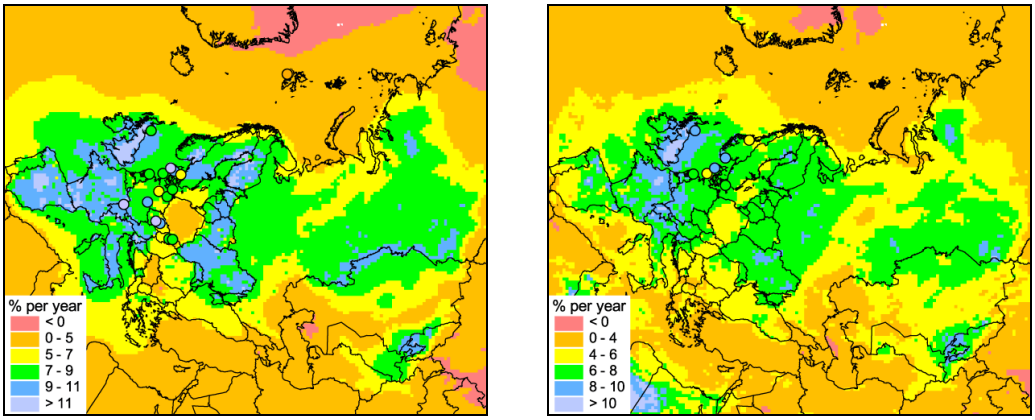

***Figure 4.5**: Average reduction rate of modelled (field) and observed (circles) Pb concentrations in air (left) and wet deposition fluxes (right) for the period from 1990 to 2012*

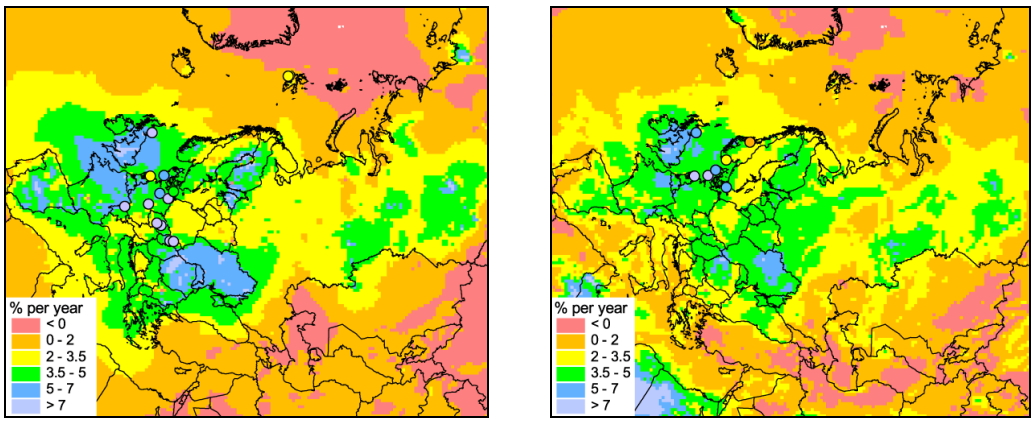

***Figure 4.6**: Average reduction rate of modelled (field) and observed (circles) Cd concentrations in air (left) and wet deposition fluxes (right) for the period from 1990 to 2012*

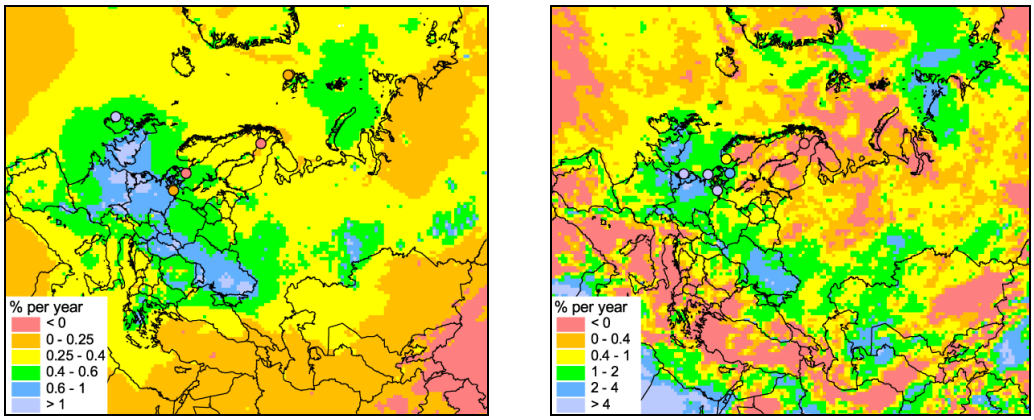

***Figure 4.7:** Average reduction rate of modelled (field) and observed (circles) Hg concentrations in air (left) and wet deposition fluxes (right) for the period from 1990 to 2012*

On average for the period from 1990 to 2012, the mean annual reduction rate of observed and modelled concentrations and wet deposition are given in *Figure 4.8*. For lead it amounted to about 7 to 9%. For cadmium the reduction rate of modelled levels was around 4%, and that of observed levels was about 5 to 8%. Somewhat higher reduction rate of observed compared to modelled levels was caused by underestimation of high observed values in the beginning of the considered period. Reduction rate of modelled and measured mercury air concentrations was low (less than 0.5% per year). Reduction rate of observed mercury wet deposition was higher (about 3% per year) than that of modelled levels. However, the range of reductions of observed mercury deposition was quite high and fully overlapped the range for modelled values.

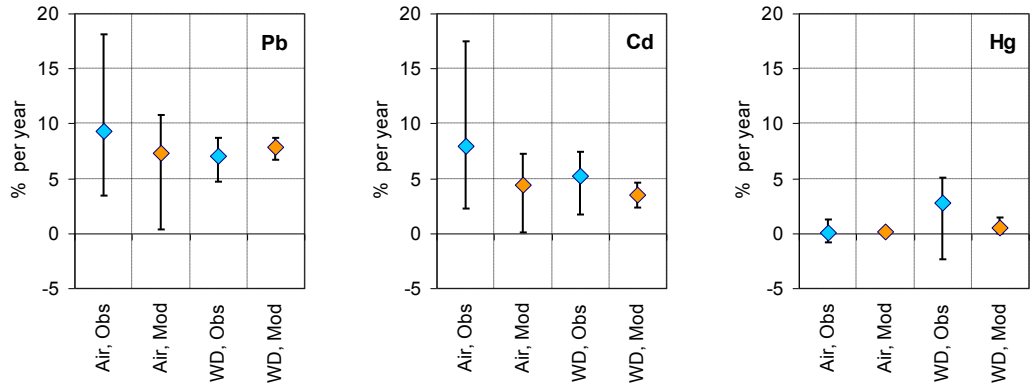

***Figure 4.8**: Mean annual reduction rates for modelled and observed air concentrations and wet deposition fluxes of lead (left), cadmium (middle) and mercury (right) over selected monitoring stations. Whiskers mean range of average reduction rates among stations.*

4.2 Persistent Organic Pollutants

4.2.1 POP trends based on modelling results

Calculated trends of average air concentrations in the EMEP region for the period from 1990 to 2012 for selected POPs are shown in *Figure 4.9*. To describe the general tendencies in changes of air concentrations, trends of annual averages (not taking into account seasonal variations) are considered. Reduction rates refer to the main trend component. Dashed lines indicate 95% confidence interval.

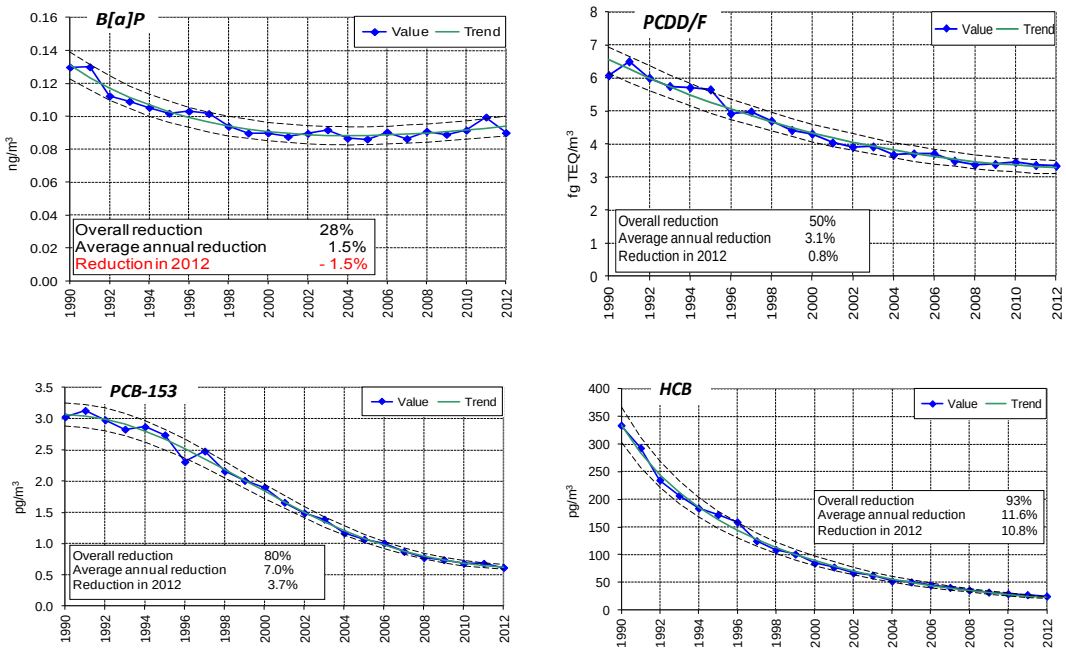

Figure 4.9: *Trends of modelled annual mean air concentrations of (a) B[a]P, (b) PCDD/Fs, (c) PCB-153 and (d) HCB in the EMEP region for the period from 1990 to 2012. Negative reduction denotes increase of air concentrations. Dashed lines indicate 95% confidence interval.*

The maximum reduction for the selected POPs occurred in the beginning of the period, whereas at the end of the period (in 2012), the reduction rate diminished or even was replaced by growth. **The largest reduction is obtained for HCB (over 90%), and the smallest for B[a]P (about 30%). In 2012 an increase of B[a]P pollution was obtained, and for PCDD/Fs the concentrations reached a stationary level, with a reduction of only about 0.8%.** It is noted that the growth of B[a]P air concentrations in the EMEP region from 2005 to 2012 occurred to be statistically significant at the 90% confidence level.

Similar trends can also be seen in temporal variations of B[a]P deposition fluxes to various ecosystems which is important for the evaluation of harmful effects of POPs pollution. As shown in *Figure 4.10*, the reduction of B[a]P deposition to deciduous forests and arable lands is estimated to about 25% for the period 1990 – 2012. However, the general trend started to increase from 2005. The main characteristics of the long-term trends in the EMEP region for the full period (1990-2012) and for the two parts: 1990-2001 and 2002-2012 for the considered POPs are summarized in *Table 4.2*.

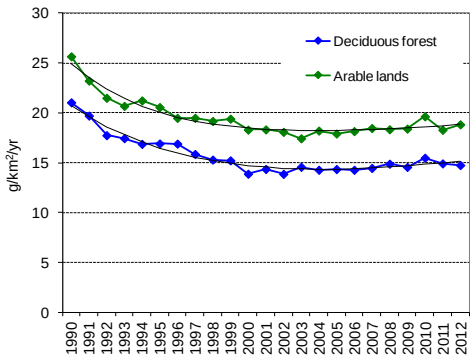

Figure 4.10: *Trends of modelled B[a]P deposition to deciduous forest and arable lands within the EMEP region.*

Table 4.2: *Main characteristics of modelled long-term deposition trends of selected POPs, 1990-2012, the range of annual reduction rates within the period is indicated in brackets.*

Parameter	B[a]P	PCDD/Fs	PCB-153	HCB
Total reduction (full period), %	28	50	80	93
Total reduction (1990-2001), %	32	36	46	76
Total reduction (2002-2012), %	-6	19	58	68
Average reduction (full period), % per year	1.5 (–1.4 – 5.7)*	3.1 (0.8 – 4.4)	6.7 (0.8 – 10.4)	11.6 (10.8 – 14.8)
Average reduction (1990-2001), % per year	3.4 (1.23 – 5.7)	4.0 (3.4 – 4.4)	5.4 (0.8 – 9.3)	12.3 (11.0 – 14.8)
Average reduction (2002-2012), % per year	– 0.6 (–1.4 – 0.7)	2.0 (0.8 – 3.3)	8.4 (3.7 – 10.4)	10.8 (10.8 – 11.0)

The seasonal variability of the concentrations for some POPs is an important characteristic in the evaluation of long-term trends. In particular, the intra-annual variations of PAH concentrations can reach an order of magnitude that needs to be considered in the trend analysis. The approach developed for the analysis of trends takes into account seasonal variations of pollution and provides approximation of changes on the level of monthly mean air concentrations. As an example, the results of the analysis of long-term trends in seasonal variations of B[a]P air concentrations in the EMEP region are shown in *Figure 4.11*. Due to the substantial seasonal variability, B[a]P air concentration in the cold period of year can exceed several times the annual average value.

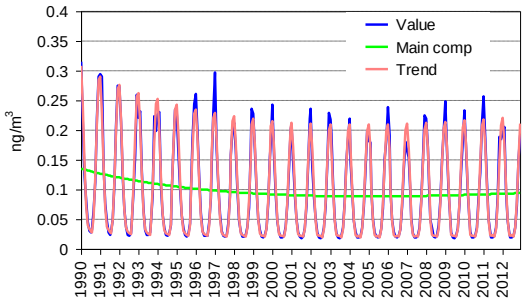

Figure 4.11: *Trend of modelled monthly mean B[a]P air concentrations in the EMEP region for the period from 1990 to 2012.*

Along with the changes of POP pollution in the EMEP region as a whole the analysis of trends was performed also for individual EMEP countries. For illustration purposes, the results of the trend analysis for B[a]P air concentrations in particular EMEP countries are given in Figure 4.12. It was found that the growth of concentrations in the end of the period (2012) is characteristic for most EMEP countries. In particularly, such increases take place in 90% of the EECCA countries and in 80% of the EU28 countries.

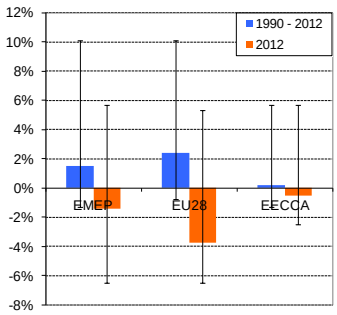

Figure 4.12: *Average annual reduction rates of modelled B[a]P air concentrations for the period from 1990 to 2012 and reduction rates in 2012 for three groups of countries: the EECCA, the EU28, and other EMEP countries. Negative values denote growth of pollution. Whiskers indicate variations between countries.*

The trends of B[a]P pollution in the EMEP countries are further illustrated for instance in Germany (*Figure 4.13*). Along with large total reduction (68%), an increase of contamination in Germany in the end of the period (from 2005) is found, reaching 5% in the last year 2012. It should be noted that the growth of the general trend of B[a]P air concentrations from 2005 to 2012 is statistically significant.

For comparison purposes, the calculated trend of B[a]P emissions in Germany is also shown in *Figure 4.13*. It is seen that the trend of air concentrations is consistent with that of emission totals (on the level of annual averages). Differences in values of reduction parameters for modelled air concentrations and emissions are attributed to transboundary transport.

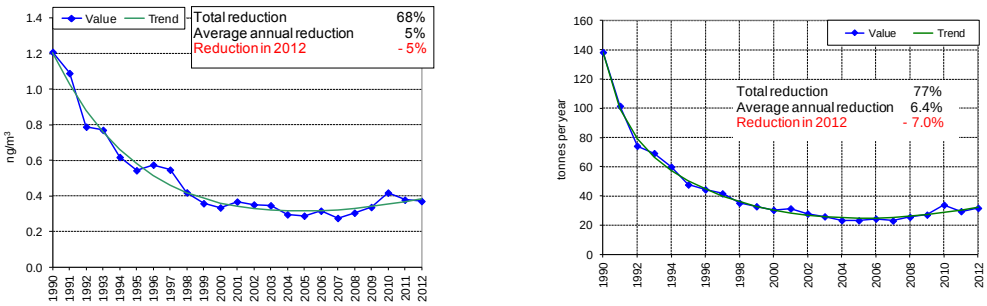

Figure 4.13: *Trends of modelled annual mean air concentrations (a) and emissions (b) in Germany for the period from 1990 to 2012. Reduction rates refer to general trend. Negative reduction denotes increase of air concentrations.*

POP concentrations in the air in the EMEP region varies significantly across the territories of the countries. According to modelling results, in spite of generally low annual mean B[a]P air concentrations over the major part of the countries there are areas where EU target value for B[a]P (1 ng/m^3 as defined in the Directive 2008/50 EC), is exceeded. The number of people living in these areas in particular EMEP countries is shown in Figure 4.14.

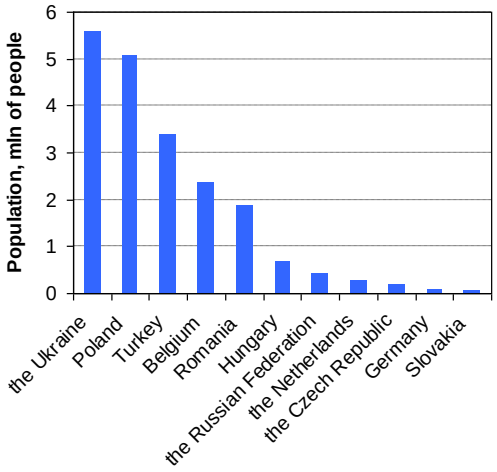

Figure 4.14: *Number of people living in regions where B[a]P air concentrations exceed EU target value of 1 ng/m^3 in EMEP countries in 2012 according to modelling results.*

As shown above in Figure 4.11, the seasonal variations in the entire EMEP region can change the main component by as much as 100%. However, seasonality varies strongly between countries (from 45% of the main component for Spain to over 150% for Turkmenistan). Nevertheless, seasonal variations of air concentrations are important in all EMEP countries.

4.2.2 Comparison of modelled and observed POP levels

Model simulations provide information on changes of pollution levels for the whole EMEP region. In the particular grid cells of modelling domain where the long-term measurements of POP concentrations were carried out, it was possible to perform combined analysis of trends in the pollution levels (*Figure 4.15*). It

should be taken into account that measurement data describe pollution levels at particular locations whereas model calculations provide values averaged over the 50×50 km grid cells. As follows from the figure, the highest mean reduction of modelled B[a]P levels in the EMEP region for 1990-2012 took place in the central, western and north-western parts of Europe. In a number of countries, located mainly in eastern, south-eastern and northern parts of Europe and in Central Asia a long-term growth of B[a]P concentrations occurred.

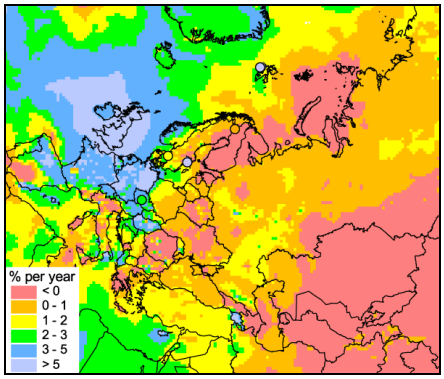

Figure 4.15: *Average reduction rate of modelled (field) and observed (circles) B[a]P concentrations in air for the period from 1990 to 2012*

Measurements of B[a]P, PCB-153 and HCB air concentrations for a sufficiently long period of time were available for the following EMEP monitoring sites: CZ3 (Kosetice), FI96 (Pallas), IS91 (Storhofdi), NO42 (Zeppelin), NO99 (Lista) SE2/14 (Rörvik/Råö) and SE12 (Aspvreten). It should be noted that these sites are located mainly in the north-west of the EMEP domain. Since the time periods of measurements performed at the selected sites are different, average annual reduction rates are used to evaluate the decline of pollution levels.

Comparison of estimates of trends for B[a]P, HCB and PCB-153, performed on the basis of model data and measurements, shows that model predictions generally capture the observed long-term tendencies in changes of pollution levels. The main findings obtained from the comparison are summarized in *Figure **4.16***.

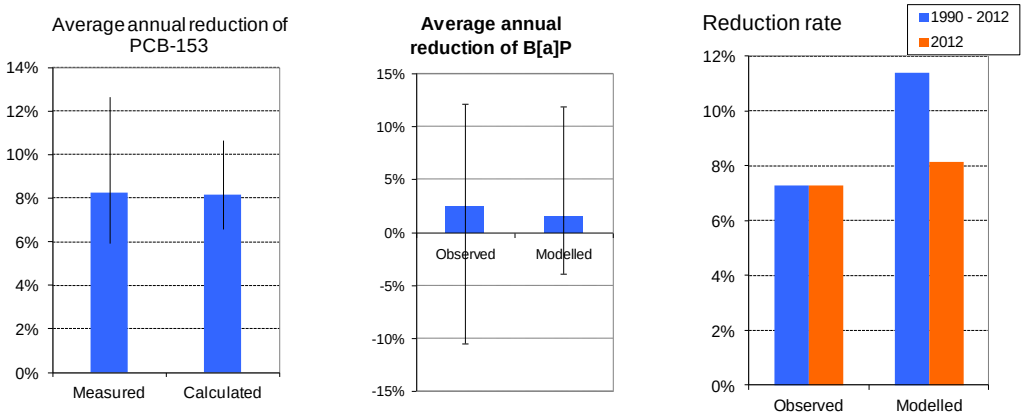

Figure 4.16: Average annual reduction of air concentration according to modeling results and measurements for PCB-153 (left), BaP (middle, for the period 2004-2012) and HCB (for the period 1990-2012 and the year 2012). The whiskers indicate the variation of the parameter between site locations

For PCB-153, the analysis was carried out for six sites, namely, CZ3, FI96, IS91, NO42, SE2/SE14, and SE12. The average annual reduction rate of PCB-153 is about 8%. Recalculation of reduction from observed annual average to the period from 1990 to 2012 results in overall decline about 85% that is in agreement with modelling results (*Figure 4.9*). The analysis of both measured and modelled data shows that seasonal variations can change pollution levels of PCB-153 by about 60%.

The majority of long-term measurements of B[a]P air concentrations in the EMEP countries were carried out during the recent decade. Analysis of modelled and measured time-series of B[a]P air concentrations indicates reasonable agreement between their reduction rates. According to the modelling results and available measurements, the average annual reduction rate of B[a]P concentrations in period 2004-2012 is about 2% per year. Recalculation of reduction from observed annual average to the period from 1990 to 2012 results in a total reduction of about 30%.

For HCB, sufficiently long time series of measured air concentrations were available for the following EMEP monitoring sites: CZ3, NO42, NO99 and IS91. Similar to PCB-153, the average annual reduction of HCB is high (9% – 10% per year). The analysis of temporal variations of HCB air concentrations for the two remote sites, NO42 and IS91, indicates larger differences in estimates of trends. The reason for the differences is due to the fact that the levels of pollution at these sites are likely influenced by the emission sources outside the EMEP domain. Thus, a refinement of the description of global scale HCB emissions and their temporal changes in various regions of the world is required.

Regular measurements of air concentrations of dioxins and furans at the EMEP monitoring sites are not currently performed. At the same time, it is possible to use available long-term measurements of PCDD/F air concentrations in the EMEP countries reported in literature for the analysis of long-term changes of pollution. A number of studies provided results of long-term measurements of air concentrations of dioxins and furans. A significant decrease of PCDD/F air concentrations (about 70%) was observed in Spain in the period 1994-2004 (Abad et al., 2007). Monitoring of PCDD/F air concentrations in the UK at urban and rural sites indicated a sharp decline in early 1990s and a smaller decline subsequently (Katsoyiannis et al., 2010). A pronounced decrease of PCDD/F air concentrations and deposition (about a factor of 5) was also observed in Germany from 1988-1992 to 2005 (Bruckmann et al., 2013), which has almost levelled off since 2005. In general, results of model simulations are in line with available measurements and demonstrate similar declines of PCDD/F pollution in the EU countries from 1990 to 2012 (about 80%).

4.2.3 Integrated monitoring of POPs

In addition to data on atmospheric monitoring of pollution levels, measurement data in other environmental compartments are important for better understanding of the behaviour of POPs in the environment. For other matrices (needles, moss, wet deposition, surface water and soil) only data from Košetice EMEP station (CZ03) are available. Needles, moss, surface water and soil data are measured

annually, which eliminates the possibility of using of the bi-exponential curve, which is based on the intra-annual variations. For these matrices, only the Mann-Kendall trend test was computed.

In the case of wet deposition, the data is of different quality, allowing to interpolate by the bi-exponential curve for benzo[a]pyrene and γ-HCH, with a relatively low share of values under quantification limit, but not for other parameters, where the share of left censored values is higher than 50%. As well as in the case of passive air sampling, there is an apparent decrease of PCB 153 in all matrices and less significant decrease of γ-HCH and *p,p'*-DDE. In the case of benzo[a]pyrene, the significance is rather low. There is a lack of convincing data for HCB. The results of the trend analysis for other matrices are listed in *Table 4.3*.

Table 4.3: *results of POPs trends identification at Košetice EMEP site for matrices other than air concentrations*

	benzo[a]pyrene		γ-HCH		HCB		PCB 153		*p,p'*-DDE	
	MK test	**bi-exp**	**MK test**	**bi-exp**	**MK test**	**bi-exp**	**MK test**	**bi-exp**	**MK test**	**bi-exp**
Needles	↓		↑		↑		↓		↑	
Moss	↓		↑		↓		↓		↑	
Surface water	↑		↓		↓				↓	
Wet deposition	↓	↓	↓	↕			↓		↓	
Soil	↓		↑		↑		↓		↓	

↓	insignificant decrease	↑	increase (significance is not known)
↑	insignificant increase	↓	decrease (significance is not known)
↔	constant trend	↕	non-monotonic trend
↓	significant decrease		
↑	significant increase		

Appendix A

Methods - Main Pollutants

A Methods – Main Pollutants

The present section provides the practicalities of the trend assessment for ozone, nitrogen dioxide, particulate matter, secondary inorganic aerosol, and sulfur and nitrogen concentration in precipitation. All the data, as well as trend diagnostics, are available on the TFMM wiki website[9].

A.1 Selection of monitoring sites

A.1.1 Selection of monitoring sites for ozone

The EMEP database EBAS (ebas.nilu.no) was the basis for the monitoring data used in this assessment. The data were extracted from the database during the period April-October 2015. The surface monitoring network within EMEP has changed substantially during the period studied here, 1990-2012, both with respect to the number of stations and with respect to the geographical coverage. The latter could be even more important than the former since it may introduce a possible bias to the overall analyses. For instance, for ozone in the first part of the period the monitoring sites were concentrated in certain parts of Europe like Germany, Switzerland, UK and Scandinavia whereas southern and eastern Europe were poorly covered. Gradually, the network has been extended to these regions as well. Still, by 2012 the monitoring network is very limited in SE-Europe.

For each of the three periods 1990-2001, 2002-2012 and 1990-2012 the sites were selected based on the criteria that i) the data capture should be at least 75 % for a specific year to be counted and ii) the number of these counted years should be at least 75 % of the total number of years in the period. Thus, for the period 2002-2012, the station should have at least 9 years with 75 % data capture. Depending on the compounds and metric, the annual data capture was evaluated on the basis of the available monitoring temporal frequency. Note that only the sites located below 1000m of altitude are included in Chapter 2.

For illustration purposes, the locations of the selected sites for ozone for the three periods are shown in Figure A.*1* (where 53 sites are used for calculation of trend in summertime peaks and 55 for the annual mean). As mentioned above, there is a strong bias to central and Northern Europe for the 1990-2001 and 1990-2012 periods.

[9] https://wiki.met.no/emep/emep-experts/tfmmtrendstations

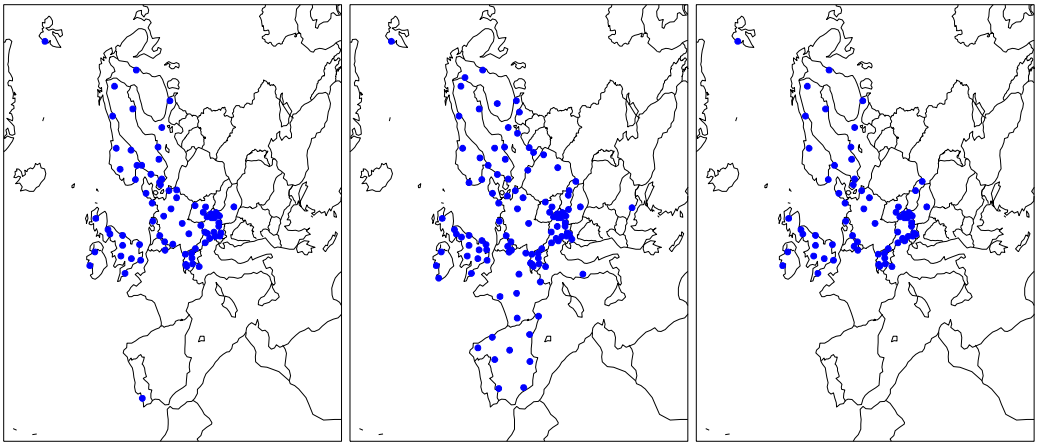

Figure A.1: *Location of selected ozone monitoring sites for the periods 1990-2001 (left), 2002-2012 (middle) and 1990-2012 (right).*

Table A.1*: List of EMEP stations passing the completion criteria for annual mean ozone and corresponding period covered: X: 1990-2012, a: 1990-2001, b: 2002-2012. It should be noted that several sites provide valuable information albeit over a shorter time period and therefore do not appear on this list.*

Station code	period	Station code	period	Station code	period
AT0002	abX	ES0009	b	LT0015	b
AT0005	bX	ES0010	b	LV0010	b
AT0030	bX	ES0011	b	NL0009	abX
AT0032	abX	ES0012	b	NL0010	abX
AT0034	abX	ES0013	b	NO0001	abX
AT0037	abX	ES0014	b	NO0015	abX
AT0038	abX	ES0016	b	NO0039	abX
AT0040	abX	FI0009	abX	NO0042	abX
AT0041	abX	FI0017	abX	NO0043	abX
AT0042	abX	FI0022	abX	NO0052	b
AT0043	abX	FI0037	b	NO0056	b
AT0044	abX	FI0096	b	PL0002	b
AT0045	abX	FR0008	b	PL0003	b
AT0046	abX	FR0009	b	PL0004	b
AT0047	abX	FR0010	b	PL0005	b
AT0048	b	FR0013	b	SE0011	abX
BE0001	bX	FR0014	b	SE0012	abX
BE0032	abX	FR0015	b	SE0013	abX
BE0035	bX	FR0016	b	SE0014	b
BG0053	b	FR0017	b	SE0032	abX
CH0001	abX	GB0002	abX	SE0035	abX
CH0002	abX	GB0006	abX	SE0039	b
CH0003	abX	GB0013	abX	SI0008	b
CH0004	abX	GB0014	abX	SI0031	bX
CH0005	abX	GB0015	abX	SI0032	abX
CY0002	b	GB0031	abX	SI0033	bX

Station code	period	Station code	period	Station code	period
CZ0001	bX	GB0033	abX	SK0002	b
CZ0003	bX	GB0035	b	SK0004	bX
DE0001	abX	GB0036	abX	SK0006	b
DE0002	abX	GB0037	bX	SK0007	b
DE0003	abX	GB0038	abX		
DE0007	abX	GB0039	abX		
DE0008	abX	GB0045	b		
DE0009	abX	GB0049	b		
DK0005	b	GB0050	b		
DK0031	abX	HU0002	bX		
EE0009	b	IE0001	b		
EE0011	b	IE0031	abX		
ES0007	b	IT0001	b		
ES0008	b	IT0004	abX		

A.1.2 Selection of monitoring sites for acidifying and eutrophying compounds

The list of sites selected for the trend analysis of sulfur and nitrogen in the gas phase, particulate matter and precipitation is given in *Table A.2*. Particulate sulfate was not sea salt corrected because of the lack of long term measurements of sea salt ions in aerosol. There was an exception for the Irish site (IE0001) that has significant sea salt influence. However, sea salt corrected sulfate is only available for 2005-2012, so that for the years between 1990-2004, the sea salt contribution was subtracted from the total sulfate measured based on the average sea salt sulfate contribution for the period between 2005-2012.

Table A.2: *List of EMEP stations passing the completion criteria for the constituents addressed in Chapter 3 (nss SO_4^{2-} (precip): sea-salt corrected sulfate in precipitation, SO_4^{2-}: particulate sulfate, SO_2: sulfur dioxide, NO_2: nitrogen dioxide, NO_3^-(precip): nitrate in precipitation, $HNO_3+NO_3^-$: nitric acid plus particulate nitrate, NH_4^+ (precip): ammonium in precipitation, $NH_4^++NH_3$: ammonia plus particulate ammonium. Symbols indicate a satisfactory coverage for: (X): the 1990-2012 period, (a): the 1990-2001 period, (b): the 2002-2012 period. It should be noted that several sites provide valuable information albeit over a shorter time period and therefore do not appear on this list.*

Code	Station name	nssSO_4^{2-} (precip)	SO_4^2	SO_2	NO_2	NO_3^- (precip)	$HNO_3+NO_3^-$	NH_4^+ (precip)	$NH_3+NH_4^+$
AT0002R	Illmitz	a		Xb	b	a		a	
AT0004R	St. Koloman	a				a		a	
AT0005R	Vorhegg			Xb	b				
BE0001R	Offagne				b				
BE0003R	Brugge					a		a	
BE0011R	Moerkerke				X				
BE0013R	Houtem				X				
BE0014R	Koksijde					b		b	
BE0032R	Eupen				X				
CH0002R	Payerne	X	X	X	X	X		X	

Code	Station name	nssSO_4^{2-} (precip)	SO_4^2	SO_2	NO_2	NO_3^- (precip)	HNO_3+ NO_3^-	NH_4^+ (precip)	NH_3+ NH_4^+
CH0003R	Tänikon	b			b				
CH0004R	Chaumont				b	b		b	
CH0005R	Rigi	b		b	b	b	b	b	b
CZ0001R	Svratouch	X	Xab	X		X	b	X	b
CZ0003R	Kosetice	X	Xab	X	X	X	b	X	X
DE0001R	Westerland	X		X	X	X		X	
DE0002R	Waldhof	X		X	X	X		X	
DE0003R	Schauinsland	X			X	X		X	
DE0004R	Deuselbach	X			a	X		X	
DE0005R	Brotjacklriegel	X			a	Xb		Xb	
DE0007R	Neuglobsow	Xb		X	b	Xb		Xb	
DE0008R	Schmücke	b			b			X	
DE0009R	Zingst	b			b	b		b	
DE0044R	Melpitz	b				b		b	
DK0003R	Tange		X	X			X		X
DK0005R	Keldsnor	X		a		X	a	b	a
DK0008R	Anholt	b	X	X		X	X	X	X
DK0022R	Sepstrup Sande	b				b		b	
DK0031R	Ulborg						a		
EE0009R	Lahemaa	b			b	X		Xb	
EE0011R	Vilsandi	b			b	b		b	
ES0001R	San Pablo de los Montes	a				a		a	
ES0003R	Roquetas	a				a		a	
ES0004R	Logroño	a	a	a		a	a	a	a
ES0007R	Víznar	b	b	b	b	b	b	b	b
ES0008R	Niembro	b	b	b	b	b	b	b	b
ES0009R	Campisabalos	b		b	b	b	b	b	b
ES0010R	Cabo de Creus		b	b	b		b		b
ES0011R	Barcarrota	b	b	b	b		b	b	b
ES0012R	Zarra	b	b	b	b	b	b	b	b
ES0013R	Penausende		b	b	b		b	b	b
ES0014R	Els Torms		b	b	b		b		b
ES0016R	O Saviñao	b	b	b	b	b	b	b	b
FI0004(37)R	Ähtäri (I and II)	X	X	X	b	X	X	X	X
FI0009R	Utö	a	X	X		a	X	a	X
FI0017R	Virolahti II	X	X	X	b	X	X	X	X
FI0022R	Oulanka	X	X	X	a	X	X	X	X
FI0036R	Pallas (Matorova)		b	b		b	b	b	b
FI0053R	Hailuoto II					b		b	

Code	Station name	nssSO_4^{2-} (precip)	SO_4^2	SO_2	NO_2	NO_3^- (precip)	HNO_3+ NO_3^-	NH_4^+ (precip)	NH_3+ NH_4^+
FR0003R	La Crouzille	a	a			a		a	
FR0005R	La Hague							a	
FR0008R	Donon	X	a			X		X	
FR0009R	Revin	X				X		X	
FR0010R	Morvan	X	a	a		X		X	
FR0012R	Iraty	a	a			a		a	
FR0013R	Peyrusse Vieille	b	b			b		b	
FR0014R	Montandon	b				b		b	
FR0015R	La Tardière	b				b		b	
FR0016R	Le Casset	b				b		b	
FR0090R	Porspoder					b		b	
GB0002R	Eskdalemuir	X	a	a		X	a	X	a
GB0006R	Lough Navar	X	a	a		X		X	
GB0007R	Barcombe Mills		a	a					
GB0013R	Yarner Wood	X	a	a		X		X	
GB0014R	High Muffles	X	a			Xb	X	X	X
GB0015R	Strath Vaich Dam	X	a			X		X	
GB0016R	Glen Dye		a	a					
GB0036R	Harwell			b					
GB0037R	Ladybower Res.			X	X				
GB0038R	Lullington Heath			b	X				
GB0043R	Narberth				b				
GB0045R	Wicken Fen			b	b				
GB0050R	St. Osyth				b				
HR0002R	Puntijarka	Xa		b		X		X	
HR0004R	Zavizan	Xa				X		X	
HU0002R	K-puszta	b	b			X	X	Xa	X
IE0001R	Valentia Observatory	Xa	X	X	X	X		X	
IE0002R	Turlough Hill	a						a	
IS0002R	Irafoss	X							
IS0090R	Reykjavik	b				b		b	
IS0091R	Storhofdi					b		b	
IT0001R	Montelibretti	b	b	b	b	b	b	b	b
IT0004R	Ispra	X	a	X	Xa	X		X	
LT0015R	Preila	X	X	X	X	X	b	X	X
LV0010R	Rucava	X	a	X	X	X		X	
NL0009R	Kollumerwaard	b	b	X	X			b	
NL0010R	Vredepeel		b	a	X				

Code	Station name	nssSO_4^{2-} (precip)	SO_4^2	SO_2	NO_2	NO_3^- (precip)	HNO_3+ NO_3^-	NH_4^+ (precip)	NH_3+ NH_4^+
NL0091R	De Zilk				b	b		b	b
NO0001(2)R	Birkenes (I and II)	X	X	X	X	X	X	X	X
NO0008R	Skreådalen	a			a	a	a	a	a
NO0015R	Tustervatn	X	X	X	X	X			
NO0039R	Kårvatn	X	X	X	X	X	X	X	X
NO0041R	Osen	a	a		a	a			
NO0042G	Zeppelin mountain		X	X					
NO0099R	Lista					a			
PL0002R	Jarczew	X	X	X	X	X	X	X	b
PL0003R	Sniezka	X	X	X	X	X	b	X	X
PL0004R	Leba	b	b	b	b	b	b	b	b
PL0005R	Diabla Gora	b	b	b	b	b	b	b	b
PT0001R	Braganca	a				a		a	
PT0003R	Viana do Castelo	a				a		a	
PT0004R	Monte Velho	a				a		a	
RS0005R	Kamenicki vis	X				X		X	
RU0001R	Janiskoski	X	a	a		X		X	
RU0013R	Pinega	X				X		X	
RU0018R	Danki	b	b	b		b			
SE0002(14)R	Rörvik (Råö)	X	X	X	X	X	X	X	X
SE0005R	Bredkälen	a	X	X	X		b	a	X
SE0008R	Hoburgen		a	a	a				
SE0011R	Vavihill	X	X	X	X	X	X	X	X
SE0012R	Aspvreten	a				a		a	
SI0008R	Iskrba	b	b	b		b	b	b	b
SK0004R	Stará Lesná	b				b		b	
SK0006R	Starina	b		b	b	b	b	b	
SK0007R	Topolniky	b				b		b	

Finally, to complement the analysis, the monitoring stations from the EEA´s Air Quality Database (http://www.eea.europa.eu/data-and-maps/data/aqereporting, former AIRBASE) were also considered (for further details, see Colette *et. al.*, 2015).

A.1.3 Selection of monitoring sites for NMHC

EMEP stations were chosen for inclusion in the analysis of NMHC concentrations based on the availability of multi-year measurement records for a suite of commonly measured NMHCs: acetylene (ethyne), benzene, i-butane, n-butane, ethylene, hexane, i-pentane, n-pentane, propene, and toluene. An annual data capture criterion of 75% (based on the regular sampling frequency for each type

of measurement) was applied for each individual species at each station. Arithmetic annual means were calculated for each species at each station and year. In cases where one or more species was missing for a given year at a given station, no sum is calculated (i.e., a data point for that station and year will be missing from *Figure 2.5*). With the exception of stations GB48 (Auchencorth Moss), GB36 (Harwell), and DE54 (Zugspitze), all NMHC data was extracted from the EBAS database. In the case of DE54, monitoring data not available in EBAS was provided by a national expert. In the case of GB48 and GB36, additional data flagged as missing in EBAS were provided by a national expert. A more detailed treatment of VOC trends in the UK, including at the GB48 and GB36 sites, can be found in (Derwent et al., 2014).

A.2 Metrics

For nitrogen dioxide, particulate matter, secondary inorganic aerosol, and wet sulfur and nitrogen concentration in precipitation, annual averages were computed on the basis of the highest available temporal resolution. Diagnostics were also computed for each season.

For ozone, more elaborate metrics must be considered, the following were selected for the analysis (following acronyms in Figure 3):

- O3 Avg: annual mean
- MDA8: the daily maximum of 8-hr running mean hourly ozone
- SOMO35: the sum of MDA8 levels over 35 ppb (70 $\mu g/m^3$) accumulated over one year. A measure of accumulated annual ozone concentrations used as an indicator of human health risks.
- ndays Max>60ppb: number of days with MDA8 exceeding 60 ppb
- annual max: annual maximum of the MDA8
- 3-months AOT40 (May-July): AOT is the accumulated hourly ozone above the level of 40 ppb (80 $\mu g/m^3$), a measure of cumulative annual ozone concentrations that is used as indicator of risks to vegetation.

Certain remarks to these metrics should be noted: The daily max running 8 h averages were allocated to the day the 8 h period ended, as stated in the EU air quality directive 2008/50/EC. The AOT40s were only calculated when the data capture (based on hourly data) was at least 75 % for the requested period (month or 3-months). Furthermore, a UN-ECE approach was used for selecting the hours of the day for the AOT calculations, implying that only the hours with a global radiation > 50 W/m^2 based on zenith angle and a climatological relationship between zenith angle and radiation assuming clear sky conditions were considered. The AOT values were also normalised by the inverse of the data capture, i.e.:

$$AOT = AOT_{measured} / (\text{fractional data capture})$$

All calculations were based on hourly ozone data in ppb whereas EBAS presently stores these data in a proxy $\mu g/m^3$ unit (in which 1 ppb = 2 proxy $\mu g/m^3$).

It should be noted that the selection of sites could differ depending on the metrics. For a three-months AOT40 based on the months May-July, the 75 % data capture requirement was applied to these months. Thus, a site could be rejected if the data capture in this three-months period was less than 75 % although it was above 75 % for the whole year.

A focus on the 4th highest MDA8 day is given in the main text. It represents approximately the annual 99th percentile when the data coverage is complete. Alternative higher percentiles of MDA8 can be found in the literature, it should be noted however that the 95th percentile is considered too low because it is approximately the 18th highest day, it can therefore include several non-episode days and be influenced by the background. Using the annual maximum (100th percentile) is not a good statistical practice either, because of the imperfect statistical distribution of high ozone episode days. But it should be noted that for the trend analysis presented here, very similar results were found when using the 98th, 99th and 100th percentiles.

A.3 Trend calculations

The trend calculations were based on the Mann Kendall (MK) method for identifying significant trends combined with the Sen's slope method for estimating slopes and confidence intervals. These simple and straight-forward methods were programmed and run in IDL based on the documentation given by (Gilbert, 1987). Comparisons with other existing MK software (e.g. Makesens in Excel or R) showed a very good agreement between the results from these programs.

The essence of the MK method is that the signs of all forward differences in a time series are counted and then the probability of having that amount of negative or positive differences is computed. A high fraction of positive differences implies a high probability of a positive trend and vice versa. The main advantages of the MK method are that (i) it doesn't require normally distributed data, (ii) it is not affected by outliers (which often is a problem for atmospheric monitoring data), and (iii) it removes the effect of temporal auto-correlation in the data. It should be said, though, that for long-term aggregated quantities like annual means etc., the reasons for using a MK method instead of a standard linear regression is not that strong since the aggregated quantities will normally be less influenced by outliers than single (hourly) data points, and also less auto-correlated.

The Sen's slope method is commonly used in conjunction with the MK method. If the MK statistics indicates the presence of a significant trend, the Sen method is used to compute the slope and the confidence intervals. The essence of this method is simply that the estimated (Sen's) slope is set equal to the median of the slopes when looking at all forward differences in the time series. The Sen method also provides the coefficients (y_0 and a) in a linear equation:

$$y = y_0 + a(t-t_0),$$

where y is the estimated value, t is the time, t_0 is the start time of the time series and a the slope (positive for an increasing trend).

In the calculations applied in this assessment a significance level of p=0.05 was used, i.e. corresponding to a 95 % probability of a significant upward or downward trend. The relative trends were also estimated, given in a %/year unit. The relative trends were computed based on the estimated value at the start ($t=t_0$) as reference, i.e.:

$$\text{Rel. trend (in \%/year)} = 100\ a/y_0$$

refering to the equation above. Using the estimated value at the start allows using a reference that is less sensitive to inter-annual variability than the actual observed value at t_0. To assess the relative change over a given time span, the relative annual trend over the period is simply multiplied by the number of years during that period minus one.

A.4 Model results

The model outputs of the EURODELTA multi-model exercise were also included in relevant sections of the Assessment. It builds upon previous iteration of the CITYDELTA and EURODELTA exercises in support of past TFMM activities (Thunis et al., 2007;Bessagnet et al., 2014;Cuvelier et al., 2007).

The EURODELTA phase was initiated late 2014, it involves 6 regional Chemistry-Transport Models (CTM) in addition to EMEP-MSCW (Chimere, CMAQ, LOTOS-EUROS, MINNI, Polair3D, WRF-Chem), although only 6 models (all but Polair 3D) had delivered all required data to be included in the present report. A synthetic presentation of most participating models can be found in (Bessagnet et al., 2016)

The exercise consists in performing an air quality hindcast over Europe over the 1990-2010 period at regional-scale resolution (25km). The setup is quite constrained with prescribed identical anthropogenic emissions and boundary conditions. A common meteorological driver is also used by most CTMs. The full 21-yr hindcast is supplemented by a number of sensitivity experiment designed to isolate the contribution of (i) European emission changes, (ii) boundary conditions, (iii) meteorology.

Further details are available on the TFMM wiki: https://wiki.met.no/emep/emep-experts/tfmmtrendeurodelta, and will be published when the analysis progresses.

For the quickviews in the present report, the multi-model ensemble is a simple 6-model average at each grid point. One of the model uses a slightly smaller modelling domain, hence the undefined values in the south-east corner of the region.

Appendix B

Methods – Heavy Metals and POPs

B Methods – Heavy Metals and POPs

B.1 Selection of monitoring sites

For HMs, the EMEP database includes data from the early 1970s for a few sites, although most of the time series start in the 1990s. The targeted HMs within the EMEP protocol are Cd, Pb and Hg. These are also the HMs for which most EMEP measurement data are available.

Table B.1: *Long-term data on HMs in air and precipitation at EMEP sites showing the starting year.*

Site (code)	Air			Precipitation		
	Cd	Pb	Hg	Cd	Pb	Hg
Svratouch (CZ01)	1988	1988	-	1994	1994	-
Kosetice (CZ03)	1988	1988	2007	1994	1994	-
Westerland (DE01)	1987	1987	-	1990	1989	-
Waldhof (DE02)	1987	1987	2009	2002	2002	2002
Schauinsland (DE03)	1987	1987	-	2004	2004	2007
Neuglobsow (DE07)	1987	1987	-	2005	2005	-
Schmücke (DE08)	1987	1987	-	2004	2004	-
Zingst (DE09)	1990	1990	-	1996	1995	-
Anholt (DK08)	2010	2010	-	1999	1999	-
Niembro (ES08)	2004	2004	-	2004	2004	2008
Campisabalos (ES09)	2001*	2003	-	2004	2009	-
Virolahti II (FI17)	2008	2007	-	1995	1995	-
Pallas (FI36)	1996	1996	1996	1996	1996	1996
Peyrusse Vieille (FR13)	2003	2003	-	2003	2003	-
Storhofdi (IS91) *	1995	1995	1998	2002	2002	-
Rucava (LV10)	1994	1994	-	1993	1993	2007
De Zilk (NL09)	1994	1990	-	1990	1990	-
Birkenes (NO01/02/99)	1991	1991	1999	1973	1973	1990
Zeppelin (NO42)	1994	1993	1994	-	-	-
Diabla Gora (PL05)	2005	2005	2004	1992*	1992*	-
Bredkalen (SE05)	2009	2009	2009	1987*	1987	1998*
Råöo/Rörvik (SE02/14)	2002	2002	1979	2010	1987	1989
CHOPOK (SK02)	1987	1987	-	2000	2000	-
Stara lesna (sk04)	1988	1988		2000	2000	

**Not continuous sampling*

For POPs, the length of the monitoring data sets varies between sites and type of POP compound (*Table B.2*). The number of EMEP POPs monitoring sites has increased from 7 in 1999 to 30 in 2013. Long-term data series for POPs in the air starting from the 1990s are only available from Zeppelin and Birkenes in Norway, Pallas in Finland, Aspvreten and Råö in Sweden, Storhofdi in Iceland, and Kosetice in Czech Republic while long-term data of POPs in precipitations are also available from Westerland and Zingst in Germany. The following section

provides a trend analysis for benzo(a)pyrene (B[a]P) as a representative of polycyclic aromatic hydrocarbons (PAHs), PCB-153 as a representative of polychlorinated biphenyls (PCBs), hexachlorobenzene (HCB) and the polychlorinated dibenzo-*p*-dioxins and dibenzofurans (PCDD/F) using a combination of modelling and measurements.

Table B.2: *Long-term data on POPs in air and precipitation at EMEP sites showing the starting year.*

Site	Air						Precipitation				
(code)	PCBs	HCB	HCHs	DDTs	CHLs	PAHs	PCBs	HCB	DDTs	HCHs	PAHs
Kosetice (CZ03)	2002	2006	1999	1999		1999	2003		2003	2006	2003
Westerland (DE01)							1996	1996	1996	1996	1996
Zingst (DE09)							1999	1999	1999	1999	1999
Pallas (FI36)	1996		1996	1996		1996	1996			1996	1996
Storhofdi (IS91) *	1995	1995	1995	1995	1995		1995	1995	1995	1995	
Zeppelin (NO42)	1998	1993	1993	1994	1993	1994					
Birkenes (NO02/99)	2004	1991	1991	2010	2010	2009	2004	1991		1991	
Aspvreten (SE12)	1995		1995	1995		1995	1996			1995	1995
Råö/Rörvik (SE02/14)	1994		1994	1996		1994	1995			1995	1995

* Stopped measuring POPs after 2012

B.2 Trend calculations

In order to account for the specificity of heavy metals and POPs phenomenology in the atmosphere, the statistical analysis used to assess trends differs from that of the main pollutants presented in Annex A. The present section prepared by MSC-East in support to the TFMM introduces the relevant approaches.

Typical measurement data on air quality for a sufficiently long period (1990 – 2010) is exemplified in *Figure B.1*, where air concentrations of B[a]P and lead at EMEP sites CZ3 and DE7, respectively, are shown.

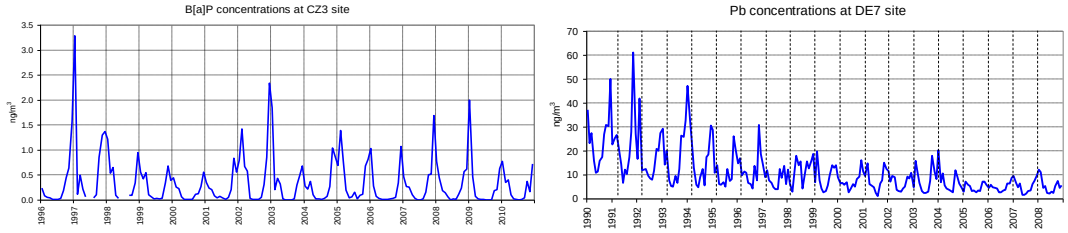

Figure B.1*:* Air concentrations of B[a]P and lead at EMEP sites CZ3 and DE7, 1990 – 2010, monthly means

It is seen that the dynamics of air concentrations can be decomposed to the following three components. First, there is a general decrease of air concentrations during the considered period (main component). Second, air concentrations are subject to strong seasonal variations (seasonal component). Finally, these two tendencies are perturbed by variations not described by the two above components (residues).

B.3 Decomposition of time series

The above mentioned decomposition is illustrated in *Figure B.2* by the time series of air concentrations in Germany (monthly means) from 1990 to 2010.

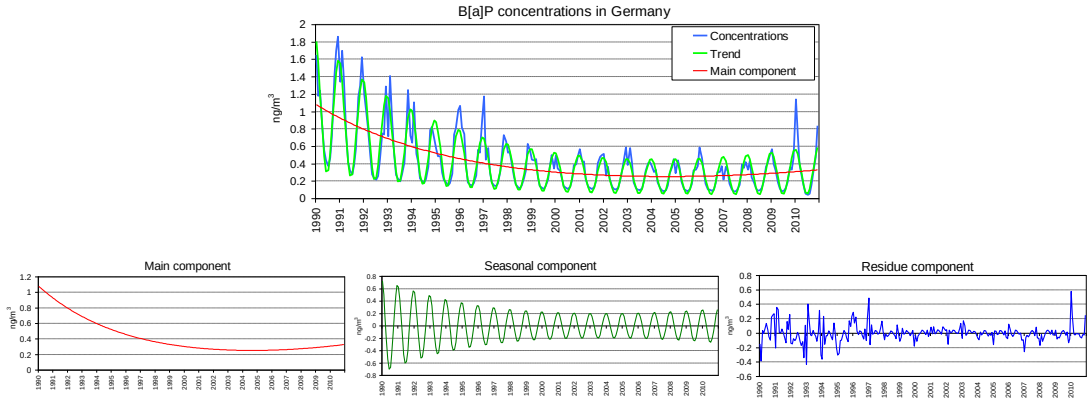

Figure B.2: *Decomposition of time series (B[a]P concentrations in Germany for the period from 1990 to 2010).*

In fact, the approach is based on the combination of exponential trends with standard description of periodic time series (Anderson, 1994).

Analytically, the decomposition is described by the following formulas:

$$C = C_{main} + C_{seas} + C_{res}, \qquad (1)$$

where for each time t

$$C_{main,t} = a_1 \cdot \exp(- t / \tau_1) + a_2 \cdot \exp(- t / \tau_2) \qquad (2)$$

is the main component ;

$$C_{seas,t} = a_1 \cdot \exp(- t / \tau_1) \cdot (b_{1,1} \cdot \cos(2\pi \cdot t - \varphi_{1,1}) + b_{1,2} \cdot \cos(4\pi \cdot t - \varphi_{1,2}) + ...)$$

$$+ a_2 \cdot \exp(- t / \tau_2) \cdot (b_{2,1} \cdot \cos(2\pi \cdot t - \varphi_{2,1}) + b_{2,2} \cdot \cos(4\pi \cdot t - \varphi_{2,2}) + ...) \qquad (3)$$

is the seasonal component; and

$$C_{res,t} = C_t - C_{main,t} - C_{seas,t} \qquad (4)$$

Are the residues. Here a, b are coefficients, τ are characteristic times, and φ are phase shifts. All these parameters are calculated by the least square method.

Quantification of trend

Below parameters describing the above components are described.

Main component. This component is characterized by the following parameters (which are positive for a decline) *Figure B.3*:

total reduction:

$$R_{tot} = (C_{beg} - C_{end}) / C_{beg} = 1 - C_{end} / C_{beg}, \quad (5)$$

maximum and minimum annual reductions

$$R_{max} = \max R_i, R_{min} = \min R_i, \quad (6)$$

where R_i are annual reductions for year i: $R_i = \Delta C_i / C_i = 1 - C_{i+1} / C_i$, and

average annual reduction (geometric mean of annual reductions over all years):

$$R_{av} = 1 - (\Pi_i \, C_i/C_{i-1})^{1/(N-1)} = 1 - (C_{end} / C_{beg})^{1/(N-1)} \quad (7)$$

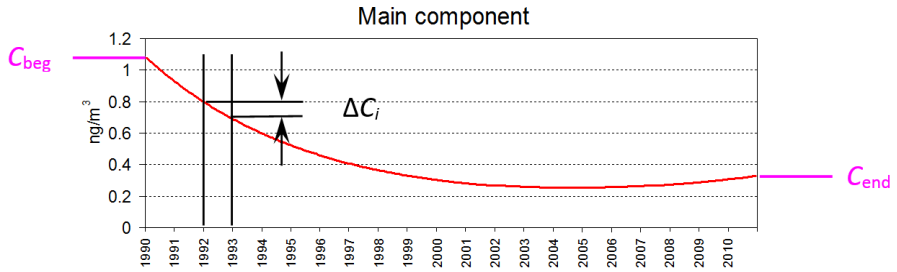

Figure B.3*: Characterization of the main component*

Seasonal component. It can be found that the amplitude of the seasonal component follows the values of the main component (*Figure B.4*):

(a) (b)

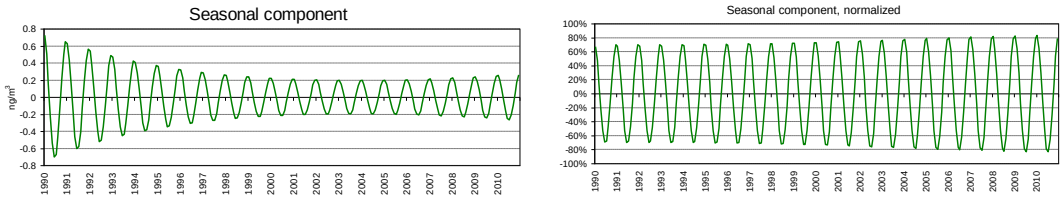

Figure B.4: *Characterization of the seasonal component*

Therefore, it is reasonable to normalize values of this component by values of the main component obtaining the relative contribution of the seasonal component to the trend values (*Figure B.4*). The amplitudes of the normalized seasonal component for each year can be calculated as

$$A_i = (\max(C_{seas,\,i} / C_{main,\,i}) - \min(C_{seas,\,i} / C_{main,\,i})) / 2, \quad (8)$$

where max and min are taken within the year *i*. Average of these amplitudes over all years of the considered period can characterize the change of trend of the main component due to seasonal variations, so that the parameter quantifying seasonal variations will be:

seasonal variation fraction

$$F_{seas} = \langle A_i \rangle, \qquad (9)$$

where <…> stands for average value taken over all years of the considered period. Threshold A t value of 10% is proposed for determination whether seasonal component is essential.

One more important characteristic of seasonal variations is the shift of the maximum value of contamination with respect to the beginning of the year. This shift varies from year to year, and for its characterization the following parameter can be used:

phase shift

$$S = \langle S_i \rangle, \qquad (10)$$

where S_i are shifts (in months) within the year *i* (see *Figure B.5*). Maximum of the trend values is searched using its analytical expression (see formulas (2) and (3)).

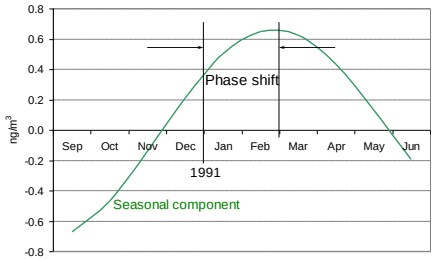

Figure B.5: *Definition of phase shift*

Residues. Similar to theseasonal component, the values of the residues also follow the values of the main component and they should be normalized in a similar way (*Figure B.6*):

(a) (b)

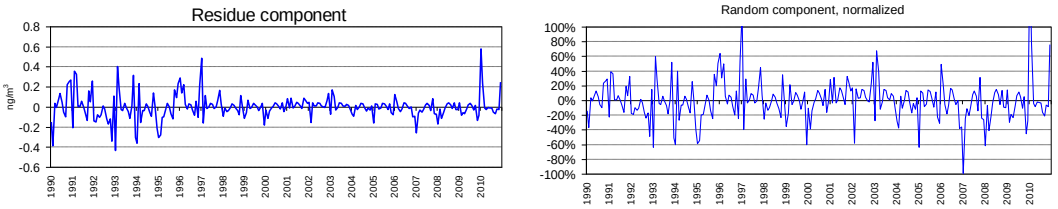

Figure B.6: *Characterization of residues*

So, the parameter characterizing the residues can be defined as

$$F_{res} = \sigma(C_{res,i} / C_{main,i}) \qquad (11)$$

where σ stands for standard deviation over the considered period.

Full list of parameters for quantification of trends is presented in *Table B.3*:

Table B.3*: List of parameters for trend quantification*

Main component	Total reduction over the period R_{tot}	formula (5)
	Maximum annual reduction R_{max}	formula (6)
	Minimum annual reduction R_{min}	
	Average annual reduction R_{av}	formula (7)
Seasonal component	Relative contribution of seasonality F_{seas}	formula (9)
	Shift of maximum contamination S	formula (10)
Residual component	Relative contribution of residues F_{res}	formula (11)

The example of trend evaluation (monthly averages of B[a]P concentrations in Germany in the period from 1990 to 2010) are given in *Table B.4*:

Table B.4: *Trend evaluation (monthly averages of B[a]P concentrations in Germany in the period from 1990 to 2010)*

Considered series	Main component				Seasonality		Residues
	R_{tot}	R_{av}	R_{max}	R_{min}	F_{seas}	S	F_{res}
B[a]P concentrations in Germany, 1990 – 2010	70%	5%	14%	–7%	75%	11.97	28%

The results show that the total reduction of air concentrations over Germany within the considered period is about 70% with an annual average of 5% per year. In the beginning of the period the annual reduction was 14%, but in the last year of the period air concentrations increased by 7%. Air contamination in Germany is subject to strong seasonal variations (around 75% of the main component). Maximum value of contamination takes place mainly in December. The fraction of contamination not explained by the constructed trend is about 30% of main component.

Note. The same approach can be used for trend evaluation at the level of annual averages. In this case all parameters from *Table B.3*, except for parameters for seasonal variations, can be applied.

Appendix C

Trends in air pollutant emissions

C Trends in air pollutant emissions

C.1 Emission trends of photo-oxidant, acidifying and eutrophying pollutants precursors and particulate matter

This annex, contributed by CEIP (EMEP Centre on Emission Inventories and Projections), summarises information on trends and socio-economic drivers of acidifying pollutants and particulate matter (PM) emissions in the EMEP region.

C.1.1 Emission data used in EMEP models

Emissions used in the models are based on data reported by the Parties under the LRTAP Convention (UNECE, 2014), gap-filled with expert estimates.[10] About 40 to 48 Parties regularly report emissions data to EMEP[11], however, the quality of submitted data differs quite significantly across countries. The uncertainty of the reported data (national totals, sectoral data) is considered relatively high particularly for the EMEP East region: the completeness of the reported data has not turned out satisfactory for all pollutants nor sectors. Before emissions can be gridded for use in the models (Fagerli, H. et al., 2015), missing data are gap-filled with expert estimates.

C.1.2 Contribution of individual SNAP sectors to total EMEP emissions

The share of the individual sectors typically does not change significantly over the years. Figure C.*1* shows the contribution of each sector to the total emissions of individual air pollutants (NO_X, NMVOC, SO_X, NH_3, CO and $PM_{2.5}$) in 2013.

[10] For detailed information on gap-filling, see EEA & CEIP technical inventory review report, Annex C: http://www.ceip.at/review_proces_intro/review_reports.

[11] For details, see http://www.ceip.at/status_reporting/2015_submissions.

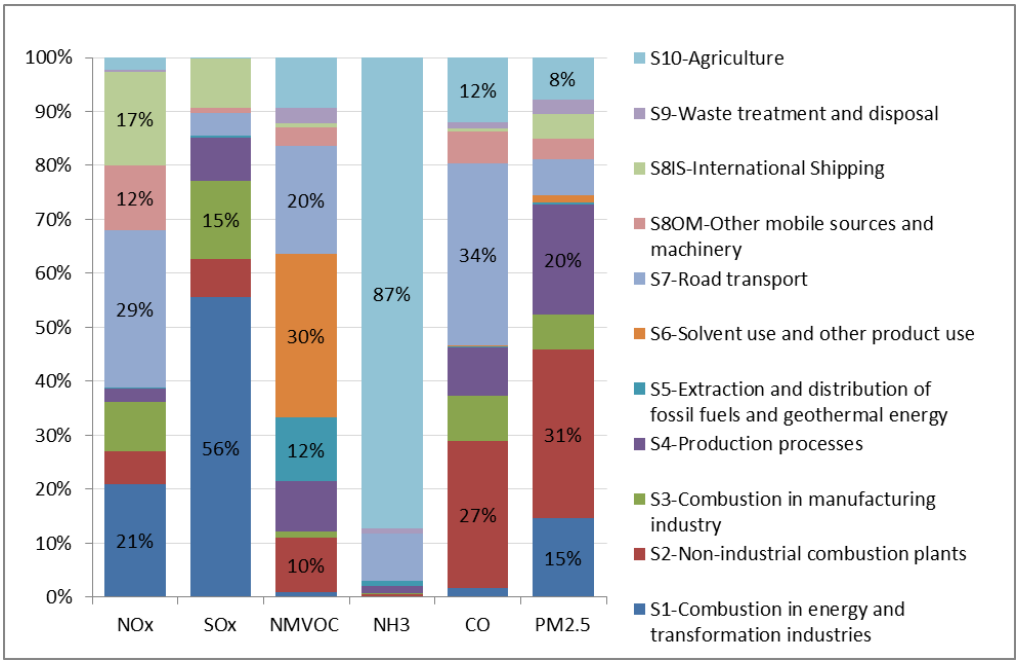

***Figure C.1**: SNAP sector contribution to national total emissions, EMEP extended area (2013)*

The combustion of fossil fuels is responsible for a substantial part of all emissions. 58% of NO_X emissions are produced by the transport sector (S7 and S8), while 21% of NO_X come from large power plants (S1). The main source of SO_X emissions are large-point sources from combustion in energy and transformation industries (56%) although in 2013 this share decreased by 4 percentage points compared to 2012. CO emissions originate primarily from road transport (34%) and residential heating (27%). The main sources (up to 62%) of primary PM emissions are various combustion processes (S1, S2, S7 and S8) but also production processes (S4), which contribute between 13% and 20%, as well as agriculture (S10) with a share of 8%. NMVOC sources are distributed more evenly among the sectors such as solvent use (30%), road transport (20%), extraction of fossil fuels (12%) as well as non-industrial combustion plants (10%). Ammonia arises mainly from agricultural activities (S10), more than 85% across all years.

C.1.3 Emission trends of NO_X, NMVOC, SO_X, NH_3, CO, and $PM_{2.5}$

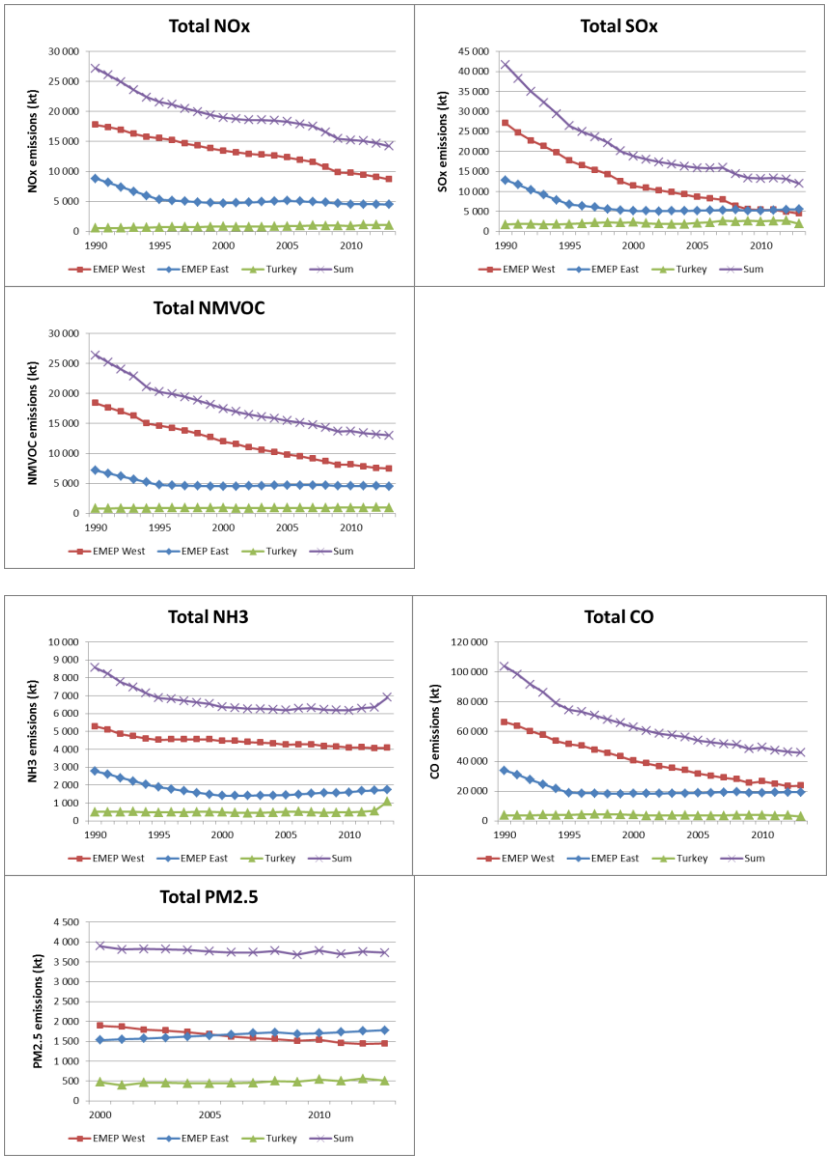

Figure C.2: *Emission trends in the EMEP area, 1990-2013*
Source: EMEP/CEIP data, 1990-2013

For all air pollutants, overall emissions trended downwards between 1990 and 2013 for the EMEP West and EMEP East regions combined (see Figure C.2). This general decline is primarily due to emission reductions in EMEP West in the early 1990s. Both East and West regions registered steep declines in all pollutants; since the mid-1990s however, emissions in EMEP East have stagnated or even increased, while in EMEP West for most pollutants emissions continued to decline considerably.

C.1.4 Socioeconomic drivers

One reason for this divergence in trends is the continuous improvement in technologies employed in the industry, transport and residential sectors in the EMEP West region following the implementation of various energy- and

pollution-related EU directives into national law. This also led to substantial increases in energy efficiency in the EU - especially in the formerly communist new member states, which caught up strongly - but also in the UK and Germany. For example, in Romania, output (GDP) per unit of energy input (kg of oil equivalent) rose by 150% between 1990 and 2012, according to data from the World Development Indicators (see Panel A in Figure C.*3* below).

PANEL A

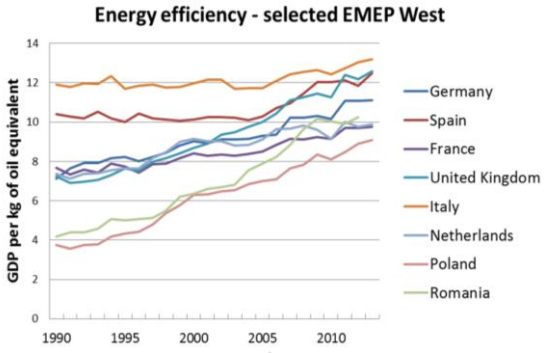

PANEL B

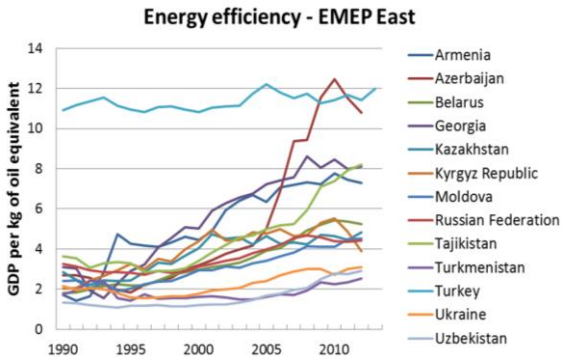

Figure C.3*: Energy efficiency developments in EMEP East and West, 1990-2013. Source: World Bank World Development Indicators, http://data.worldbank.org, accessed February 2016. Note: Energy efficiency defined as GDP per unit of energy input, where GDP is measured in constant 2011 US-Dollars at purchasing power parities (PPP $).*

The overall downward trend in EMEP West for all six pollutants reflects substantial emission reductions in large industrial economies like Germany, the UK, France, Italy and Spain. Especially in the first two, SO_X emissions from burning fossil fuels in the energy and manufacturing industries fell dramatically, among others because of a regulation-induced decline in the sulfur content of mineral oils and a reduction in the use of coal. Similarly, NO_X and CO emissions in the transport sector declined substantially due to fleet renewal as well as improvements in combustion processes and abatement techniques in vehicles such as the catalytic converter. However, it is noteworthy that emissions of these pollutants especially in Poland either increased over the period (NO_X, SO_X) or remained stable (CO). Poland is a large economy with considerable coal resources, and its energy efficiency improvements between 1990 and 2013 were comparatively low (see Panel A of Figure C.*3*). The small dents in emissions of NO_X, SO_X and CO between 2008 and 2009 are related to the drop in production and transport activity resulting from the financial crisis.

A second reason for the divergence in trends between EMEP East and West is the economic recovery in the East region following the collapse of the Soviet Union and the initial years of economic turmoil in the early 1990s. From 1990 to 1995, all EMEP East countries registered negative annual rates of GDP growth on average, as the economic system changed from a planned to a market economy. In the five years that followed, some countries still experienced crises (notably Russia in 1998), but the production and transport infrastructure was improved and the region returned to strong growth in the early 2000s. GDP growth in Azerbaijan, Armenia, Kazakhstan and Turkmenistan was even close to or above 10% for several years between 2000 and 2010.

As a result of the economic recovery, emissions in EMEP East began to stabilise or even increase slightly between 1995 and 2000. The increases were small despite the recovery because energy efficiency also improved with the replacement of outdated Soviet-era infrastructure (see Panel B of Figure C.3). Note however that energy efficiency in the two countries that drive the main trends in the EMEP East region, Russia and Ukraine, is among the lowest and also improved only slightly over the period. Particularly emissions of NO_X, SO_X and CO resulting from fuel combustion in manufacturing industries and from production processes increased. On the other hand, NO_X emissions in the energy industry and in transport as well as CO emissions in transport declined or remained stable, as did emissions in the residential sector. This sectoral heterogeneity explains why emissions from all pollutants are fairly stable overall from the mid-1990s onwards. In addition, improved mitigation technology in industry and transport as well as rising energy efficiency appear to have counterbalanced the growth in emissions from economic development, which led to higher industrial production and greater car use.

C.1.5 Emission trends in the energy and industry sectors

SO_X and NO_X emissions in the energy sector have been regulated in the EU-28 member states with diverse legislation such as the IPPC directive (Switch to best available technologies) as well as national action plans in order to reduce emissions to be in compliance with the NEC Directive.

In the EU-28 energy and transformation sector (S1), NO_X emissions declined because of measures such as the introduction of combustion modification technologies (e.g. the use of low-NO_X burners), implementation of flue gas abatement techniques (e.g. NO_X scrubbers, selective catalytic reduction (SCR) and non-selective catalytic reduction (SNCR) techniques), and fuel switches from coal to gas. SO_X emissions in this sector fell due to measures like switching from high-sulfur solid and liquid fuels to low-sulfur fuels (e.g. natural gas) and the installation of flue gas desulfurisation abatement technology in existing power plants. The $PM_{2.5}$ emissions were reduced mostly as a consequence of installing secondary abatement technologies such as electrostatic precipitators and wet scrubbers. Other countries like Albania, Bosnia and Herzegovina, Iceland, Macedonia, Montenegro, Norway, Serbia and Switzerland do not show a significant reduction between 1990 and 2013.

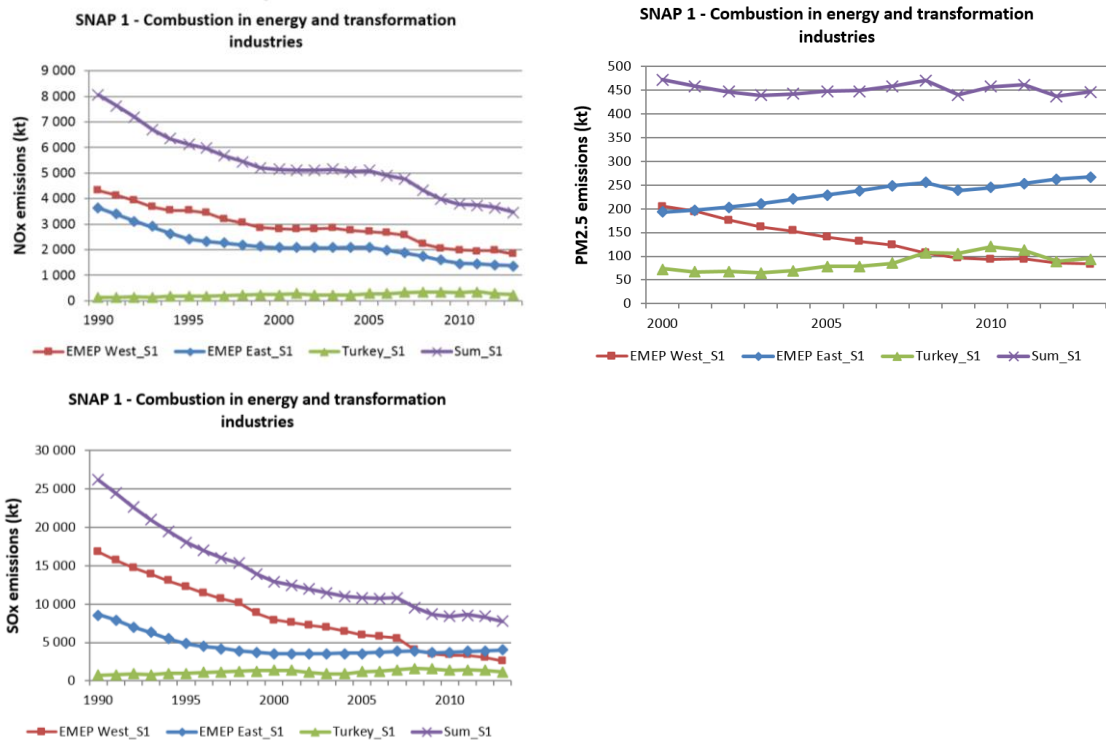

Figure C.4: *NO_X, SO_X and $PM_{2.5}$ emission trends in the energy and transformation industries. Source: EMEP/CEIP data, 1990-2013*

The countries that dominate emissions of NO_X, SO_X and $PM_{2.5}$ from the energy sector (S1) in the EMEP East region are the Russian federation, Ukraine and Belarus. Together, they contributed 65% of total EMEP East emissions in 2013. The decrease of emissions in the early 1990s is due to a decrease of electricity production from thermal power plants, triggered by the socioeconomic changes of the period. Although electricity production from thermal power plants in the Russian federation reached the same level in 2013 as in 1990, NO_X and SO_X emissions were reduced following a switch to coal with low sulfur content and the installation of primary abatement technologies such as low-NOx burners in existing power plants. The switch to low-sulfur coal has also reduced $PM_{2.5}$ emissions. While the countries within the EMEP East and West regions reduced their $PM_{2.5}$ emissions, the overall trend is dominated by the "Rest of the Russian Federation", which shows a substantial increase. NO_X, SO_X and $PM_{2.5}$ emissions emissions in Turkey increased because of the installation of new coal and gas power plants since 1990.

NO_X emissions from non-industrial combustion plants (S2) do not show a significant decrease for the EMEP West region. The main reasons for the emission reduction are the switch from coal and high-sulfur fuels to natural gas and district heating and improved boiler technologies, induced by legislated lower emission limits. SO_X emissions decreased considerably because of a switch from coal to other fuels and because of a legal limit on the sulfur content of liquid fuels. $PM_{2.5}$ emission trends vary among the EU-28 member states. Italy and Romania

registered a rather strong increase because of increased use of biomass, while France reports a significant reduction due to a switch from coal to natural gas and a switch to more efficient biomass boilers.

In the early 1990s, emissions in EMEP East followed the declining fuel use (coal, oil) in this sector (S2) due to the socioeconomic changes in this region. Since 2000, emissions trends have been quite stable, and it appears that the change to modern low-emission boilers is not taking place very widely.

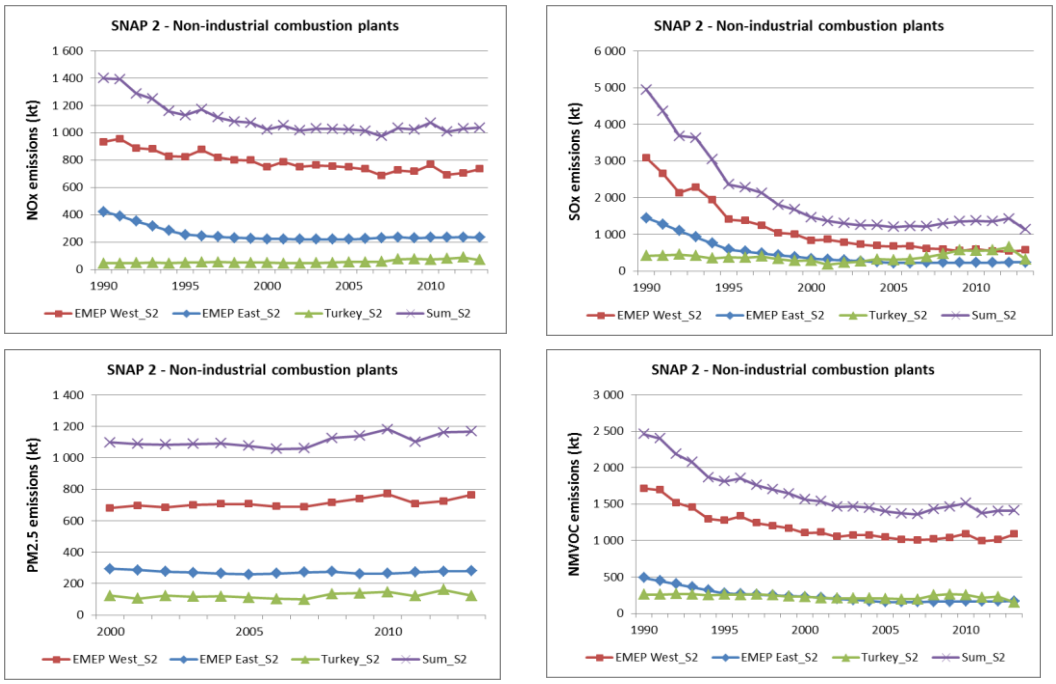

Figure C.5: *NO_X, SO_X, NMVOC and $PM_{2.5}$ emission trends in non-industrial combustion plants. Source: EMEP/CEIP data, 1990-2013*

NO_X and SO_X emissions declined substantially in the industrial production sector (S3 and S4). SO_X emissions fell mainly because of the limitation of sulfur in residual fuel oils and a switch to coal with lower sulfur content. NO_X emissions decreased due to installation of primary and secondary abatement technologies. The decreasing trend of $PM_{2.5}$ emission results from the increased implementation of flue gas cleaning within production industries since the year 2000.

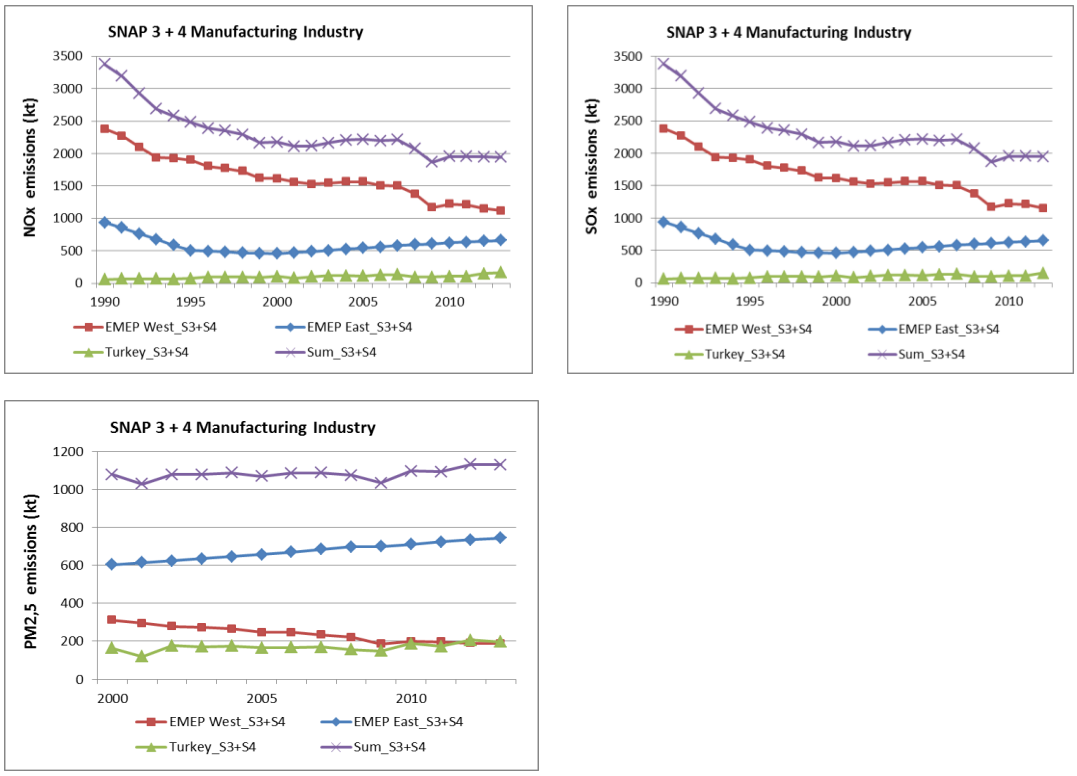

***Figure C.6**: NOx, SOx and $PM_{2.5}$ emission trends in manufacturing industries (S3+S4). Source: EMEP/CEIP data, 1990-2013*

C.1.6 Emission trends in road transport (S7)

Transport sector (S7) contributes significantly to emissions of NOx, NMVOC, CO and partly $PM_{2.5}$ (Figure C.*1*). The trends in the transport time series data result from the general growth in mobility demand and consumption on the one hand, and from the introduction of advanced technologies limiting emissions in modern vehicles (e.g. catalytic converters) and the ongoing economic crisis on the other hand. The NMVOC trends are also influenced by the expansion of the two-wheeler fleet.

NOx emissions in EMEP West decreased by 22% between 1990 and 2000 and by an additional 42% in the period 2000 to 2013. CO emissions declined by 47% between 1990 and 2000 and by 72% in the period 2000 to 2013. NMVOC emissions fell by 48% between 1990 and 2000 and by an additional 72% in the period 2000 to 2013. In EMEP East, the emission trends of NOx, NMVOC and CO between 1990 and 2000 are comparable to EMEP West. However, the reduction between 2000 and 2013 is limited, and in a number of countries emissions even increased. SO_X emissions from *road transport* (S7) have been reduced by more than 90% since 1990 and do not contribute significantly to overall SOx emissions in the EMEP area.

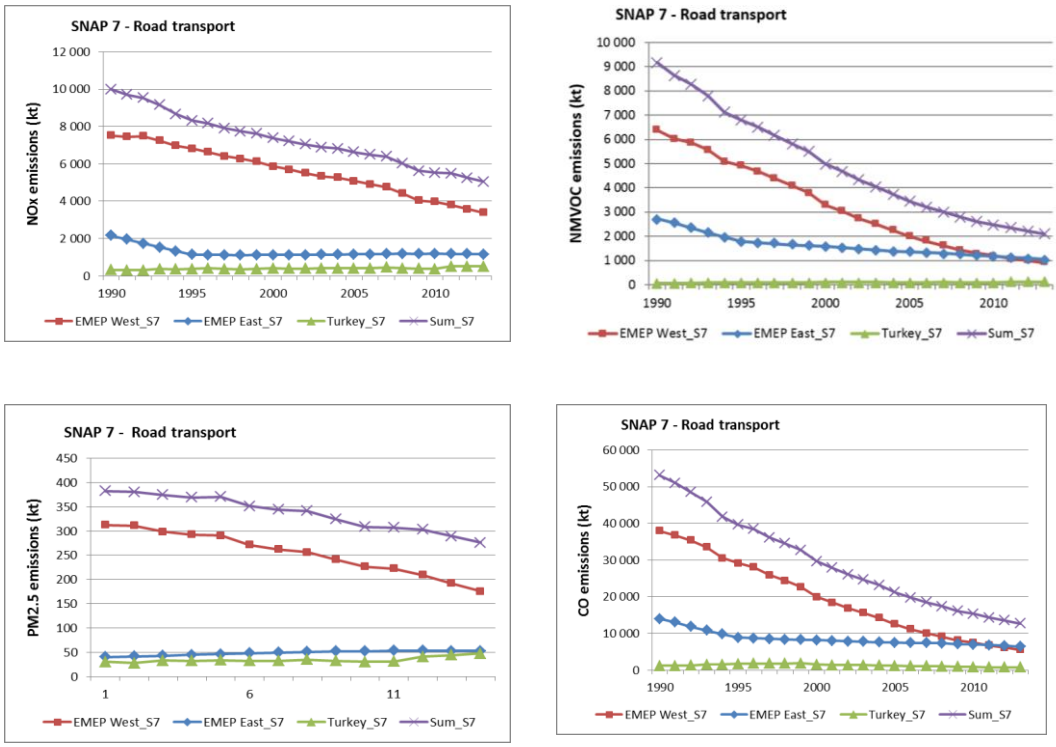

***Figure C.7**: NOX, NMVOC, CO and PM2.5 emission trends in road transport (S7). Source: EMEP/CEIP data, 1990-2013*

C.1.7 Emission trends in agriculture (S10)

Agriculture is the main source of NH_3, contributing more than 90% of overall emissions. Emissions mainly occur during the housing of animals, storage and application of animal manures. Application of inorganic N-fertilizers is also a relevant source of ammonia emissions, especially when using urea. Between 1990 and 2013, emissions decreased by 25% in the EMEP West region and by 39% in EMEP East. The main drivers are declining animal numbers, especially at the beginning of the 1990s. Thus, emissions declined the most between 1990 and 2000 (-18% for EMEP West and -50% for EMEP East). After 2000, the decrease in the EU-28 lost pace, and emissions even tended to increase in EMEP East and Turkey. Improved management practices in the whole nitrogen cycle (livestock feeding strategies, measures in the areas of housing, storage and application techniques) supported the declining trend in the EMEP West region.

With a share of 3% in 2013, agriculture is only a minor source of total reported NO_X emissions. The main activity resulting in NO_X emissions is the application of organic and inorganic N-fertilizers; a minor source is the field burning of agricultural residues. At present estimates are highly uncertain. Reported emissions are incomplete and heavily differ between countries. In the EMEP West region, a reduced application of fertilizers is responsible for decreasing of NO_X emissions between 1990 and 2013 (-20%). Most of the decrease (-15%) occurred in the 1990s, while a smaller decrease could be achieved over the 2000s (-6% from 2000 to 2013). In EMEP East, the trend (+15% from 1990 to 2013) partly

follows GDP trends observing reductions in the 1990s (-32%) and a continuous increase of emissions over the 2000s (+69% from 2000 to 2013).

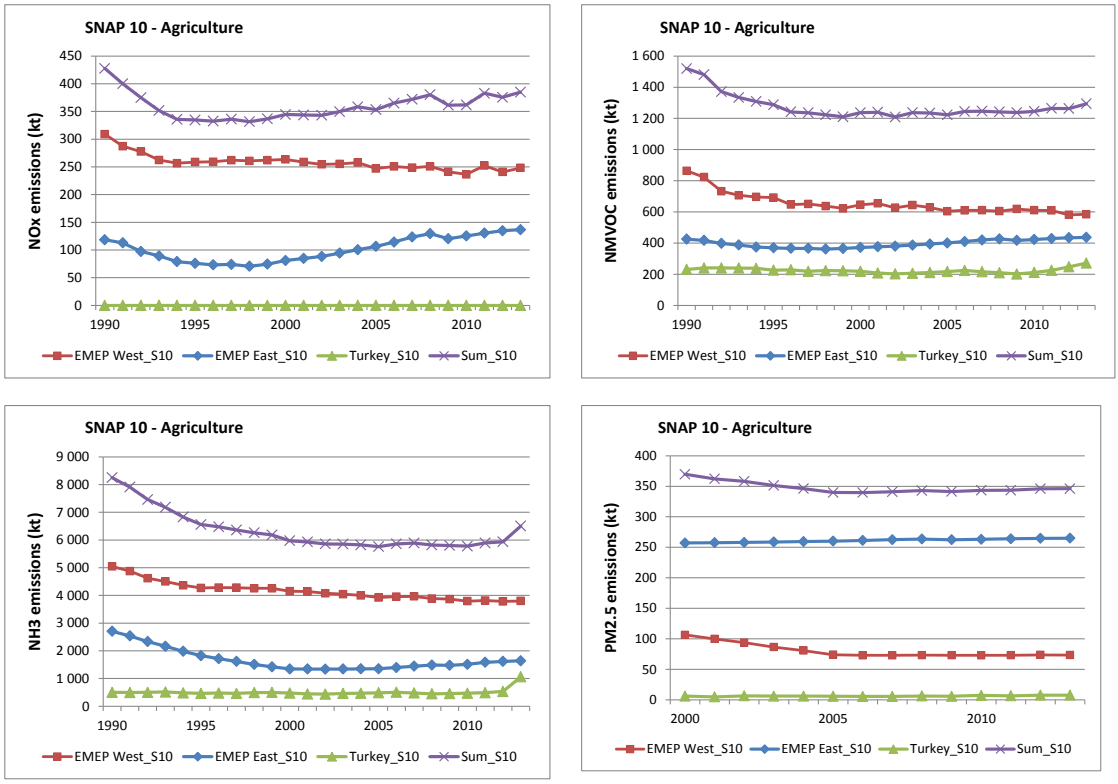

***Figure C.8**: NOX, NMVOC, NH3 and PM2.5 emission trends in agriculture (S10). Source: EMEP/CEIP data, 1990-2013*

Around 9% of NMVOC emissions come from agriculture. The main source of NMVOC is manure management; minor sources are the field burning of agricultural residues and the cultivation of agricultural crops. Emissions are highly variable and uncertain. Reported emissions are incomplete and differ between countries as manure management is a new source to be reported for NMVOC. In EMEP West, emissions declined by 32% between 1990 and 2013, mainly attributable to decreasing livestock numbers in the 1990s. From 1990 to 2000, emissions fell by 25%. Looking at the entire period 1990 to 2013, the EMEP East region registered an increase of NMVOC emission of 3%. While emissions decreased by 13% between 1990 and 2000, they increased by 18% from 2000 to 2013.

Animal husbandry and to a smaller extent field burning activities and agricultural crop operations are the relevant sources of $PM_{2.5}$ emissions in agriculture, covering 5% of total $PM_{2.5}$ emissions in EMEP West and 15% of the total in EMEP East. Emission trends in EMEP West (-31% from 2000 to 2013) predominantly reflect declining livestock numbers. In EMEP East (+3% from 2000 to 2013), they partly follow the GDP trend.

The contribution of agriculture to SO_X and CO emissions is rather limited. The main source of both is the field burning of agricultural residues. Until the 1990s, stubble burning was a widespread agricultural practice. Improvements such as ploughing the stubble back into the ground and legal restrictions resulted in decreased emissions in EMEP West from 1990-2013 (-37% for SO_X and -49% for

CO). All of the decrease in EMEP East occurred in the 1990s (-18% for SO_X and -20% for CO), while during the 2000s, emissions trended upwards (+30% for SO_X and +35% for CO).

C.2 Heavy Metals emissions

This Chapter, prepared by MSC-E, provide the Heavy Metals and POPs emission data used in the model simulation of trends supporting the present report.

Heavy metal emissions are presented in *Figure C.9*. Total anthropogenic emissions of lead, cadmium and mercury were 43631 tonnes, 500 tonnes and 402 tonnes, respectively in 1990. In 2012 emissions of HMs amounted to 3895 tonnes for Pb, 182 tonnes for Cd and 164 tonnes for Hg.

(a)

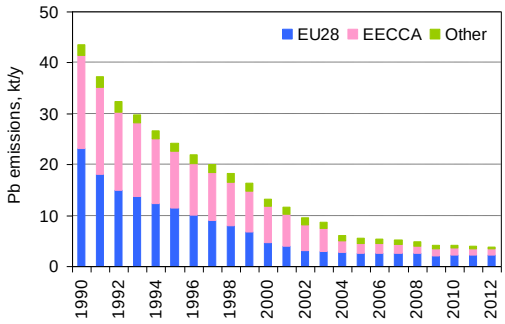

(b)

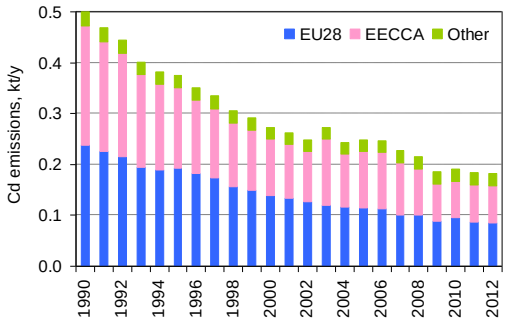

(c)

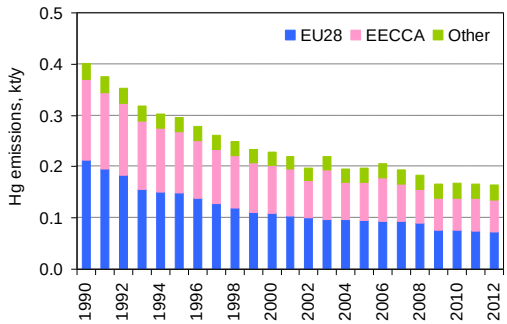

Figure C.9: *Temporal changes of lead (a), cadmium (b), and mercury (c) anthropogenic emissions in the EU28, EECCA, and other EMEP countries from 1990 to 2012*

Emissions of HMs have considerably decreased in the EMEP region over the last two decades. Lead emissions have dropped by 90% since 1990, whereas emissions of cadmium and mercury have decreased approximately by 60%. Maps of spatial distribution of emissions of heavy metals are given in *Figure C.10*.

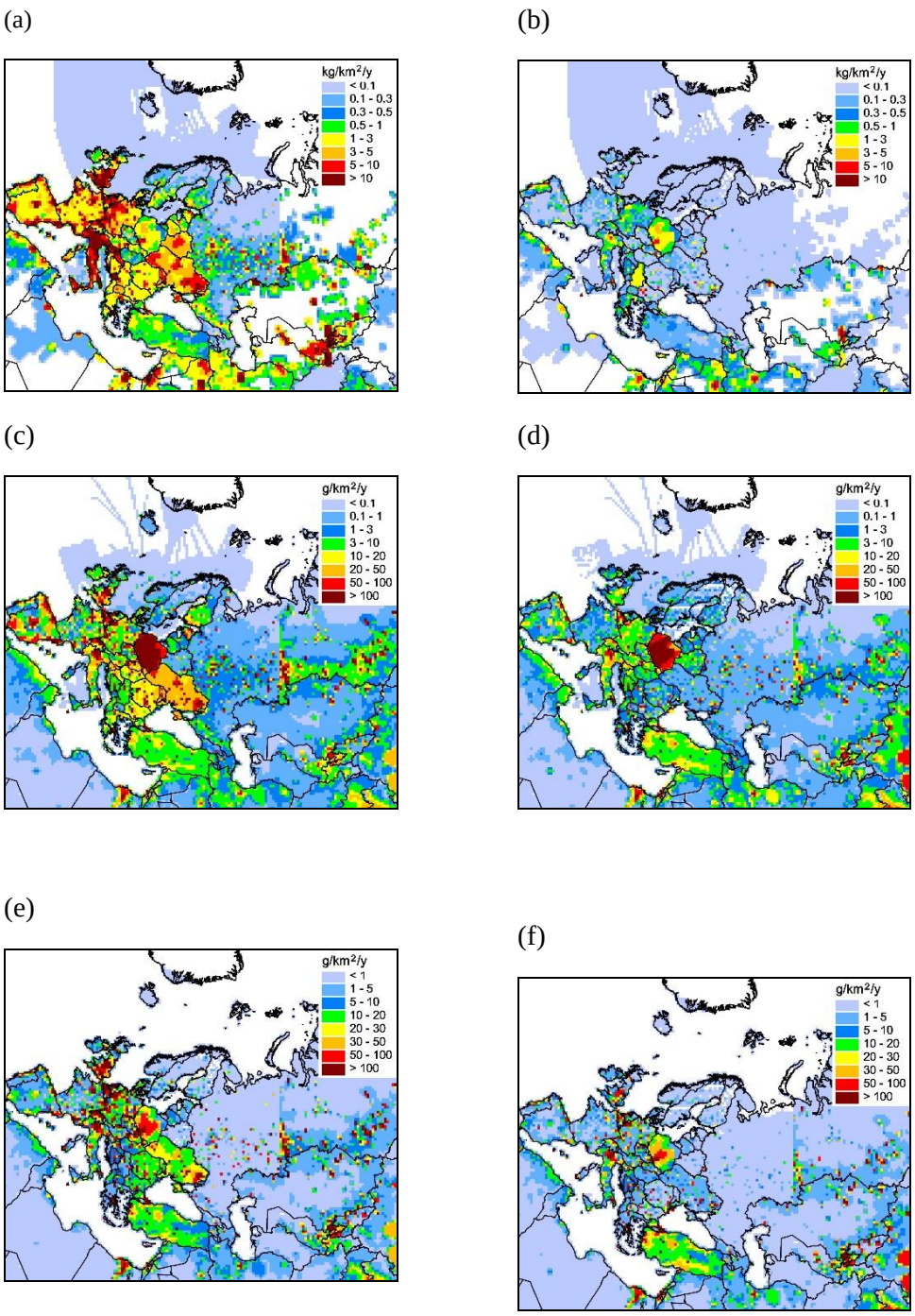

Figure C.10: *Spatial distribution of anthropogenic emissions over the EMEP domain for lead in 1990 (a) and 2012 (b), cadmium in 1990 (c) and 2012 (d), and mercury in 1990 (e) and 2012 (f)*

The most noticeable HM emission reduction was in the EU28 countries. Lead, cadmium and mercury emissions declined by 93%, 69%, and 60% respectively.

A slight decrease of emissions is observed in the EECCA countries for cadmium and mercury (about 15%). At the same time, for lead the reduction of emissions in the EECCA countries is very close to the EU28 countries.

The other EMEP countries are characterized by almost the same dynamics of changes as in the EU28 countries.

Pollution levels in the EMEP region can be significantly affected by mercury emissions from distant global sources. In order to take into account this effect global inventories of mercury anthropogenic emissions to the atmosphere are used in modeling (Pacyna and Pacyna, 2002;Pacyna et al., 2006;Pacyna et al., 2009;AMAP/UNEP, 2008, 2013;Ilyin et al., 2015).The spatial distribution of mercury on a global scale is given in Figure C.*10*.

C.3 Emission data of POPs used for model assessment

Emission data of persistent organic pollutants used for model assessment of trends are presented in *Figure C.11*. Total anthropogenic emissions of 4 PAHs, PCDD/Fs, HCB and PCB-153 were 2487 tonnes, 14.8 kg TEQ, 6.1 tonnes and 9.6 tonnes, respectively in 1990. In 2012 emission of POPs amounted to 1517 tonnes for 4 PAHs, 5.7 kg TEQ for PCDD/Fs, 0.95 tonnes for HCB and 1.5 tonnes for PCB-153.

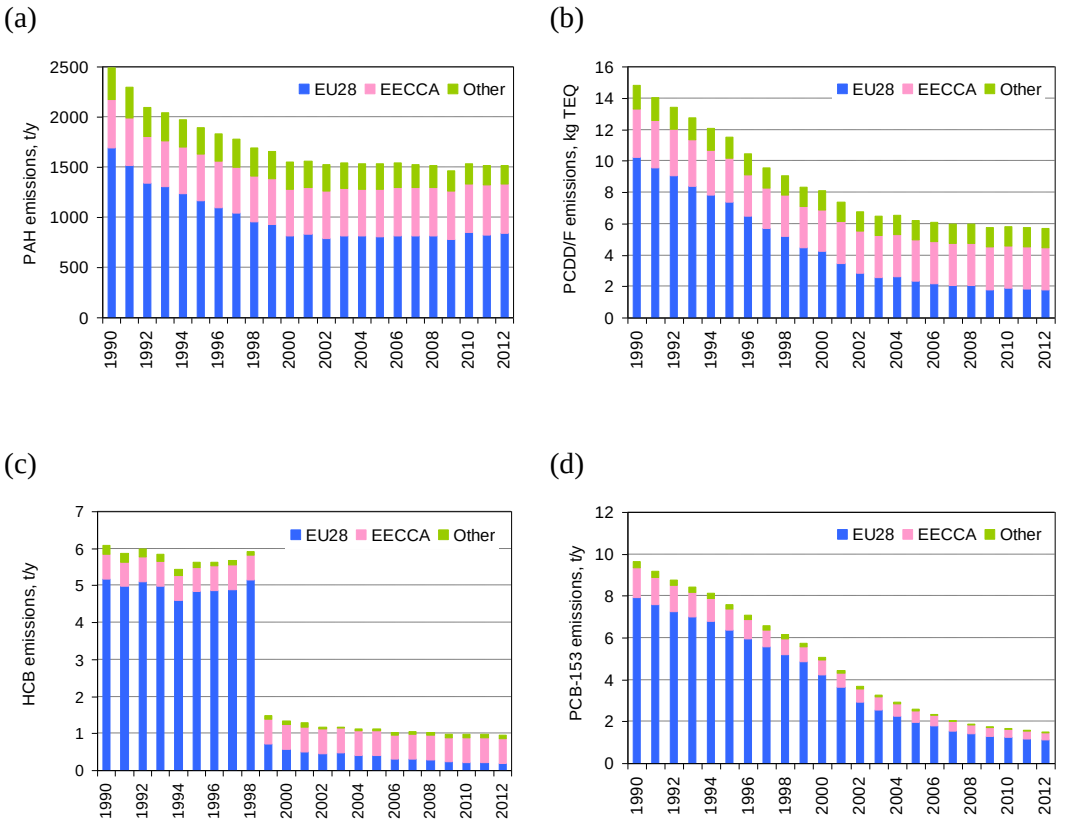

Figure C.11: *Temporal changes of 4 PAHs (a), PCDD/Fs (b), HCB (c), and PCB-153 (d) emissions in the EU28, EECCA, and other EMEP countries from 1990 to 2012*

According to officially reported data and expert estimates anthropogenic emissions of POPs in the EMEP countries have decreased from 1990 to 2012 by 84% for HCB and PCB-153, by 61% for PCDD/Fs, and by 39% for PAHs. Maps of spatial distribution of emissions of POPs are given in *Figure C.12*.

(a) (b)

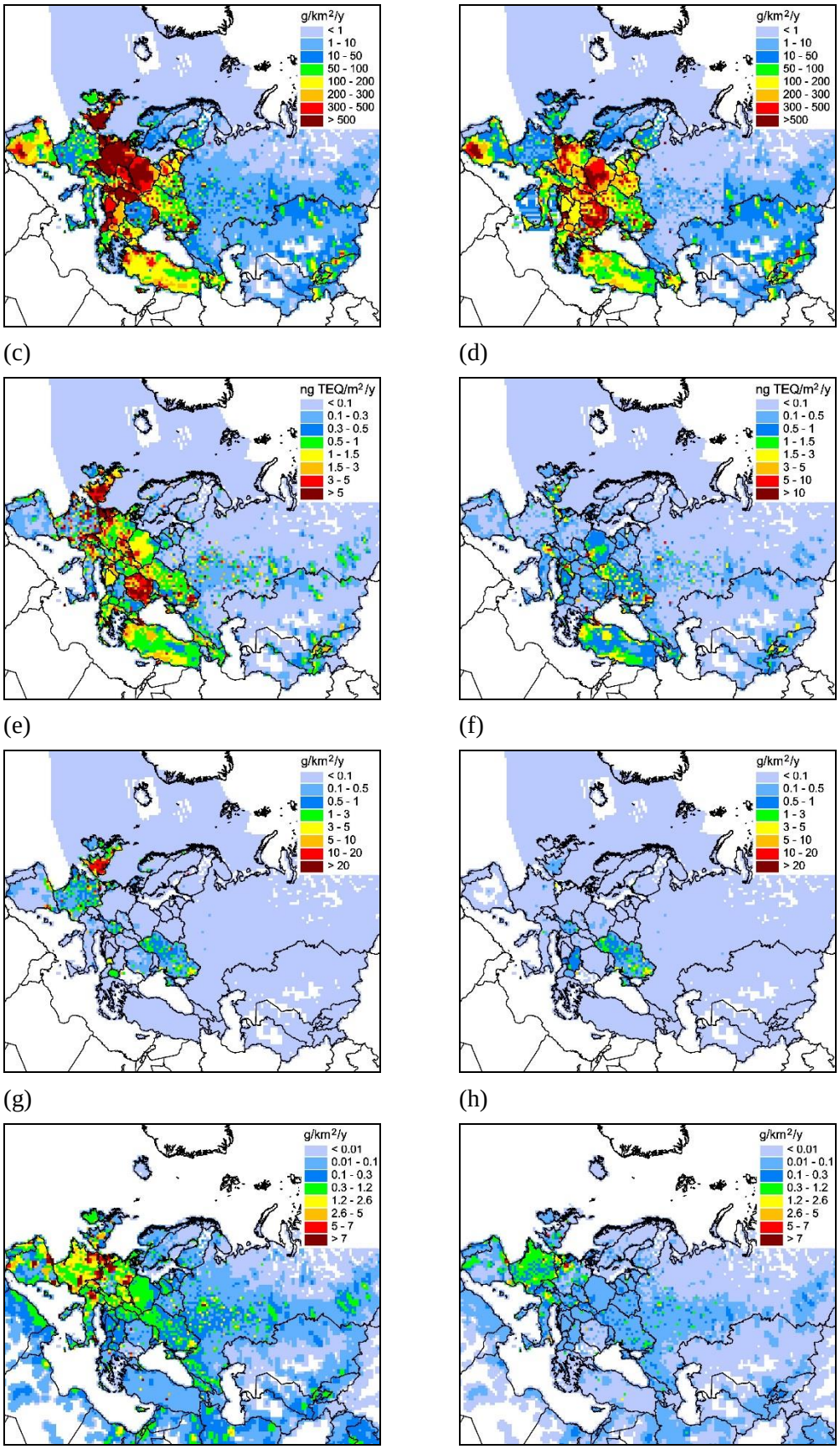

***Figure C.12**: Spatial distribution of emissions in the EMEP countries with resolution 50x50 km2 for the sum of 4 PAHs in 1990 (a) and in 2013 (b), PCDD/F in 1990 (c) and in 2013 (d),HCB in 1990 (e) and 2013 (f), PCB-153 in 1990 (g) and 2013 (h)*

Changes of POP emissions in the EMEP region during the considered period were inhomogeneous. Substantially different rates of changes can be seen in the EU28, EECCA, and the other EMEP countries. The most significant decline of POP emissions took place in the EU28 countries. Particularly, emissions of HCB, PCB-153, PCDD/Fs, and PAHs dropped by 96%, 86%, 83%, and 50% respectively. Marked change of anthropogenic HCB emissions from 1998 to 1999 was conditioned by sharp decrease of releases reported by the UK.

The lowest decrease of emissions is seen in the EECCA countries for PCDD/Fs, PAHs, and HCB. In particular, it varies from about 10% for PCDD/Fs to almost no decrease for PAHs and HCB. At the same time, for PCB-153 the decline of emissions in the EECCA countries is almost similar to the EU28 countries according to the available expert estimates. The other EMEP countries are characterized by moderate changes.

Pollution by POPs is formed by different sources including anthropogenic emissions of the EMEP countries, distant emissions outside of the EMEP domain, and secondary emissions both within the EMEP region and beyond its boundaries.

Model evaluation of HCB pollution was performed on the basis of officially reported emissions of the EMEP countries and experimental dataset of global HCB emissions, which described contemporary levels of HCB releases as well as historical emissions for the period from 1945 to 2013 (Shatalov et al., 2010). Model simulations of PCB-153 were carried out on the basis of expert estimates of global PCB emissions (Breivik et al., 2007). Emissions used for modelling of PCDD/Fs are based on experimental emission scenarios constructed on the basis of official data and data of the UNEP SC inventory.

Appendix D

Glossary

D Glossary

ACTRIS: Aerosol, Clouds, and Trace gases Research InfraStructure Network.

AOT40: Accumulated ozone exposure over 40ppb

CCC: Chemical Coordinating Centre

CEIP: Centre for Emission Inventories and Projections

CH_4: Methane

CIAM: Centre for Integrated Assessment Modelling

CLRTAP: Convention on Long-range Transboundary Air Pollution

EEA: European Environment Agency

EECCA: Eastern Europe, Caucasus and Central Asia

EMEP: Cooperative Programme for Monitoring and Evaluation of the Long-range Transmission of Air Pollutants in Europe

EU28: The 28 Member State of the European Union

GAW: Global Atmosphere Watch

HCB: Hexachlorobenzene

MDA8: maximum daily 8-hours mean ozone

MSC-W: Meteorological Synthesizing Centre-West

MSC-E: Meteorological Synthesizing Centre-East

NMVOCs: non-methane volatile organic compounds

NO_2, NOx, NO_3^-: nitrogen dioxide, nitrogen oxides, nitrate

NH_3, NH_4^+: ammonia, ammonium

O3: Ozone

OECD: Organisation for Economic Co-operation and Development

PAH: Polycyclic aromatic hydrocarbon

PCB: polychlorinated biphenyl

PCCD: Polychlorinated dibenzodioxins

ppb: part per billion

PM, PM_{10}, $PM_{2.5}$: Particulate Matter, finer than 10 and 2.5 µm aerodynamic diameter, respectively

POP: Persistent Organic Pollutants

SO_2, SOx, SO_4^{2-}: sulfur dioxide, sulfur oxides, sulfate

SOMO35: Sum of ozone means (MDA8) over 35ppb

TFMM: Task Force on Measurements and Modelling

WGE: Working Group on Effects

WHO: World Health Organisation

WMO: World Meteorological Organisation

Appendix E

References

E References

Aas, W., Bohlin-Nizzetto, P. (2015) Heavy metals and POP measurements 2013. Kjeller, NILU (EMEP/CCC, 3/2015).

Abad, E., Martínez, K., Gustems, L., Gomez, R., Guinart, X., Hernández, I., Rivera, J. (2007) Ten years measuring PCDDs/PCDFs in ambient air in Catalonia (Spain). *Chemosphere, 67,* 1709-1714.

AMAP/UNEP (2008) Technical background report to the global atmospheric mercury assessment. Oslo, Norway, Arctic Monitoring and Assessment Programme / Geneva, Switzerland, UNEP Chemicals Branch.

AMAP/UNEP (2013) Technical background report for the global mercury assessment 2013. Oslo, Norway, Arctic Monitoringand Assessment Programme / Geneva, Switzerland, UNEP Chemicals Branch.

Anderson, T. W. (1994) The statistical analysis of time series. Hoboken, NJ, John Wiley & Sons.

Banzhaf, S., Schaap, M., Kranenburg, R., Manders, A. M. M., Segers, A. J., Visschedijk, A. J. H., Denier van der Gon, H. A. C., Kuenen, J. J. P., van Meijgaard, E., van Ulft, L. H., Cofala, J., Builtjes, P. J. H. (2015) Dynamic model evaluation for secondary inorganic aerosol and its precursors over Europe between 1990 and 2009. *Geosci. Model Dev., 8,* 1047-1070, doi:10.5194/gmd-8-1047-2015.

Bessagnet, B., Colette, A., Meleux, F., Rouïl, L., Ung, A., Favez, O., Cuvelier, C., Thunis, P., Tsyro, S., Stern, R., Manders, A. M. M., Kranenburg, R., Aulinger, A., Bieser, J., Mircea, M., Briganti, G., Cappelletti, A., Calori, G., Finardi, S., Silibello, C., Ciarelli, G., Aksoyoglu, S., Prevot, A., Pay, M. T., Baldasano, J. M., Garcia, M., Garrido, J., Palomino, I., Martin F., Pirovano, G., Roberts., P., Gonzales, L. (2014) The EURODELTA III exercise – Model evaluation with observations issued from the 2009 MEP intensive period and standard measurements in Feb/Mar 2009. TFMM & MSC-W (Technical report, 1/2014).

Bessagnet, B., Pirovano, G., Mircea, M., Cuvelier, C., Aulinger, A., Calori, G., Ciarelli, G., Manders, A., Stern, R., Tsyro, S., García Vivanco, M., Thunis, P., Pay, M. T., Colette, A., Couvidat, F., Meleux, F., Rouïl, L., Ung, A., Aksoyoglu, S., Baldasano, J. M., Bieser, J., Briganti, G., Cappelletti, A., D'Isodoro, M., Finardi, S., Kranenburg, R., Silibello, C., Carnevale, C., Aas, W., Dupont, J. C., Fagerli, H., Gonzalez, L., Menut, L., Prévôt, A. S. H., Roberts, P., White, L. (2016) Presentation of the EURODELTA III inter-comparison exercise – Evaluation of the chemistry transport models performance on criteria pollutants and joint analysis with meteorology. *Atmos. Chem. Phys. Discuss.,* doi:10.5194/acp-2015-736, *in review*.

Breivik, K., Sweetman, A., Pacyna, J. M., Jones, K. C. (2007) Towards a global historical emission inventory for selected PCB congeners - A mass balance approach-3. An update. *Sci. Total Environ., 377,* 296-307.

Bruckmann, P., Hiester, E., Klees, M., Zetzsch, C. (2013) Trends of PCDD/F and PCB concentrations and depositions in ambient air in Northwestern Germany. *Chemosphere, 93,* 1471-1478, doi:10.1016/j.chemosphere.2013.07.029.

Colette, A., Beauchamp, M., Malherbe, L., Solberg, S. (2015) Air quality trends in AIRBASE in the context of the LRTAP Convention. Bilthoven, European Topic Centre on Air Pollution and Climate Change Mitigation (ETC/ACM Technical Paper 2015/4).

Cooper, O. R., Parrish, D. D., Ziemke, J., Balashov, N. V., Cupeiro, M., Galbally, I. E., Gilge, S., Horowitz, L., Jensen, N. R., Lamarque, J.-F., Naik, V., Oltmans, S. J., Schwab, J., Shindell, D. T., Thompson, A. M., Thouret, V., Wang, Y., Zbinden, R. M. (2014) Global distribution and trends of tropospheric ozone: An observation-based review *Elem. Sci. Anth., 2,* 000029, doi:10.12952/journal.elementa.000029.

Cuvelier, C., Thunis, P., Vautard, R., Amann, M., Bessagnet, B., Bedogni, M., Berkowicz, R., Brandt, J., Brocheton, F., Builtjes, P., Carnavale, C., Coppalle, A., Denby, B., Douros, J., Graf, A., Hellmuth, O., Hodzic, A., Honoré, C., Jonson, J., Kerschbaumer, A., de Leeuw, F., Minguzzi, E., Moussiopoulos, N., Pertot, C., Peuch, V. H., Pirovano, G., Rouil, L., Sauter, F., Schaap, M., Stern, R., Tarrason, L., Vignati, E., Volta, M., White, L., Wind, P., Zuber, A. (2007) CityDelta: A model intercomparison study to explore the impact of emission reductions in European cities in 2010. *Atmos. Environ., 41,* 189-207.

De Wit, H. A., Hettelingh, J. P., Harmens, H. (2015) Trends in ecosystem and health responses to long-range transported atmospheric pollutants. Oslo, NIVA (NIVA report, 6946-2015) (ICP Waters report, 125/2015).

Dentener, F., Keating, T, Akimoto, H. (eds.) (2010) Hemispheric transport of air Pollution 2010, Part A: Ozone and particulate matter. Prepared by the Task Force on Hemispheric Transport of Air Pollution. New York and Geneva, United Nations (Air pollution studies, 17).

Derwent, R. G., Dernie, J. I. R., Dollard, G. J., Dumitrean, P., Mitchell, R. F., Murrells, T. P., Telling, S. P., Field, R. A. (2014) Twenty years of continuous high time resolution volatile organic compound monitoring in the United Kingdom from 1993 to 2012. *Atmos. Environ., 99,* 239-247, doi:10.1016/j.atmosenv.2014.10.001.

EC (2008) Directive 2008/50/EC of the European Parliament and of the Council of 21 May 2008 on ambient air quality and cleaner air for Europe, *Off. J. Eur. Union: Legis, L 152,* 1-44.

Fagerli, H., Tsyro, S., Simpson, D., Schulz, M., Gauss, M., Jonson, J.E., Benedictow, A., Wind, P., Nyíri, A., Steensen, B.M., Valiyaveetil, S., Aas, W., Hjellbrekke, A.-G., Solberg, S., Stebel, K., Tørseth, K., Yttri, K.E., Mareckova, K., Wankmüller, R., Pinterits, M., Ullrich, B., Posch, M., van der Gon, H.D., Alastuey, A., Theys, N. (2015) Transboundary particulate matter, photo-oxidants, acidifying and eutrophying components. EMEP Status Report 2015. Oslo, Norwegian Meteorological Institute - MSC-W (EMEP report, 1/2015).

Fowler, D., Muller, J., Smith, R. I., Cape, J. N., Erisman, J. W. (2005) Nonlinearities in source receptor relationships for sulfur and nitrogen compounds. *Ambio, 34,* 41-46, doi: 10.1579/0044-7447-34.1.41.

Fowler, D., Smith, R., Muller, J., Cape, J., Sutton, M., Erisman, J., Fagerli, H. (2007) Long term trends in sulphur and nitrogen deposition in Europe and the cause of non-linearities. *Water Air Soil Pollut. Focus, 7,* 41-47, doi:10.1007/s11267-006-9102-x.

Fowler, D., Steadman, C. E., Stevenson, D., Coyle, M., Rees, R. M., Skiba, U. M., Sutton, M. A., Cape, J. N., Dore, A. J., Vieno, M., Simpson, D., Zaehle, S., Stocker, B. D., Rinaldi, M., Facchini, M. C., Flechard, C. R., Nemitz, E., Twigg, M., Erisman, J. W., Butterbach-Bahl, K., Galloway, J. N. (2015) Effects of global change during the 21st century on the nitrogen cycle. *Atmos. Chem. Phys., 15,* 13849-13893, doi:10.5194/acp-15-13849-2015.

Gilbert, R. O. (1987) Statistical methods for environmental pollution monitoring. New York, John Wiley & Sons.

Hellén, H., Kouznetsov, R., Anttila, P., Hakola, H. (2015) Increasing influence of easterly air masses on NMHC concentrations at the Pallas-Sodankylä GAW station. *Boreal Environ. Res., 20,* 542-552.

Ilyin, I., Rozovskaya, O., Travnikov, O., Varygina, M., Aas, W. (2015) Heavy metals: Analysis of long-term trends, country-specific research and progress in mercury regional and global modelling. Moscow/Kjeller, Meteorological Synthesizing Centre - East/Chemical Coordinating Centre (EMEP Status Report 2/2015).

Katsoyiannis, A., Gioia, R., Sweetman, A. J.,Jones, K. C. (2010) Continuous monitoring of PCDD/Fs in the UK atmosphere: 1991−2008. *Environ. Sci. Technol., 44,* 5735-5740.

Lövblad, G., Tarrasón, L., Tørseth, K., Dutchak, S. (2004) EMEP Assessment. Part I - European Perspective. Oslo, Meteorological Synthesizing Centre-West.

Maas, R., Grennfelt , P. (eds.) (2016) Towards cleaner air - Scientific Assessment Report 2016. EMEP-Steering body and Working Group on Effects - Convention on Long-Range Transboundary Air Pollution 2016. Geneva, UNECE.

Martin, S. T. (2000) Phase transitions of aqueous atmospheric particles. *Chem. Rev., 100,* 3403-3454, doi:10.1021/cr990034t.

Melymuk, L., Bohlin, P., Sáňka, O., Pozo, K., Klánová, J. (2014) Current challenges in air sampling of semivolatile organic contaminants: sampling artifacts and their influence on data comparability. *Environ. Sci. Technol., 48,* 14077-14091.

Monks, P. S., Archibald, A. T., Colette, A., Cooper, O., Coyle, M., Derwent, R., Fowler, D., Granier, C., Law, K. S., Mills, G. E., Stevenson, D. S., Tarasova, O., Thouret, V., von Schneidemesser, E., Sommariva, R., Wild, O., Williams, M. L. (2015) Tropospheric ozone and its precursors from the urban to the global scale from air quality to short-lived climate forcer. *Atmos. Chem. Phys., 15,* 8889-8973.

Paatero, P., Tapper, U. (1994) Positive matrix factorization: A non-negative factor model with optimal utilization of error estimates of data values. *Environmetrics, 5,* 111-126, doi:10.1002/env.3170050203.

Pacyna, E. G., Pacyna, J. M. (2002) Global emission of mercury from anthropogenic sources in 1995. *Water Air Soil Pollut., 137,* 149-165.

Pacyna, E. G., Pacyna, J. M., Steenhuisen, F., Wilson, S. (2006) Global anthropogenic mercury emission inventory for 2000. *Atmos. Environ., 40,* 4048-4063.

Pacyna, E. G., Pacyna, J. M., Sundseth, K., Munthe, J., Kindbom, K., Wilson, S., Steenhuisen, F., Maxson, P. (2009) Global emission of mercury to the atmosphere from anthropogenic sources in 2005 and projections to 2020. *Atmos. Environ., 44,* 2487-2499.

Peñuelas, J., Staudt, M. (2010) BVOCs and global change. *Trends Plant Sci., 15,* 133-144.

Querol, X., Alastuey, A., Pey, J., Cusack, M., Pérez, N., Mihalopoulos, N., Theodosi, C., Gerasopoulos, E., Kubilay, N., Koçak, M. (2009) Variability in regional background aerosols within the Mediterranean. *Atmos. Chem. Phys., 9,* 4575-4591, doi:10.5194/acp-9-4575-2009.

Querol, X., Alastuey, A., Pandolfi, M., Reche, C., Pérez, N., Minguillón, M. C., Moreno, T., Viana, M., Escudero, M., Orio, A., Pallarés, M., Reina, F. (2014) 2001–2012 trends on air quality in Spain. *Sci. Total Environ., 490,* 957-969.

Sauvage, S., Plaisance, H., Locoge, N., Wroblewski, A., Coddeville, P., Galloo, J. C. (2009) Long term measurement and source apportionment of non-methane hydrocarbons in three French rural areas. *Atmos. Environ., 43,* 2430-2441, doi:10.1016/j.atmosenv.2009.02.001.

Schlabach, M., Farag-Clement, R., Hung, H., Kallenborn, R., Su, Y., Aas, W. (2011) AMAP/EMEP/NCP inter-laboratory study for POP analysis 2010. Kjeller, NILU (EMEP/CCC, 07/2011).

Shatalov, V., Gusev, A., Dutchak, S., Rozovskaya, O., Sokovykh, V., Vulykh, N., Aas, W., Breivik, K. (2010) Persistent organic pollutants in the environment. Moscow/Kjeller, Meteorological Synthesizing Centre - East - MSC-E, NILU (EMEP Status Report, 3/2010).

Shatalov, V., Ilyin, I., Gusev, A., Rozovskaya, O., and Travnikov, O.: Heavy Metals and Persistent Organic Pollutants: Model Assessment of Pollution and Research Activities. Moscow, Meteorological Synthesizing Centre - East (EMEP/MSC-E Technical report, 4/2014).

Simpson, D., Benedictow, A., Berge, H., Bergstrom, R., Emberson, L. D., Fagerli, H., Flechard, C. R., Hayman, G. D., Gauss, M., Jonson, J. E., Jenkin, M. E., Nyiri, A., Richter, C., Semeena, V. S., Tsyro, S., Tuovinen, J. P., Valdebenito, A., Wind, P. (2012) The EMEP MSC-W chemical transport model - technical description. *Atmos. Chem. Phys., 12,* 7825-7865.

Spindler, G., Gnauk, T., Gruener, A., Iinuma, Y., Mueller, K., Scheinhardt, S., Herrmann, H. (2012) Size-segregated characterization of PM10 at the EMEP site Melpitz (Germany) using a five-stage impactor: a six year study. *J. Atmos. Chem., 69,* 127-157, doi:10.1007/s10874-012-9233-6.

Spindler, G., Gruener, A., Mueller, K., Schlimper, S., Herrmann, H. (2013) Long-term size-segregated particle (PM10, PM2.5, PM1) characterization study at Melpitz - influence of air mass inflow, weather conditions and season. *J. Atmos. Chem., 70,* 165-195, doi:10.1007/s10874-013-9263-8.

Thunis, P., Rouil, L., Cuvelier, C., Stern, R., Kerschbaumer, A., Bessagnet, B., Schaap, M., Builtjes, P., Tarrason, L., Douros, J., Mousslopoulos, N., Pirovano, G., Bedogni, M. (2007) Analysis of model responses to emission-reduction scenarios within the CityDelta project. *Atmos. Environ., 41,* 208-220, 10.1016/j.atmosenv.2006.09.001.

Thunis, P., Cuvelier, C., Roberts, P., White, L., Post, L., Tarrason, L., Tsyro, S., Stern, R., Kerschbaumer, A., Rouil, L., Bessagnet, B., Builtjes, J., Bergstroem, R., Schaap, M., Boersen, G. (2008) Evaluation of a sectoral approach to integrated assessment modelling including the Mediterranean Sea. Ispra, JRC.

Tørseth, K., Aas, W., Breivik, K., Fjæraa, A. M., Fiebig, M., Hjellbrekke, A. G., Lund Myhre, C., Solberg, S., Yttri, K. E. (2012) Introduction to the European Monitoring and Evaluation Programme (EMEP) and observed atmospheric composition change during 1972-2009. *Atmos. Chem. Phys., 12,* 5447-5481, doi:10.5194/acp-12-5447-2012.

Travnikov, O., Ilyin, I. (2005) Regional model MSCE-HM of heavy metal transboundary air pollution in Europe. Moscow, Meteorological Synthesizing Centre - East, (EMEP/MSC-E Technical Report, 6/2005).

UNECE (2014) Guidelines for reporting emission data under the Convention on Long-range Transboundary Air Pollution. Geneva, UNECE (ECE/EB.AIR/125).